8-30-2018

Evaluation of Undrained Shear Strength and Soil Classification from Cone Penetration Test

Md Imran Hossain
Louisiana State University and Agricultural and Mechanical College, mhoss35@lsu.edu

EVALUATION OF UNDRAINED SHEAR STRENGTH AND SOIL CLASSIFICATION FROM CONE PENETRATION TEST

A Thesis

Submitted to the Graduate Faculty of the
Louisiana State University and
Agricultural and Mechanical College
in partial fulfillment of the
requirements for the degree of
Master of Science in Civil Engineering

in

The Department of Civil and Environmental Engineering

by
Md Imran Hossain
B.Sc., Bangladesh University of Engineering and Technology, 2015
December 2018

This thesis is dedicated to my:

Grandparents

Parents

Uncle and Aunt

ACKNOWLEDGEMENTS

Thanks to the God Almighty for his unbound graciousness and unlimited kindness in all the endeavors I have taken up throughout my life.

I would like to express my gratitude to my dear advisor Dr. Murad Y. Abu-Farsakh, for his guidance, helpful criticisms, inspiration, assistance and encouragement given throughout the course of this research work. It is his perseverance, insight, and supervision that made this thesis possible. He has been a great mentor and I appreciate all his help. I would also like to thank Dr. Navid Jafari, co-chair of my committee, for guidance and suggestions throughout my research and for sharing his knowledge on Advanced Geotechnical Engineering. I would like to thank Dr. George Z. Voyiadjis, my committee member and departmental head of the civil engineering department at Louisiana State University, for his inspiration toward completing my research work. Besides, I would like to give special thanks to Dr. Shengli Chen for being my committee member and for sharing his knowledge on the deep foundation. I am truly grateful to my committee members. I would also like to express my gratefulness to Dr. Zhongjie Zhang and Gavin Gautreau for their help and continuous support. I am very thankful to Dr. Nafiul Haque for being a bolster of support and encouragement. He shared his knowledge throughout my research and helped me continuously. I would like to express my gratitude to my lab mates: Abu Hakim Faisal, Md. Habibur Rahman, Mohsen Amirmojahedi, Hossein Alimohammadi, Allam Ardah and Ahmad Souri for their continuous support. Besides, I would like to thank the staffs working at Louisiana Transportation Research Centre specially Ural "Renee" Cosse, Hend Alyousef, Preston Causey and Leon Goudeau for their helping during field trips.

Finally, my deepest thanks go to my family members for their continuous support and encouragement throughout my entire life.

TABLE OF CONTENTS

LIST OF TABLES

LIST OF FIGURES

ACRONYMS, ABBREVIATIONS, AND SYMBOLS

ASCE	American Society of Civil Engineers
c_v	Vertical Coefficient of Consolidation
c_h	Horizontal Coefficient of Consolidation
COV	Coefficient of Variation
CPT	Cone Penetration Test
DOTD	Department of Transportation and Development
f_s	Sleeve Friction
ft.	Feet
I_c	Soil Behavior Type index
In.	Inch
k_h	Horizontal Permeability
LA	Louisiana
LL	Liquid Limit
M	Constrained Modulus
MC	Moisture Content
n	Number of Observations, Stress Component
N_k	An Empirical Cone factor
OCR	Overconsolidation Ratio
PCPT/CPTu	Piezocone Penetration Test
PI	Plasticity Index
PL	Plastic Limit
PWP	Pore Water Pressure
q_c	Cone Tip resistance
q_t	Corrected Cone Tip Resistance
R^2	Coefficient of Correlation/ Coefficient of Determination
RM	Regression Model

RMSE	Root Mean Square Error
SAS®	Statistical Analysis Software
s_u	Undrained Shear Strength
S_t	Sensitivity
SPT	Standard Penetration Test
u_1	Excess Pore Water Behind the Friction Sleeve
u_2	Excess Pore Water Behind the Cone
u_3	Excess Pore Water on the Cone Tip
u_o	Hydrostatic Pressure
USCS	Unified Soil Classification System
σ_{vo}	Total Overburden Pressure
σ'_{vo}	Effective Overburden Pressure
σ'_p	Preconsolidation Pressure
γ	Unit Weight

ABSTRACT

The in-situ cone and piezocone penetration tests (CPT, PCPT) has been widely used by the geotechnical engineering community for subsurface soil characterization and classification, and for the evaluation of many engineering soil properties, such as undrained shear strength (s_u), unit weight (γ), constrained modulus (M), coefficient of consolidation (c_v), and stress history (OCR). The objective of this research study was to estimate the undrained shear strength of clayey soil using CPT/PCPT data in addition to some soil boring log data. At the same time, soil classification charts/methods based on CPT/PCPT were investigated and modified. For this purpose, 70 cone penetration test data collected from 14 different parishes in Louisiana were analyzed. In each site, both laboratory and CPT tests were performed at the same location in order to evaluate the soil parameters (e.g., corrected cone tip resistance, q_t; sleeve friction, f_s; total overburden pressure, σ_{vo}; plasticity index, I_p; Liquid limit, LL; and moisture content, MC). Both linear and non-linear statistical regression models were developed and verified using the measured soil parameters to estimate s_u of clayey soil for individual soil layers. The s_u model that contains q_t, f_s, and σ_{v0} parameters is found to be the best model that satisfies all the statistical parameters, and that the estimated values of s_u are close to the measured values. In addition, three basic soil zones (e.g., sandy, silty and clayey) have been modified in some CPT/PCPT based soil classification charts. The CPT/PCPT soil classification charts investigated in this study include Douglas and Olsen (1981) chart, modified Schmertmann chart by Tumay (1985), Robertson (1990, 2009 and 2010) charts, Saye et al. (2017) chart, and Zhang and Tumay (1999) probability method. Among these charts, the Robertson (2010) chart showed better prediction to categorize soils for Louisiana. In addition, the Zhang and Tumay (1999) probability method is found to be suitable to categorize the sandy and clayey soil type behavior, but was not so clear for the silty soil behavior.

CHAPTER 1
INTRODUCTION

The cone penetration test (CPT) was introduced in the early 1930's. In 1932, the first CPT test was performed to measure the tip resistances from a depth of 4 m soil fill by the Dutch engineer P. Barentsen (Broms and Flodin, 1990). Usually, the tip resistance q_c and the sleeve friction f_s can be measured from the CPT tests. If the cone can measure the pore water pressure (u_1, u_2 *or* u_3), then it is called piezocone (e.g., Robertson et al., 1986; Abu-Farsakh et al., 2005). Pore pressure transducers are connected with the cone or friction sleeve to measure the pore water pressure during penetration in piezocone penetrometer (PCPT/CPTu). There are no standard filter locations for excess pore water pressure measurement. However, usually three locations are found in the literature for setting the pore pressure transducer and the positions are shown in Figure 1.1 (e.g., Mayne, 2007; Robertson, 2015). Usually, the filter position just behind the cone (u_2) is widely used (e.g., Lunne et al., 2014; Robertson, 1990). The other positions are on the tip of the cone (u_1) or behind the friction sleeve rod (u_3).

Nowadays, the CPT has gained popularity and worldwide acceptance for soil characterization and subsurface investigation (e.g., Robertson, 2009; Mayne, 2007). The CPT can offer continuous soundings of subsurface soil with depth in a fast and economical way (e.g., Mayne, 2007; Abu-Farsakh et al., 2003). The three most anticipated applications for CPT are:

a) To access the sub-surface soil condition and identify materials present below the ground level.

b) To evaluate the geotechnical parameters such as the undrained shear strength (s_u), unit weight (γ), constrained modulus (M), the coefficient of consolidation (c_v), stress history (σ_p', OCR), soil classification, etc.

c) To establish a guideline for geotechnical design directly using CPT results. Additionally, the CPT can preliminarily identify strata and thus can give direction on what additional tests need to perform. If the geology is uniform and well understood, and if estimates based on CPT results have been correlated and verified locally, then CPT tests alone are adequate for design.

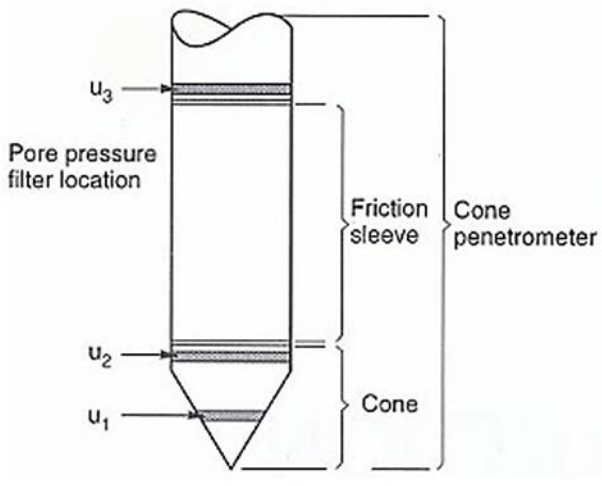

Figure 1.1: Terminology for cone penetrometers (after Lunne et al., 1997)

However, it is general exercise for the CPT to be used in parallel with other laboratory tests for identification of soil, to validate local correlations, to offer a complete information where CPT data interpretations are difficult and time consuming due to partial drainage conditions or other soil problems, or to predict future variations in soil conditions that are not predictable by CPT etc. In this study, the strength parameter (s_u) of clayey soils is evaluated from CPT. At the same time, existing CPT/PCPT soil classification methods are adjusted/modified.

1.1 Scope and Objectives of the Thesis

One of the objectives of this study is to evaluate the undrained strength (s_u) of clayey soils. For this purpose, CPT data collected from 70 different sites in Louisiana were used to perform linear

and non-linear statistical regression analyses. By direct and indirect approaches, some new correlations for s_u were developed. Thus, s_u could be assessed directly from CPT using q_t and f_s alone or the combination of these two parameters. Moreover, an attempt was made to explore indirect correlations based on CPT data along with other soil properties, e.g., total overburden stress, σ_{vo}; moisture content, *MC*; liquid limit, *LL* and plasticity index, I_p. Though initial analyses in this thesis study had acknowledged other models consisted of q_t and σ_{vo} together giving a good estimation of s_u, another attempt was made to include f_s in combination with q_t and σ_{vo} to explore new correlations. In addition, an attempt was made to develop a correlation between the cone tip factor, N_{kt} and some selected soil parameters, e.g., I_p, *MC* and *LL* to estimate s_u. Finally, the undrained shear strength parameters (s_u) predicted from CPT based correlation were compared and verified using laboratory s_u data along with in-situ measurements using data from other sites.

Another objective of this study is to investigate the existing CPT/PCPT soil classification methods. The CPT/PCPT soil classification charts actually describe the soil behavior. It does not demonstrate actual soil type or configuration. Although many soil classification charts are available, region-specific basic soil type charts are necessary. Besides, the q_c and f_s are subjected to various disturbance such as equipment disposition, stratigraphy, in-situ stresses, soil collection disturbance etc. Therefore, it is necessary to inspect the applicability of the currently available CPT/PCPT soil classification charts to characterize the soil behavior. Moreover, it is important to know the basic soil types from CPT/PCPT data. Thus, in this study, three basic soil type zones, e.g., sandy, silty and clayey zones were modified in the selected CPT/PCPT soil classification charts.

For analyzing soil types, the soils were classified according to USCS soil classification method into three major types: sandy, silty and clayey. Then, these three soil zones were adjusted in some

CPT soil classification charts named Douglas and Olsen (1981) chart, Modified Schmertmann chart by Tumay (1985), Robertson (1990, 2009, 2010) charts and Saye et. al (2017) chart. In addition, the effectiveness of Zhang and Tumay (1999) CPT soil probability method was investigated.

1.2 Thesis Outline

The thesis consists of six different chapters. The first chapter introduces the research background, summaries the scopes and objectives of the research. A brief overview of the CPT/PCPT test method and existing methods for evaluating the undrained shear strength form CPT/PCPT is also discussed. Chapter Two also provides the detailed review of the existing CPT/PCPT soil classification methods. Test sites details and the summaries of soil properties of each site are described in Chapter Three. Chapter Four gives the outline for the statistical regression analyses of data. Results of the linear and nonlinear regression analyses to develop new s_u models are discussed in details. Adjusting/modifying some CPT/PCPT soil classification methods are highlighted in Chapter Five. Chapter Six summarizes the conclusions and findings of the thesis. Furthermore, future recommendations on the practice of CPT methods and soil classifications charts are discussed here.

CHAPTER 2
LITERATURE REVIEW

This chapter would give a brief overview of the role of cone or piezocone penetration test (CPT/PCPT). A detailed procedure for estimating undrained shear strength from CPT/PCPT was also discussed. Finally, the existing CPT soil classification methods were presented.

2.1 Cone Penetration Test (CPT)

The Cone or Piezocone Penetration Test (CPT/PCPT) is an in-situ testing method. CPT/PCPT is advantageous for determining different geotechnical parameters. Nowadays, CPT/PCPT is popular because of the repeatability and reliability. During CPT, a rod is pushed into the ground at a rate of 0.79 in./sec (2 cm/sec) and data is collected every 0.79 in (2 cm). Several types of penetrometers are available such as the mechanical cone, the friction cone, the electric cone, the piezocone, or the combinations. Nowadays, piezocone is widely used for testing purposes.

A standard cone penetrometer generally has 1.55 in^2 (10 cm^2) base area with an apex angle of 60^o. The area of the friction sleeve is 23.25 in^2 (150 cm^2) and it is located above the cone (ISSMFE, 1989). The cone tip resistance, q_c, is the ratio between total force acting on the cone, Q_c, and projected cross-sectional area, A_c. Similarly, the sleeve friction, f_s, is the ratio between total force acting on the friction sleeve F_s, and the surface area of the friction sleeve, A_s. q_c and f_s are derived from the data acquisition system.

2.2 Presentation of Result

The tip resistance (q_c, q_t), sleeve friction (f_s) and pore water pressure values (u_1, u_2 or u_3) can be found directly from the PCPT. Another parameter friction ratio, F_r, that is the ratio between f_s and q_c, is also presented in PCPT result. F_r is an important parameter in soil classification since many soil classification charts were prepared using F_r. Figure 2.1 represents PCPT data for a typical site.

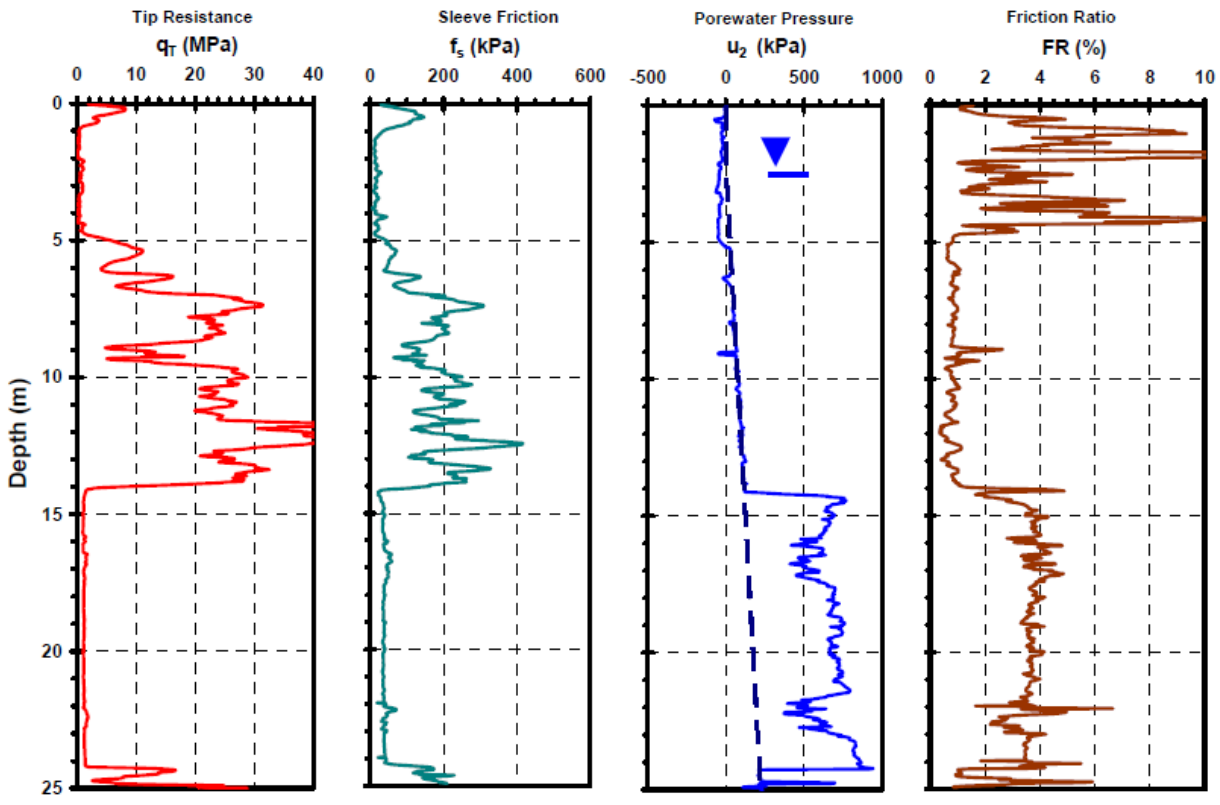

Figure 2.1: A typical CPTU result (after Mayne, 2007)

2.3 Role of CPT in Site Investigation

Good correlations observed between the laboratory measured and CPT/PCPT estimated soil parameter (e.g., Abu-Farsakh, 2003; Mayne and Kulhawy, 2002; Robertson, 2015). For example, according to Voyiadjis and Song (2003), the drainage condition and hydraulic conductivity (k) can be measured using piezocone. They used an elastoplastic, coupled theory of mixtures. Steady-state excess pore pressure generated during piezocone penetration. That study indicated that the change in the dimensionless excess pore pressure at the cone tip is nearly constant when the dimensionless k is $\leq 10^{-7}$ or $\geq 10^{-4}$. In this manner, without doing dissipation tests, hydraulic conductivity of soil can be measured form PCPT. The existing parameters that can be derived using CPT/PCPT are shown in Table 2.1.

Table 2.1: List of soil properties estimated using piezocone parameters

Serial No.	Parameter	Reference
1	Soil Classification	Begemann (1965), Schmertmann (1978), Senneset & Janbu (1985), Robertson (1990, 2009)
2	Effective Friction angle (ϕ')	Senneset and Janbu (1985), Robertson (2010)
3	In situ Stress State (K_o)	Brown and Mayne (1993), Mayne and Kulhawy (2002), Robertson (2010)
4	Stress History (σ_p' ,OCR)	Baligh et al. (1980), Sully et al. (1988), Voyiadjis et al. (1993), Abu-Farsakh (2003), Lee et al. (2011)
5	Shear Modulus (G_{max})	Mayne and Rix (1993), Mayne and Campanella (2005)
6	Constrained Modulus (M)	Buisman (1940), Khulway and Mayne (1990), Abu-Farsakh (2003 and 2007)
7	Sensitivity (S_t)	Robertson and Campenella (1988)
8	Undrained Strength (s_u)	Aas et al. (1986); Konrad and Law (1987),
9	Hydraulic Conductivity (k)	Robertson et al. (1992a), Voyiadjis and Song (2003)
10	Coefficient of Consolidation (c_v)	Senneset et al. (1982), Baligh et al. (1981), Abu-Farsakh (2003, 2007), Cai et al. (2012)
11	Effective cohesion intercept (c')	Senneset et al. (1989), Alonso et al. (2016)
12	Unit weight (γ_t)	Robertson et al. (1986), Mayne (2014)
13	Attraction, $a' = c' cot\phi'$	Senneset et al. (1989), Mayne (2014)
14	California Bearing Ratio, CBR	Pamukcu & Fang (1989), Mayne (2001)
15	Strain Rate and Partial Saturation	DeJong and Randolph (2012)

2.3.1 Cone Tip Resistance

With the purpose of correlating cone tip resistance to soil properties, Terzaghi's (1943) formula for ultimate bearing pressure is analyzed,

$$q_{ul} = cN_c + \frac{1}{2} B\gamma N_\gamma + \gamma DNq \qquad (2.1)$$

where B is footing depth, D is embedment depth of footing γ is soil density, N_γ, N_q, N_c are bearing capacity factors. The surface term $\frac{1}{2}\gamma BN_\gamma$ is negligible in case of penetrometer:

$$q_c = \gamma DN_q \text{ (for cohesionless soil)} \qquad (2.2)$$

$$q_c = \gamma D + cN_c \text{ (for cohesive soil)} \qquad (2.3)$$

On the other hand, in terms of s_u, equation (2.3) becomes:

$$q_c = \gamma D + N_{kt} * s_u \quad (2.4)$$

where N_{kt} is the cone tip factor. Vesic (1977) defined N_{kt} in terms of spherical cavity expansion theory:

$$N_{kt} = \frac{4}{3}(ln\ I_r + 1) + \frac{\pi}{2} + 1 \quad (2.5)$$

where I_r is the rigidity index. In case of a strip footing and cohesionless soil, the σ_{vo} and the maximum soil bearing pressure at the end, q_{ul}, can be correlated by Prandtl's equation:

$$q_{ul} = \sigma_{vo}\ tan^2\left(\frac{\pi}{4} + \frac{\emptyset}{2}\right)e^{\pi tan\phi} \quad (2.6)$$

For cohesive soils Caquot's theorem can be used in place of Prandtl's equation:

$$q_{ul} = \sigma_{vo}\ tan^2\left(\frac{\pi}{4} + \frac{\emptyset}{2}\right)e^{\pi tan\phi} + \frac{c}{tan\emptyset}\left\{tan^2\left(\frac{\pi}{4} + \frac{\emptyset}{2}\right)e^{\pi tan\phi} - 1\right\} \quad (2.7)$$

Considering cone penetrometer, the multiplication coefficient of 1.3 was assumed Buisman (1940):

$$q_c = 1.3\left[\sigma_{vo}\ tan^2\left(\frac{\pi}{4} + \frac{\emptyset}{2}\right)e^{\pi tan\phi} + \frac{c}{tan\emptyset}\left\{tan^2\left(\frac{\pi}{4} + \frac{\emptyset}{2}\right)e^{\pi tan\phi} - 1\right\}\right] \quad (2.8)$$

that is $q_{c=f}(\phi, c, \sigma_{vo})$

2.3.2 Sleeve Friction

No specific correlation has been suggested to determine the sleeve friction (e.g., Vesic, 1969).

2.3.3 Pore Pressure

Due to penetration in soil, the soil stress condition changes near the probe. Thus, the pore water pressure also changes. For clayey type soils, large excess pore pressures develop due to an undrained loading condition and thus generating the hydrostatic state. This excess water pressure of soil is a combination of soil displacement and probe driving along with shear stress developed near the penetrometer. In piezocone, the excess pore pressure can be measured at the cone tip (u_1),

behind the cone (u_2) and behind the friction sleeve (u_3). The excess pore water pressure, $\Delta u = u_m - u_o$, produced during cone penetration can be described using cavity expansion and critical state theory:

$$\Delta u = \Delta u_{oct} + \Delta u_{shear} \quad (2.9)$$

where Δu_{oct} is octahedral stress, Δu_{shear} is shear stress and u_o is hydrostatic pressure. According to Song and Voyiadjis (2005), distribution of pore water pressure along a penetrometer is lower at the shaft (compression induced) and higher at the face (shear-induced). It is because of the mechanism of excess pore water pressure generation. They analyzed the pore pressure response of soils with finite element analysis. It is based on the coupled theory of mixtures. For experimental purposes, they used Louisiana State University (LSU) calibration chamber. The was a misxture of sand, kaolin and deionized water. The water content was double of the liquid limit. For that particular study, they used three piezo miniature cone penetrometer. Another study performed on cohesive soils at LSU calibration chamber suggested that excess pore water pressure measurement is highly sensitive to filter location (Abu-Farsakh et al., 1998). They recommended using u_2 configuration of the filter location.

For the measurement of u_1, Baligh (1985) suggested that Δu is controlled by Δu_{oct}. He suggested that the contribution of shear stress (Δu_{shear}) is less than 20%. Therefore, Δu_{shear} is ignored for the practical purposes. On the other hand, u_2 or u_3 is considerably influenced by the shear component (Vesic, 1972). Voyiadjis and Kim (2003) performed finite element analysis (FEA) and compared FEA results the results with PCPT results from LSU calibration chamber. They observed quite large octahedral shear stress on upper and lower portions of the cone.

Usually, pore pressures that generate behind the cone, can influence the total stress measured by the cone tip. Therefore, the cone tip resistance and sleeve friction data measured

directly from the penetration test needs to be corrected. The corrected cone tip resistance (q_t) can be measured from:

$$q_t = q_c + (1 - a)\, u_2 \qquad (2.10)$$

where $a = a_n/a_c$ is the effective cone area ratio, a_n is the load cell cross-sectional area and a_c is the cone projected area. For Louisiana cone, a value o*f* $a = 0.59$ is generally used. In the same way, the corrected cone sleeve friction (f_s) can be measured from:

$$f_t = f_s - (A_{sb} * u_2 - a_{st}\, u_3)/A_s \qquad (2.11)$$

where A_{sb} and A_{st} are the bottoms and top cross-sectional areas of friction sleeve respectively, and A_s is the friction sleeve surface area.

2.4 Undrained Shear Strength

Undrained shear strength (s_u) is a parameter of soil which describes the capability of the soil of sustaining shear stress. s_u depends on the mode of soil shear failure, soil anisotropy, strain rate and stress history. The s_u value to be used in analysis depends on the design problem (Mayne, 2007). Therefore, it is very important to interpret the undrained shear strength of clays. The strength properties of soil can be determined through several approaches. Such as laboratory tests or in-situ tests (e.g., Robertson, 2009; Mayne, 2007). However, the laboratory collected soil samples does not properly represent the actual in-situ condition. Because the soil samples are always subjected to a certain level of disturbance at the time of collection. Besides, laboratory testing on a small amount of interbedded or fissures soil samples can be sometimes misleading.

In-situ tests, such as the cone and piezocone penetration tests (CPT, PCPT), can provide more reliable results than laboratory tests in evaluating the actual strength properties of the soil under in-situ stress conditions (e.g., Robertson, 2009). Several correlations have been developed to predict the s_u from PCPT/CPT depending on different approaches. Empirical correlations give

a better estimate of s_u. Besides, theoretical approaches also provide reasonable estimates of s_u (Yu and Mitchell, 1998). Most common theoretical methods are Bearing Capacity Method (BCM), Cavity Expansion Method (CEM), Strain Path Method (SPM) and Finite Element Methods (FEM) (Huang et al., 2004). Some researchers combined these approaches, such as CEM-FEM (Abu-Farsakh et al. 2003) CEM-SPM (Yu and Whittle, 1999), CEM-BCM (Salgado et al. 1997), and SPM-FEM (Teh and Houlsby, 1991). Besides, there are some other theoretical approaches available. Using the theoretical approaches, a relationship can be suggested between the q_c and s_u:

$$s_u = (q_c - \sigma_v)/N_c \text{ (for cohesive soil)} \quad (2.12)$$

$$\text{and } q_c = N_q \sigma'_v \text{ (for cohesionless soil) } N_q = q_c/\sigma'_v = 0.194exp^{(7.63tan\phi)} \quad (2.13)$$

where, N_c and N_q is the theoretical cone factor for sand and clay respectively (Yu, 2006), σ_v is the overburden pressure, σ'_v is the effective overburden pressure. Depending on the theory used, σ_v may be σ_{v0}, σ_{h0}, or σ_{oct} as summarized by Lunne et al. (1997). N_c values are summarized in Table 2.2. However, the theoretical cone factor values have some limitations. Almost all theoretical methods make some simplifying assumptions about soil condition, soil boundary conditions, and soil failure criteria. Therefore, the findings of theoretical methods need to be cross-checked from in-situ and laboratory soil parameters. However, parameters obtained from empirical correlations may have low reliability. Usually, a large factor of safety is assumed to offset the error. Laboratory tests like the triaxial test is a good way to measure s_u. Triaxial tests (for this study- unconsolidated undrained test) are performed on small samples obtained from the site location at pre-selected soil depths. However, laboratory tests are usually time-consuming and costly (Mitchell and Brandon 1998). Nowadays, in-situ testing (e.g., CPT/PCPT) is using as a better substitute for laboratory soil testing. A major breakthrough of CPT/PCPT method is that it offers a reliable and repeatable evaluation of in-situ soil profile and strength parameter such as s_u of soil at different depths from

a single test. Based on bearing capacity theory, Lunne and Kleven (1981) developed the equation (2.14). According to them, the in situ vertical stress should be the total overburden pressure, σ_{vo}:

$$s_u = \frac{(q_c - \sigma_{vo})}{N_k} \qquad (2.14)$$

where N_k denotes the cone factor for tip resistance and σ_{v0} denotes in situ vertical stress. N_k influences the cone shape factor. Depending on soil types and tests, different researchers suggested different N_k values (e.g., Chen, 2001; Almedia et al., 2010). The ranges of N_k values are between 5 to 28.4 (Table 2.3). The suggested N_k values by different researchers for different soils types are represented in Table 2.3.

Table 2.2: N_c values theoretically derived by different researchers

N_c ($\phi = 0$)	σ_i	Remarks	Reference
7.41	σ_{vo}	-	Terzaghi (1943)
7.0	σ_{vo}	-	Caquot and Kerisel (1956)
9.34	σ_{vo}	Smooth base	Meyerhof (1951)
9.74	σ_{vo}	Rough base	De Beer (1977)
9.94	σ_{vo}	Spherical cavity expansion, E_t	Meyerhof (1951)
$\frac{4}{3}[1 + ln(E_t/3s_u)] + 1$	σ_{vo}	Spherical cavity expansion, E_s	De Beer (1977)
$\frac{4}{3}[1 + ln(E_s/3s_u)] + 1$	σ_{vo}	Spherical cavity expansion	Meyerhof (1951)
$\frac{4}{3}[1 + ln(E_s/3s_u)] + cot\theta$	σ_{vo}	Spherical cavity expansion	Gibson (1950)
$\frac{4}{3}[1 + ln(E_s/s_u)] + cot\theta$	σ_{vo}	Spherical cavity expansion, finite strain theory	Gibson (1950)
$\frac{4}{3}[1 + lnI_r]$	σ_{vo}	Spherical cavity expansion	Vesic (1972)
$\frac{4}{3}[1 + lnI_r] + 2.57$	σ_{mean}	Spherical cavity expansion	Vesic (1972)
$[1 + lnI_r] + 11$	σ_{ho}	Cylindrical cavity expansion	Baligh (1975)
$(s_a/s_u) + \frac{4}{3}(s_r/s_u)\,[1 + \ln(E_r/3s_{ur})] + \frac{4}{3}$	σ_{vo}	Trilinear stress-strain relationship	Ladanyi (1967)
$\frac{\frac{Eu}{Su} - \frac{Er}{Sur}\cdot\frac{Sur}{Su}}{\frac{Eu}{Su} - \frac{Er}{Sur}} \ln\frac{Eu}{Su}\frac{Sur}{Eu} + 0.19 + 2.64\ln(I_r) - \frac{\sigma vo}{Su}(1-K_0) + 2\alpha$		Elastic perfectly plastic-strain path approach	Teh (1987)

Table 2.3: N_k value suggested by researchers

Soil Type	Name and Year	N_k values
Normally consolidated clay	Lunne and Kleven (1981)	11-19
Medium soft clay	Kiousis et al. (1988)	8.5
Scandinavian Marine clays	Jörss (1998)	20 (Marine clay) 15 (Boulder clay)
Different soil types	Gebreselassie (2003)	7.6-28.4
Malaysia soils	Chen (2001)	5-12
Boom clay	Van Empe (2004)	13-24
Fine-grained soils	Almeida et al. (2010)	4-16

After correcting tip resistance (q_t) values for water pressure, equation (2.14) has been modified:

$$s_u = \frac{(q_t - \sigma_{vo})}{N_{kt}} \qquad (2.15)$$

where N_{kt} is a cone factor dependent upon the theoretical basis. Common ranges for N_{kt} are generally between 4 to 29, which is dependent on tests performed and types of soil (e.g., Konrad & Law, 1987; Yu & Mitchell, 1998). According to Powell and Quarterman (1988), N_{kt} values in soft intact clays are commonly taken to be between 10 and 20, though it is mode-dependent. Depending on various geological conditions and tests performed, N_{kt} can be different (Table 2.4).

According to Senneset (1982), another possibility to calculate s_u from the CPT values is the use of effective cone resistance, $q_E = q_t - u_2$.

$$s_u = \frac{(q_E)=(q_t - \sigma_{vo})}{N_{ke}} \qquad (2.16)$$

where N_{ke} is an effective cone factor. The average value of N_{ke} is 12 with a variation of ±6 (e.g., Karlsrud et al., 1996; Hong et al., 2010). However, it is not recommended to use the effective cone resistance to estimate s_u for soft normally consolidated clays and heavily over-consolidated

deposits (Robertson and Campanella, 1988). This is mainly attributed to sensitivity and the small value of q_E due to the small error in q_t and u_2 measurements. Table 2.5 represents the different N_{ke} values depending on soil types and tests performed.

Table 2.4: Recommendations for cone factor N_{kt}

N_{kt} value range	Reference test	Comments	Reference
8-16	Triaxial compression, Triaxial extension and Direct shear	For clays (3% < I_p < 50%) N_{kt} increases with I_p	Aas et al. (1986)
11-18		No correlation between N_{kt} and I_p	La Rochelle et al. (1988)
8-29	Triaxial compression	N_{kt} varies with OCR	Rad and Lunne (1988)
10-20	Triaxial compression	-	Powell and Quarterman (1988)
6-15	Triaxial compression	N_{kt} decreases with B_q	Karlsrud (1996)
7-20	Triaxial compression	Busan clay, Korea 25% < I_p < 40%	Hong et al. (2010)
4-16	Vane shear	High plasticity, soft clay, 42% < I_p < 400%	Oliveira et al. (2010)
10-18	Triaxial compression, Triaxial extension	N_{kt} increases with increasing I_p	Robertson and Cabal (2015)

Table 2.5: Recommendations for cone factor N_{ke}

N_{ke} value range	Reference test	Comments	Reference
6-12		For clays (3% < I_p < 50%)	Senneset et al. (1982)
1-13		N_{ke} varies with B_q	Lunne et al. (1985)
2-10	Triaxial compression	N_{kt} decreases with B_q	Karlsrud (1996)
3-18	Triaxial compression	Busan clay, Korea 25% < I_p < 40%	Hong et al. (2010)

This disadvantage can be overcome by introducing a new cone factor $N_{\Delta u}$ (Vesic, 1972). The advantage of measuring $N_{\Delta u}$ over the effective cone resistance method is that Δu (u_2-u_o) can be very large, mainly in soft clays, making the effect of measurement errors less significant and

thus resulting in a better accuracy. The ranges of $N_{\Delta u}$ are 4 to 10 depending on soil type and tests (Table 2.6).

$$s_u = \frac{(\Delta_u)=(u_2 - u_o)}{N_{\Delta u}} \qquad (2.17)$$

where u_0 is the in-situ hydrostatic pressure, Δ_u is the difference between pore pressure behind the cone and in-situ hydrostatic pressure, and $N_{\Delta u}$ denotes cone factor based on excess pore water pressure.

Table 2.6: Recommendations for cone factor $N_{\Delta u}$ values

Name and year	$N_{\Delta u}$
Lunne et al (1985)	4-10
Karlsrud et al (1996)	6-8
Hong et al. (2010)	4-9

Some researchers (e.g., Amundsen et al.,1985; Karlsrud et al., 1996, Lunne et al., 1997) suggested a correlation between cone factor N_{kt} and pore pressure factor B_q (figure 2.2). B_q is defined as:

$$B_q = \frac{(\Delta_u)=(u_2 - u_o)}{q_t - \sigma_{vo}} \qquad (2.18)$$

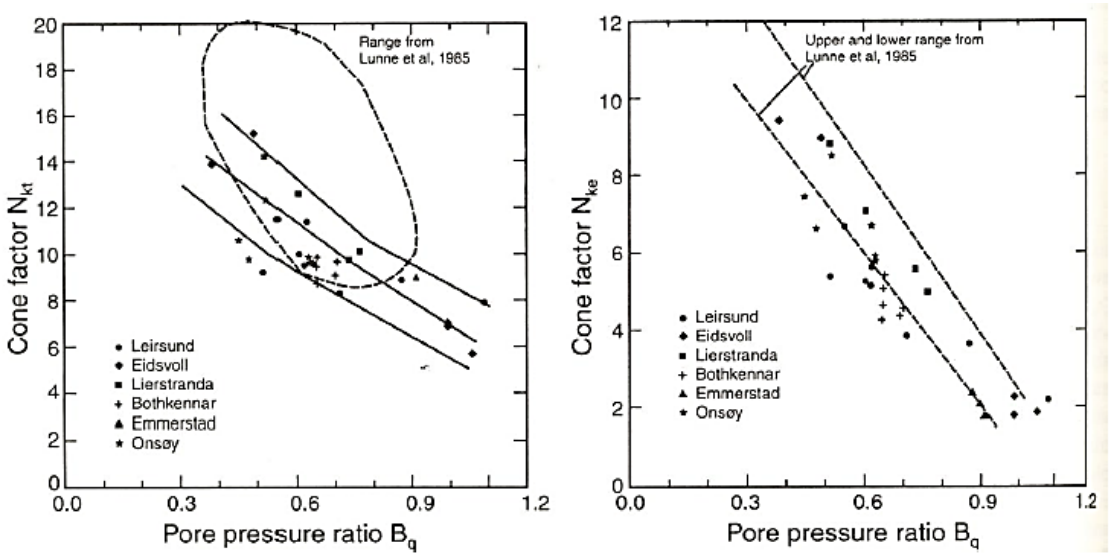

Figure 2.2: B_q vs N_{kt} and N_{ke} (after Lunne et al., 1997)

Kim et al. (2010) made an approach to correlate N_k with I_p for the clayey soils in Indiana and suggested a localized equation to estimate N_k:

$$N_k = 0.285*I_p + 7.636 \qquad (2.19)$$

where I_p is plasticity index. Equation (2.19) has coefficient of determination value, $R^2 = 0.75$. The results from Figure 2.3 showed an increasing trend N_k with I_p. However, Lunne et al. (1976) and Baligh et al. (1980) observed decreasing trends for their analyses.

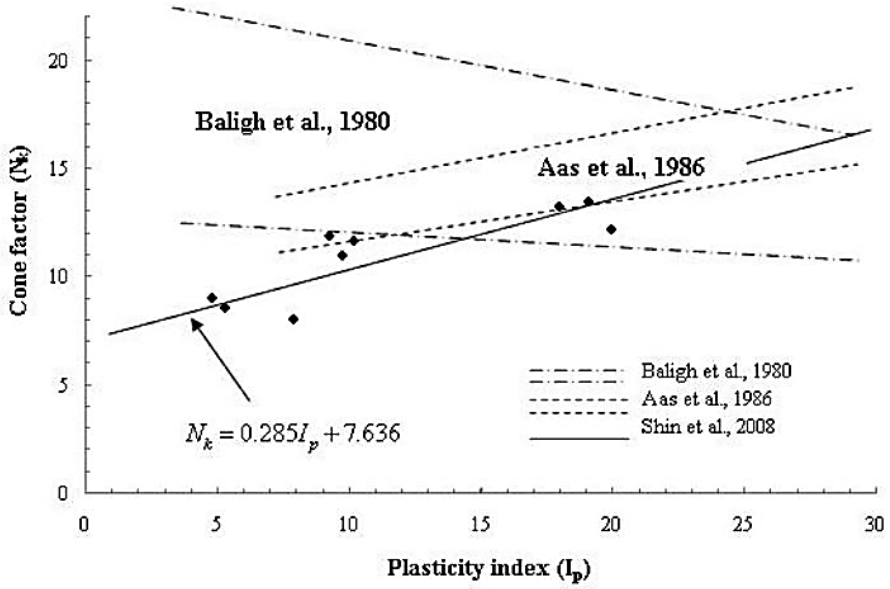

Figure 2.3: Correlation of factor N_k and I_p (after Kim et al., 2010)

Larsson and Mulabdic (1991) suggested the following equation to calculate N_{kt} for Swedish clay:

$$N_{kt} = 13.4 + 6.65*LL \qquad (2.20)$$

where LL is the liquid limit of the soil. Equation (2.20) is valid for over consolidation ratio, OCR = 1.3. OCR is defined as the ratio of the maximum past effective consolidation stress and the present effective overburden stress (Terzaghi et al.,1996):

$$OCR = \sigma_p'/\sigma_{vo}' \qquad (2.21)$$

where σ_p' is the effective preconsolidation stress. For the Norwegian clays, Thakur et al. (2016) developed a correlation between liquid limit, *LL*, and I_p :

$$LL = 15 + 1.4\, I_p \qquad (2.22)$$

In soft clays and silts, for problematic construction and field performance difficulties, sensitivity (S_t) is considered as an important index property. The sensitivity (S_t) of clay is the ratio of undisturbed s_u to totally remolded s_u (Robertson and Cabal, 2009). The field vane shear test is the reference test for determining S_t (Chandler 1988), though some other laboratory testing can also be used such as unconfined compression test (UC), fall cone test etc. Based on S_t value, equations (2.23-2.30) have been developed (Clausen et al. 2005):

For $S_t < 15$:

$$N_{kt} = 7.8 + 2.5*\log(OCR)+0.082*I_p \qquad (2.23)$$

$$N_{\Delta u} = 6.9 - 4.0*\log(OCR)+0.07*I_p \qquad (2.24)$$

$$N_{ke} = 11.5 - 9.05*B_q \qquad (2.25)$$

$$B_q = 0.88 - 0.51*\log(OCR) \qquad (2.26)$$

For $S_t > 15$:

$$N_{kt} = 8.5 + 2.5*\log(OCR) \qquad (2.27)$$

$$N_{\Delta u} = 9.8 - 4.5*\log(OCR) \qquad (2.28)$$

$$N_{ke} = 12.5 - 11.0*B_q \qquad (2.29)$$

$$B_q = 1.15 - 0.67*\log(OCR) \qquad (2.30)$$

Shear wave velocity (V_S) is another parameter to measure strength properties of soil. V_S of cohesive soils largely depend upon effective stress, void ratio, and stress history. Dickenson (1994) proposed the following correlation for San Francisco Bay cohesive soils:

$$V_S\ (m/sec) = 23 s_u^{0.475} \qquad (2.31)$$

where V_S is measured in m/sec and s_u is measured in kPa.

Rigidity index ($I_r = G/s_u$, where G is the shear modulus) is another parameter to estimate the s_u. Again, $E_s = 3G$, where E_s is the modulus of elasticity. Thus, $I_r = E_s/3s_u$. Based on I_r, Teh (1987) proposed a theoretical solution to estimate cone factor N_{kt} :

$$N_{kt} = 0.19 + 2.64\ln(I_r) - \sigma'_{vo}(1-K_0) + 2\alpha \qquad (2.32)$$

where α = roughness coefficient and K_o is earth pressure at rest. α equals 0 for smooth surface and 1 for the rough surface.

To investigate the PCPT in clayey type soils, Abu-Farsakh et al. (2003) developed a numerical model. Previously, Abu-Farsakh (1997) used an elasto-plastic coupled system to define consolidation of saturated clays. They used the stress factor, Δ, defined by Teh and Houlsby (1991):

$$\Delta = (\sigma_{vo} - \sigma_{ho})/2s_u \qquad (2.33)$$

where σ_{ho} is initial horizontal lateral stress. Figure 2.4 presents the relation between N_k and Δ. Assuming a perfectly plastic von Mises model and using strain path finite-element analyses a correlation was proposed (Teh and Houlsby, 1991):

$$N_k = 1.25 + 1.84\ln(G/s_u) \qquad (2.34)$$

Abu-Farsakh et al. (2003) investigated in a similar way. They observed that N_k increased linearly with the $\ln(G/s_u)$ value and the results are presented in Figure 2.5.

$$N_k = 2.45 + 1.80\ln(G/s_u) - 2.1\Delta \qquad (2.35)$$

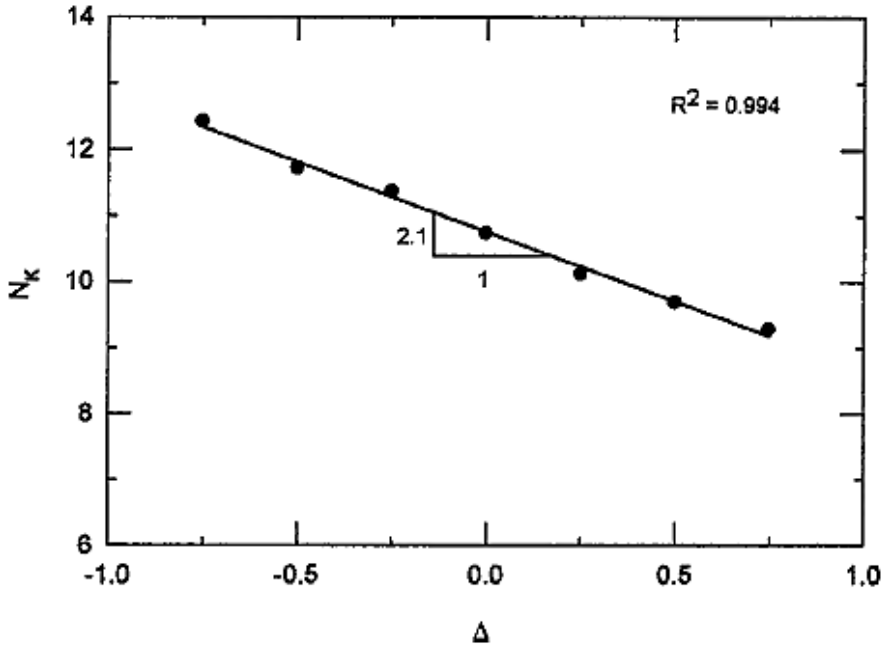

Figure 2.4: Effect of Δ on cone tip factor N_k (after Abu-Farsakh et el. 2003)

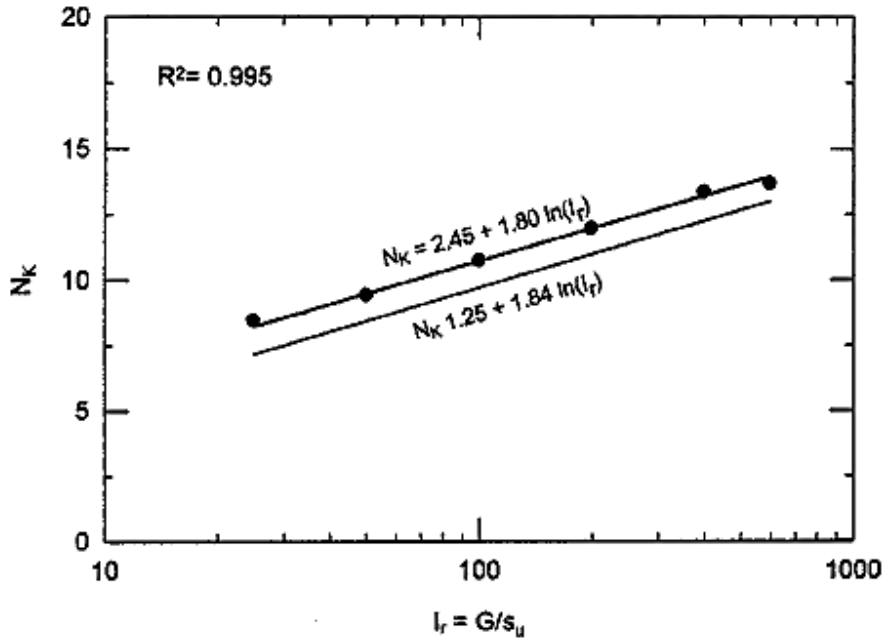

Figure 2.5: Effect of rigidity index, I_r on cone factor N_K (after Abu-Farsakh et el. 2003)

2.5 Soil Classification

Soil identification and classification is essential for any geotechnical design and investigation projects. Laboratory testing is the conventional method for soil classification (Cai et al., 2011). However, in-situ soil classification methods are also available, e.g., the Standard Penetration Test (SPT) and cone or piezocone penetration test (CPT/PCPT). CPT/PCPT is advantageous for soil characterization over other in-situ methods because it is fast, cost-effective, repeatable and reliable (e.g., Lunne et al., 1997; Robertson, P.K. & Cabal, 2012). Though CPT/PCPT provides a guideline to classify soil, CPT/PCPT cannot provide exact soil type, e.g., grain size distribution **(**Robertson et al. 2015).

2.5.1 General Approaches

Soil classification through CPT and PCPT is not a direct approach. However, there are some general approaches: (a) rules of thumb (e.g., Mayne et al. 2002), (b) experimental approach (e.g., Douglas and Olsen 1981; Modified Schmertmann, 1978 by Tumay, 1885; Saye et al., 2017) (c) Statistical approach (e.g., Zhang and Tumay, 1999) and (d) Soil behavior type approach (i.e., Robertson, 1990; 2009 and 2010). These methods should be verified for a specific geology before using practically (Mayne, 2014).

Begemann (1965) Chart

Begemann (1965) is the father of soil profiling from the CPT. He developed a chart and showed that sands exhibit higher q_c and f_s values than the clays (Figure 2.6). He also recommended that soil characterization might be the function of q_c and f_s together.

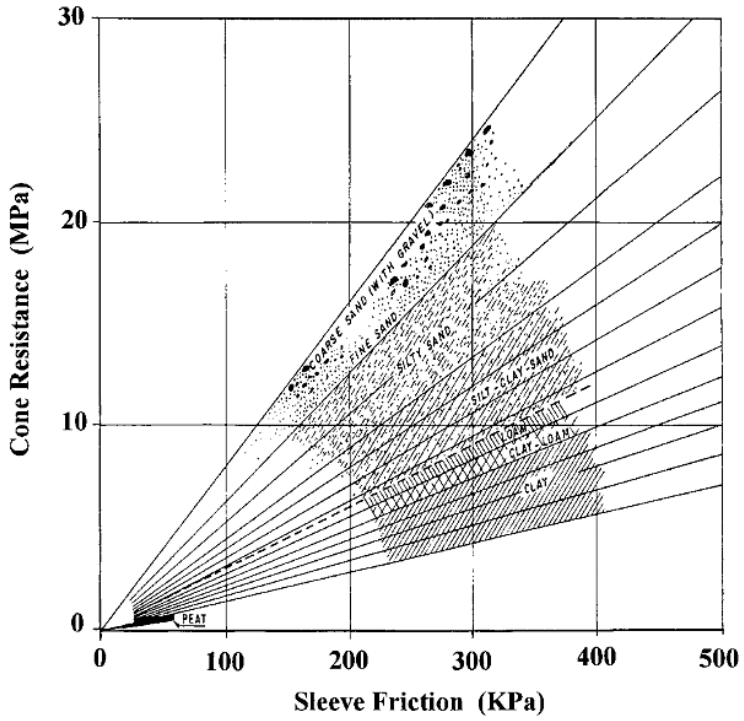

Figure 2.6: Begemann original soil profiling chart (after Begemann, 1965)

Sanglerat et al. (1974)

Sanglerat et al. (1974) developed a CPT soil classification (Figure 2.7). The chart is based on data obtained from 3.15 inch (80 mm) diameter penetrometer. The chart plots the q_c in log scale versus the F_r in linear scale. They recommended that soil type might be the function of F_r.

Schmertmann (1978) Charts

Schmertmann (1978) proposed a soil classification chart which is based on data obtained from North Central Florida (Figure 2.8). The chart specifies common soil type zones. Furthermore, it represents boundaries for different types of sands: loose and dense. The Schmertmann (1978) chart represents the q_c as a plot against the F_r like the Sanglerat et al. (1974) chart.

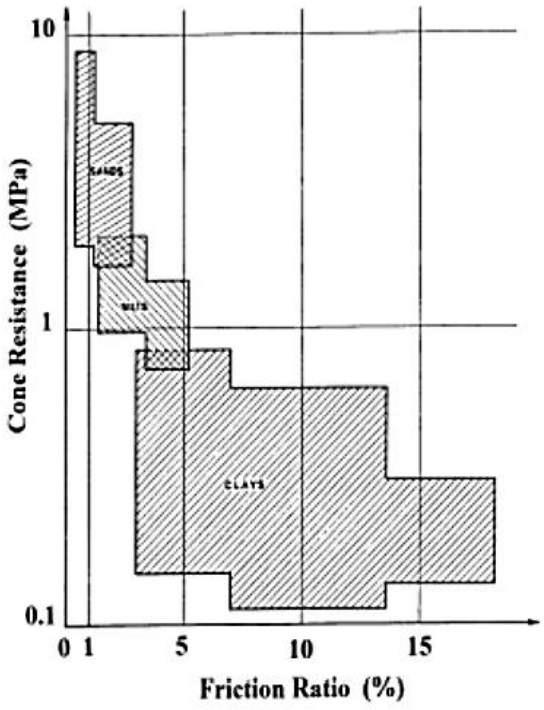

Figure 2.7: Plot of data from research penetrometer (after Sanglerat et al., 1974)

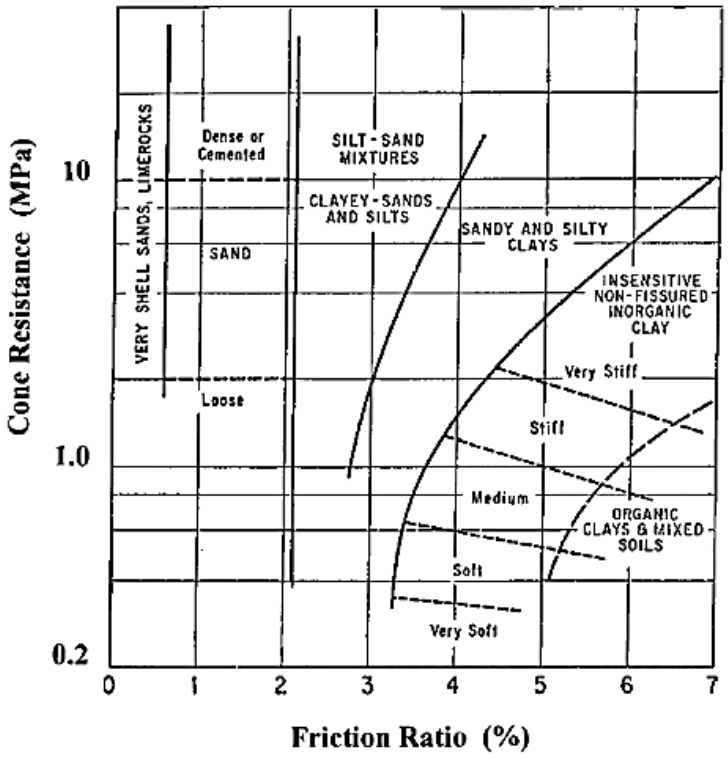

Figure 2.8: Schmertmann soil profiling chart (Schmertmann, 1978)

Douglas and Olsen (1981) Chart

Douglas and Olsen (1981) were the pioneers to analyze the electrical cone penetrometer data to classify soil. They analyzed the soil based on tge unified soil classification system (USCS) and proposed the CPT soil classification chart that represents the q_c as a plot against the F_r (Figure 2.9). This chart also incorporates liquidity index, stress condition and soil sensitivity. The upward curves represent the same f_s with an increasing percentage of coarse-grained soil. However, the sand and clay zones are almost similar to the Schmertmann (1978) chart.

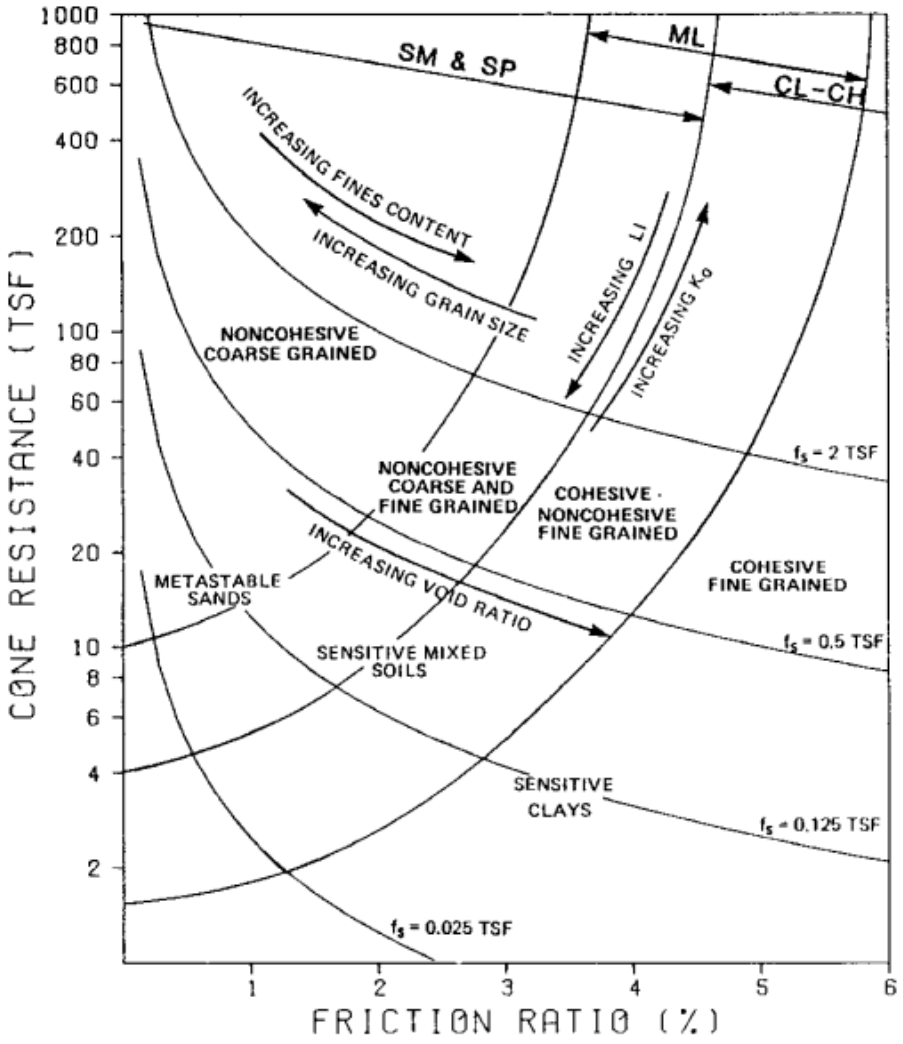

Figure 2.9: Soil profiling chart per Douglas and Olsen (1981)

Marr's method (1981)

Marr's (1981) method is one of the earliest methods to predict soil type in which, the q_c and f_s values are directly used. In this technique, a chart has been prepared with six zones that are separated by straight lines (Figure 2.10).

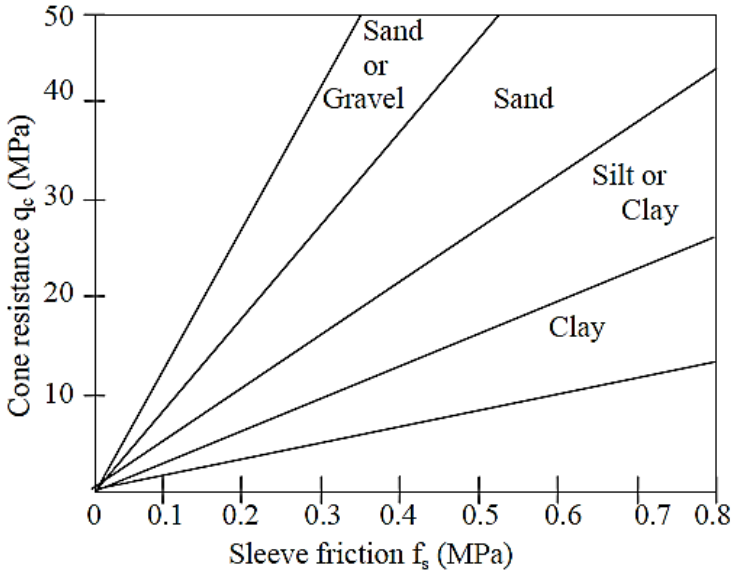

Figure 2.10: CPT based soil classification chart proposed by Marr (1981)

Vos (1982) Method

Vos (1982) developed a soil classification table based on electrical CPT on Dutch soils (Table 2.7). The table is based on the F_r. Though the F_r values are almost identical, however, they are not similar to the Begemann (1965) chart.

Table 2.7: Soil type as a function of friction ratio (Vos, 1982)

Soil type	**Friction ratio, F_r**
Coarse sand and gravel	<0.5%
Fine sand	(1.0 – 1.5)%
Silt	(1.5 – 3.0)%
Clay	(3.0 – 5.0)%
Clay	(4.1 – 7.0)%
Peat	>5.0%

Jones and Rust (1982) Chart

Based on the PCPT, Jones and Rust (1982) developed the soil profiling (Figure 2.11). They developed the chart by measuring q_c and Δu mobilized during cone penetration. The chart represents the Δu as a plot against the net cone resistance, q_c-σ_{vo}. The chart can identify the density or consistency of soil. However, this chart is not suitable for very soft clays where dilatancy can occur due to high negative pore water pressure generation.

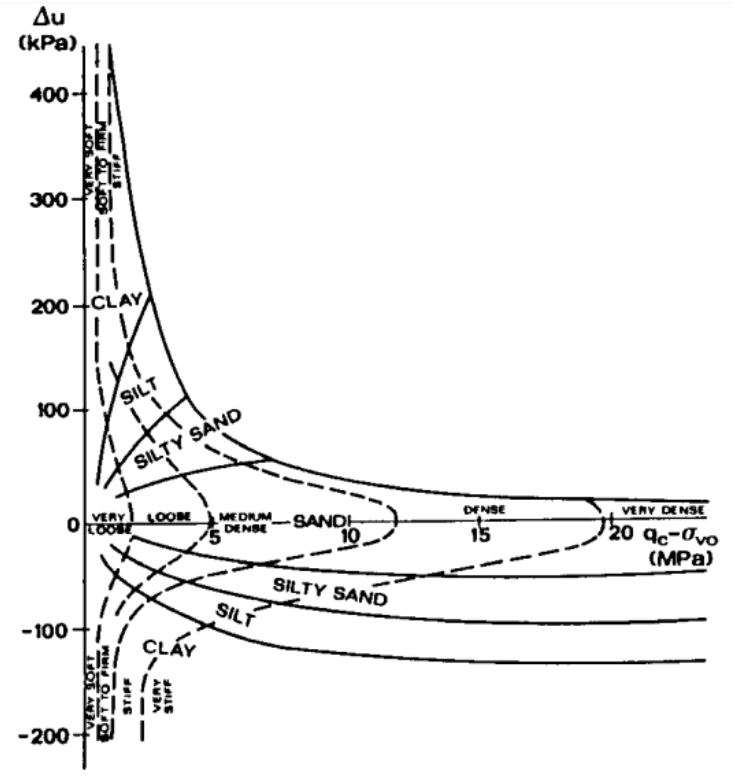

Figure 2.11: Soil profiling chart per Jones and Rust (1982)

Robertson and Campanella (1983) Chart

Robertson and Campanella (1983) proposed a simplified CPT soil classification chart. The chart represents the q_t (log scale) as a plot against the F_r and demonstrates five major soil zones (Figure 2.12).

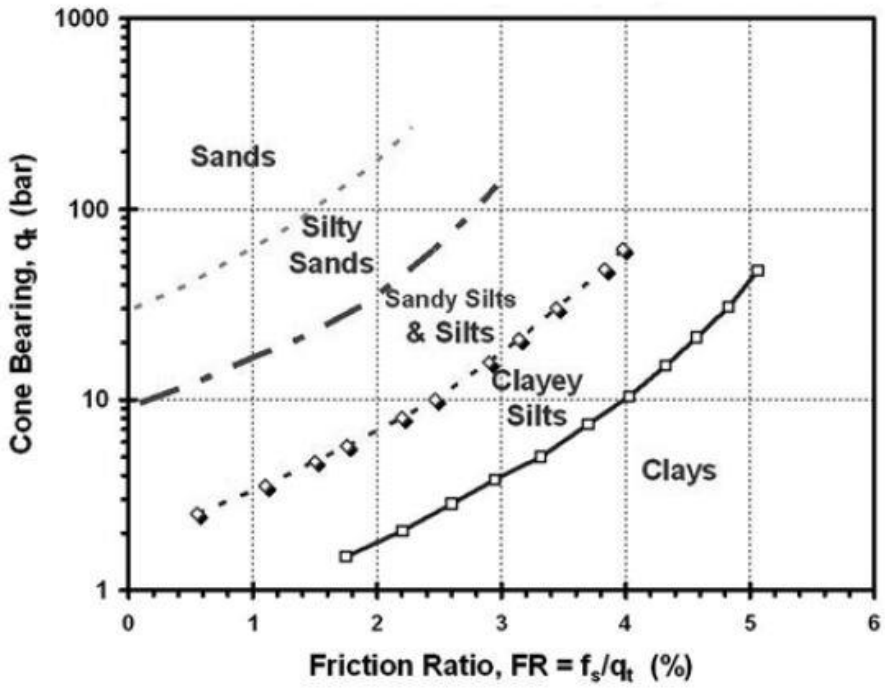

Figure 2.12: Simplified CPT soil classification chart (Robertson and Campanella, 1983)

Modified Schmertmann Chart by Tumay (1985)

Tumay (1985) modified the Schmertmann (1978) chart by incorporating Douglas and Olsen (1981) chart in it (Figure 2.13). This modified chart gives more details of soil types.

Robertson et al. (1986) Charts

Robertson et al. (1986) introduced the first soil behavioral type (SBT) classification charts which, uses the basic PCPT measurements of q_t versus f_s and q_t versus B_q. According to these charts, there are 12 major type soil zones and each zone behaves differently (Figure 2.14). The chart has one great advantage. It can be used instantly after the PCPT to classify soil, as it only requires the basic PCPT parameters.

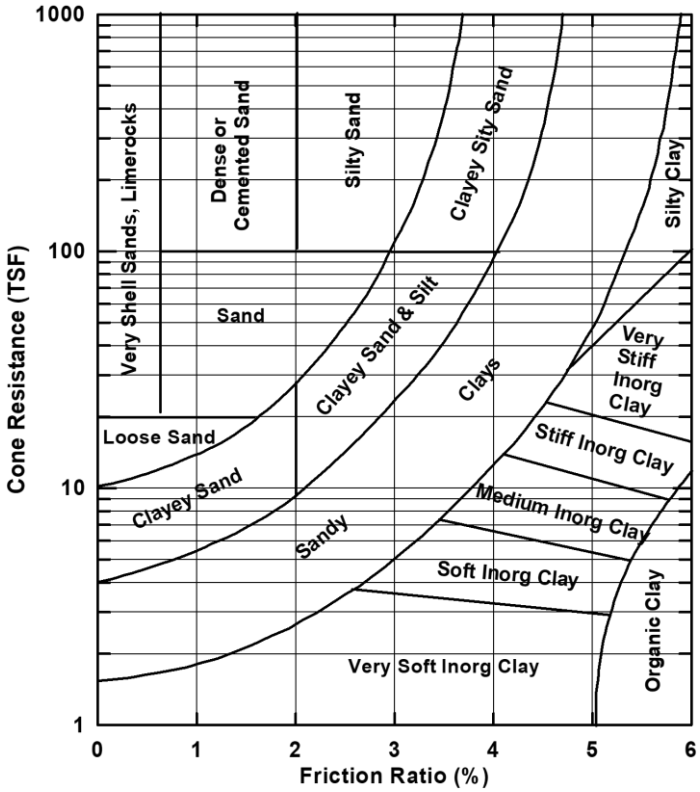

Figure 2.13: Modified Schmertmann (1978) Chart by Tumay (1985)

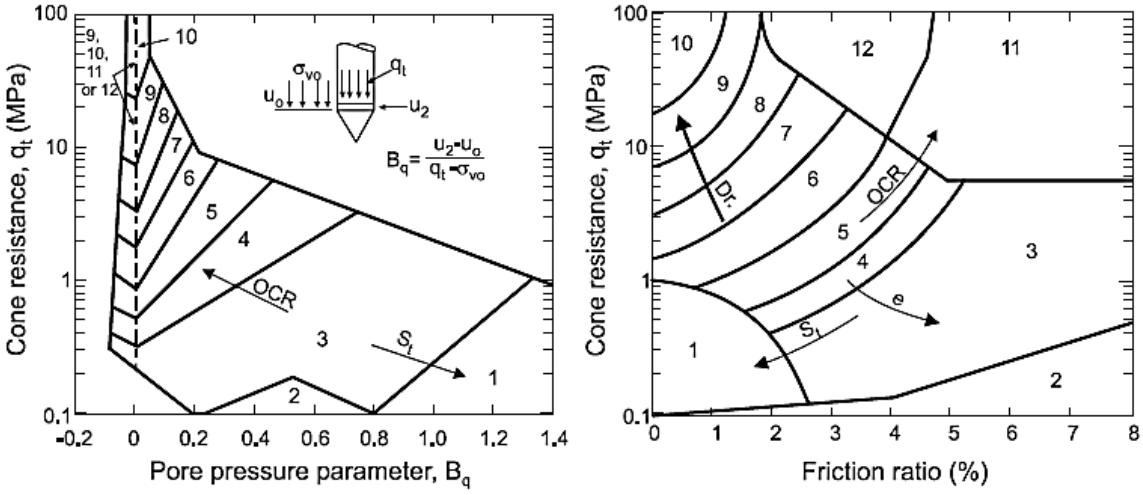

Zone:	Soil Behaviour Type:				
1.	Sensitive fine grained	5.	Clayey silt to silty clay	9.	Sand
2.	Organic material	6.	Sandy silt to clayey silt	10.	Gravelly sand to sand
3.	Clay	7.	Silty sand to sandy silt	11.	Very stiff fine grained*
4.	Silty clay to clay	8.	Sand to silty sand	12.	Sand to clayey sand*

** Overconsolidated or cemented.*

Figure 2.14: Soil behavior type classification chart (Robertson et al., 1986)

Senneset et al. (1989) Chart

Based on q_t and B_q parameters, Senneset et al. (1989) developed a chart (Figure 2.15). However, the chart is valid for some specific conditions. For example, the chart is valid when q_t < 167 tsf (16 MPa).

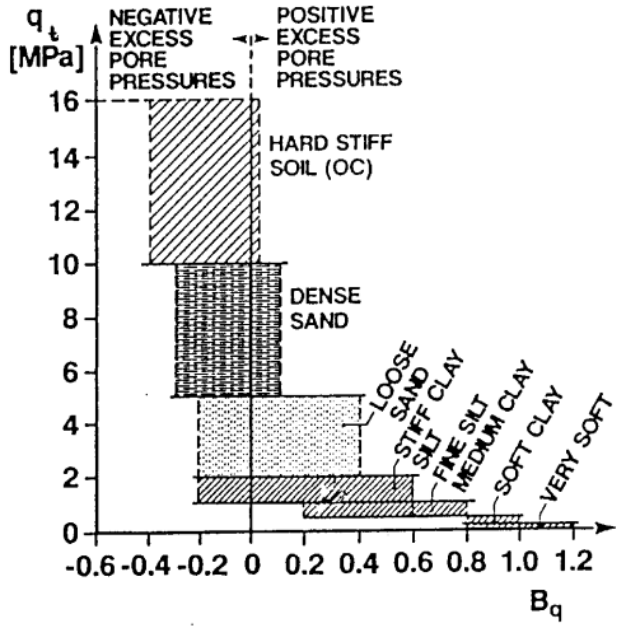

Figure 2.15: Profiling chart per Senneset et al. (1989)

Olson and Mitchell (1995) Chart

Olsen and Mitchell (1995) introduced a method for q_c and f_s normalization with an exponent component (Figure 2.16). For normalization, they used in-situ and laboratory soil data for different soil types. Normalization of q_c and f_s are defined as:

$$q_{c,1} = C_q * q_c \qquad (2.36)$$

$$f_{s,1} = C_f * f_s \qquad (2.37)$$

where $C_q = \left(\frac{Pa}{\sigma_v'}\right) * c$ and $C_f = \left(\frac{Pa}{\sigma_v'}\right) * s$, Pa is atmospheric pressure, c and s are tip and sleeve normalization exponents respectively, C_q and C_f are normalizing factors, and $q_{c,1}$ and $f_{s,1}$ are

normalized tip and sleeve resistances respectively. However, based on Olsen's work, Moss et al. (2006) proposed equations (2.38 and 2.39) for tip resistance (Q) and friction (F_r) normalization:

$$Q = \frac{q_t - \sigma_{v0}}{\sigma_{v0}'} \quad (2.38)$$

$$F_r = \frac{f_s}{q_t - \sigma_{v0}} * 100 \quad (2.39)$$

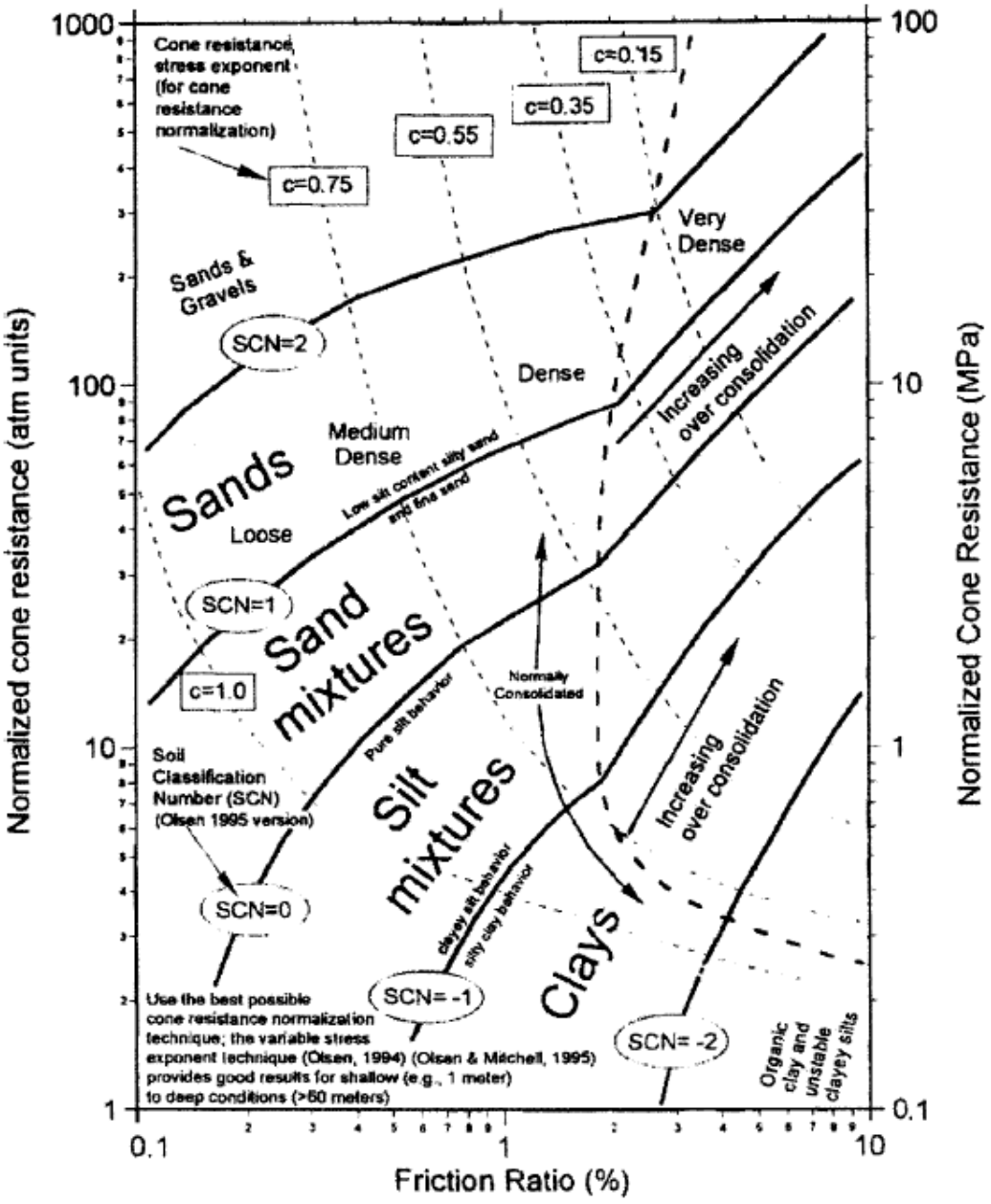

Figure 2.16: CPT normalization from Olsen and Mitchel (1995)

Eslami and Fellenius (1997) Chart

Eslami and Fellenius (1997) developed a soil classification method during studying the application of CPT for pile designs. The chart is based on q_E and f_s (non-normalized). They incorporated five soil zones in the soil classification chart (Figure 2.17). However, the chart does not perform well for cemented soils or very stiff clays.

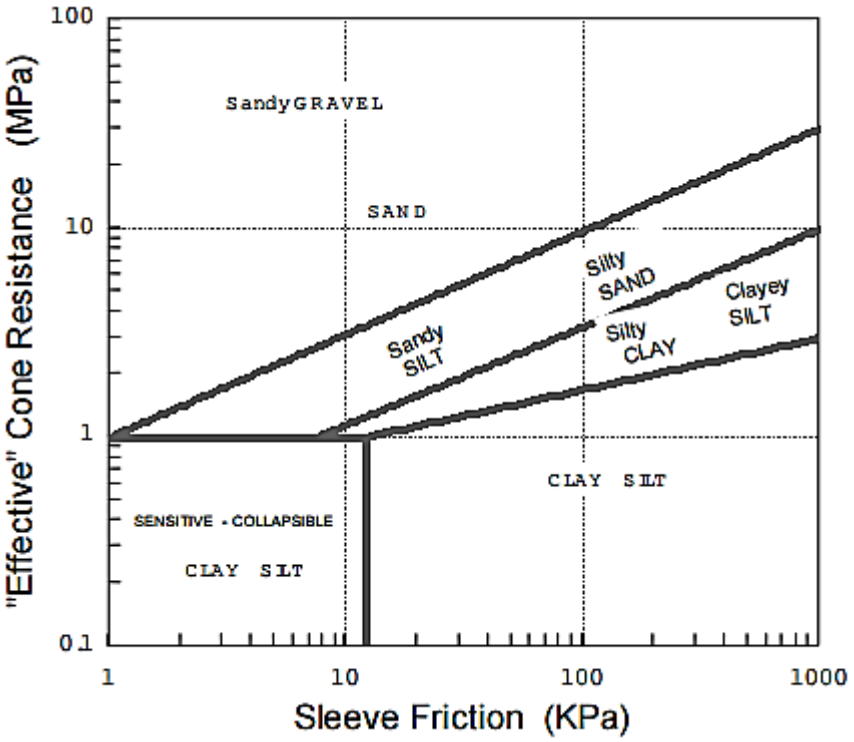

Figure 2.17: Soil profile chart (After Eslami and Fellenius, 1997)

Robertson (1990) Charts

A popular PCPT based SBT chart is first suggested by Robertson (1990) using 3 normalized parameters: Q, F_r and B_q (Figure 2.18). This chats have 9 zones and incorporate soil stress history, soil density and soil sensitivity. At times, soils will fall within various zones at the same time on each chart. In these cases, judgement is necessary to appropriately classify the SBT. The Q_t - B_q chart is useful to characterize soft and fully saturated soils.

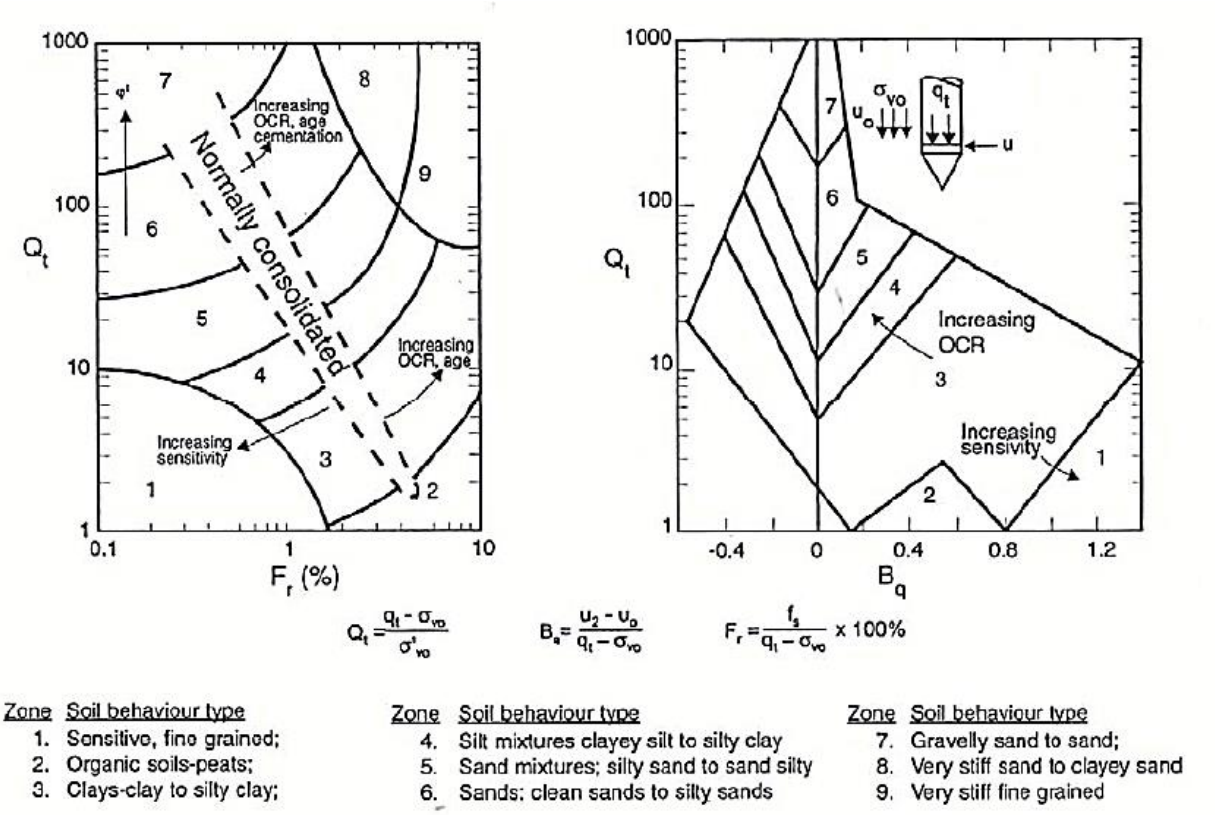

Figure 2.18: Normalized CPT SBT charts *Qt - Fr* and *Qt - Bq* (Robertson, 1990)

2.5.2 Soil Behavior Type Index

Jefferies & Davies (1993) introduced the soil behavior type index, I_c. Jefferies & Davies (1993) classified soils based on I_c values (Table 2.8). I_c can define the soil behavior type zones in the Q_t–F_r chart. I_c defines the boundaries of soil type. I_c is nothing but the radius of concentric circles. Robertson and Wride (1998) developed an equation to calculate I_c from PCPT:

$$I_c = [(3.47 - \log Q_t)^2 + (\log F_r + 1.22)^2]^{0.5} \qquad (2.40)$$

The non-normalized SBT index, I_{SBT} is essentially the same as the normalized SBTn index (I_c) however only uses the basic CPT measurements. I_{SBT} can also be defined by:

$$I_{SBT} = [(3.47 - \log(q_c/p_a))^2 + (\log R_f + 1.22)^2]^{0.5} \qquad (2.41)$$

Generally, the normalized I_c provides more reliable identification of SBT than the non-normalized I_{SBT}. However, if the field vertical effective stress is between 50 kPa to 150 kPa, then there is usually a slight difference between normalized and non-normalized SBT (Robertson 2010).

Table 2.8: SBT zones based on I_c (After Jefferies et el., 1993)

Soil classification	Zone no.*	Range of CPT Index *I_c values
Organic clay soils	2	$I_c > 3.22$
Clays	3	$2.82 < I_c < 3.22$
Silt mixtures	4	$2.54 < I_c < 2.82$
Sand mixtures	5	$1.90 < I_c < 2.54$
Sands	6	$1.25 < I_c < 1.90$
Gravelly sands	7	$I_c < 1.25$

*Notes: Zone number in according to Robertson (1990) SBT. Zone 1 is for soft to sensitive soils having similar I_c values to zones 2 or 3, and low friction F_r < 1%

Robertson (2009) Chart

Robertson (2009) incorporated I_c in his previous chart and developed a new soil classification chart. This chart is also a normalized 9 zone SBT chart (Figure 2.19 b). Zone 1 is sensitive fine-grained soil zone and the equation for this zone is:

For zone 1: $Q_{tn} < 12 \exp(-1.4 F_r)$ (2.42)

On the other hand, zone 8 and 9 are stiff soils and can be found:

For zones 8 and 9: $Q_{tn} > [1 / \{0.005 (F_r - 1) - 0.0003 (F_r - 1)^2 - 0.002\}]$ (2.43)

After detecting zones 1, 8, and 9, the soil behavior type index, I_c can subsequently be used to assign zones 2 through 7 accordingly.

Robertson (2010a) Chart

The non-normalized Robertson et al. (1986) chart has 12 defined SBT zones and the normalized Robertson (1990) chart has 9 defined SBT zones. Due to this difference, some confusions created in the past. Hence, it directed Robertson (2010) to update the charts. The updated SBT chart is shown in Figure 2.19(a). The updated chart simplified and color-coded for better understanding,

and these have 9 defined SBT zones. The updated charts have a defined zone for normally consolidated soil. This chart uses the basic CPT parameters: q_t normalized with respect to atmospheric pressure and F_r. This chart can categorize soil satisfactorily up to about 60ft (20m) depth.

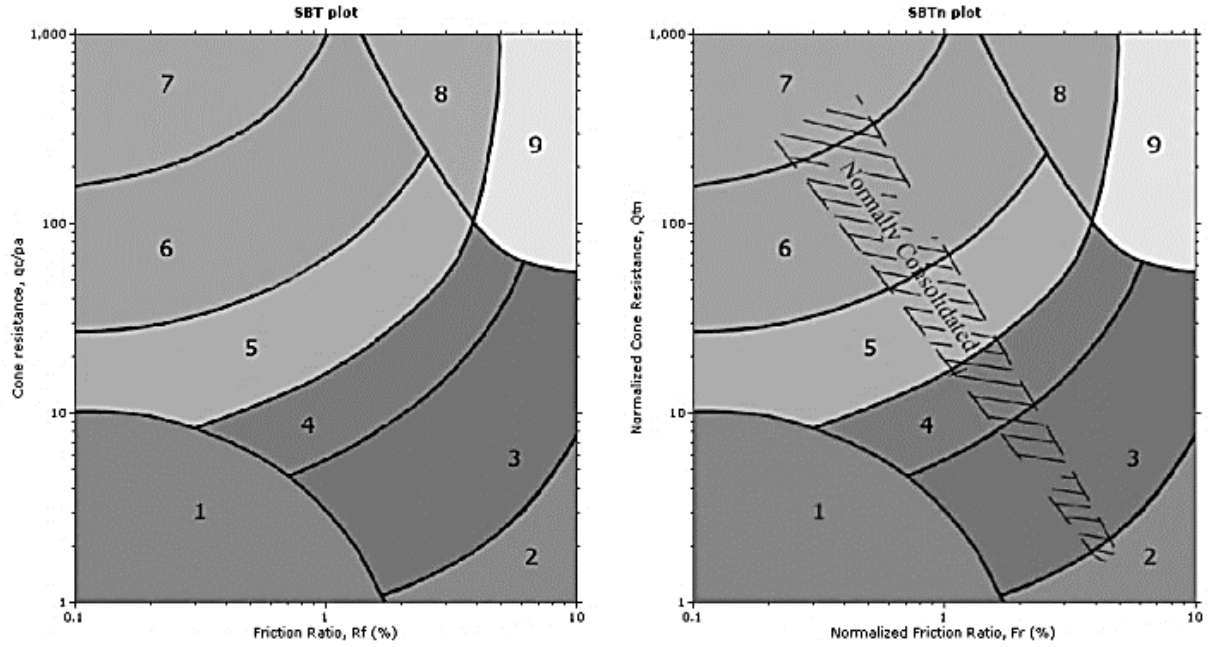

SBT zone	Proposed common SBT description
1	*Sensitive fine-grained*
2	*Clay - organic soil*
3	*Clays: clay to silty clay*
4	*Silt mixtures: clayey silt & silty clay*
5	*Sand mixtures: silty sand to sandy silt*
6	*Sands: clean sands to silty sands*
7	*Dense sand to gravelly sand*
8	*Stiff sand to clayey sand**
9	*Stiff fine-grained**

(a) (b)

Figure 2.19: (a) simplified Robertson (2010) chart and (b) normalized Robertson (2009) chart

Schneider et al. (2008) Chart

Schneider et al. (2008) incorporated pore water pressure measurements into the PCPT soil classification chart. They used Q versus the porewater pressure parameter $U^* = \Delta u_2/\sigma_{vo}'$ to classify SBT zones (Figure 2.20). They assessed undrained, partially-drained, to fully-drained soil conditions (Figure 2.20) to further investigate the soil. However, Schneider et al (2008) chart may not be usable for onshore projects where the pore water measurements are not reliable. Yet, the chart performs well for offshore conditions. The chart mainly highlights clay soils where Q is considerably small.

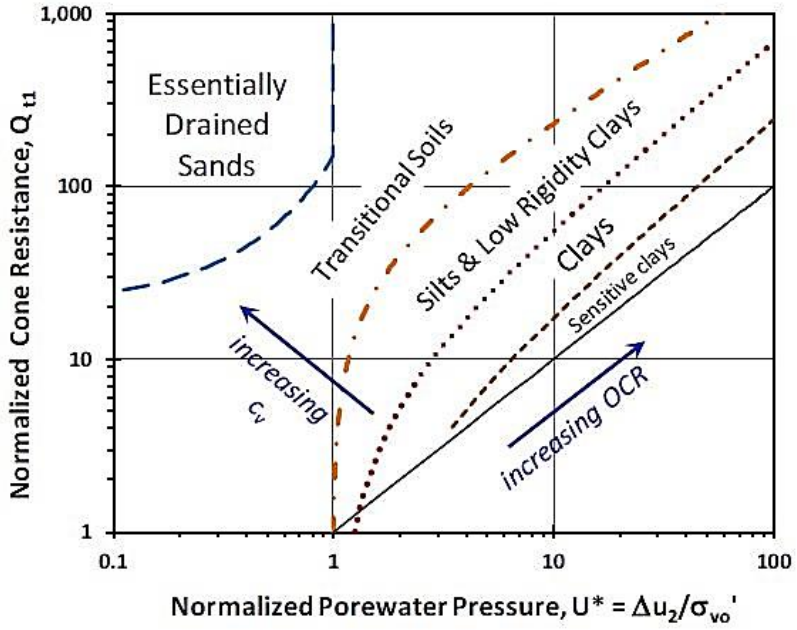

Figure 2.20: CPT indirect classification for soil behavioral type from Q_{t1}-Δ_{u2}/σ_{vo}' chart

Robertson (2012) Chart

Robertson (2012) introduced drainage condition, contractive and dilative soil behavioral zones in his previous soil chart. Soils are identified as either dilative or contractive (Figure 2.21).

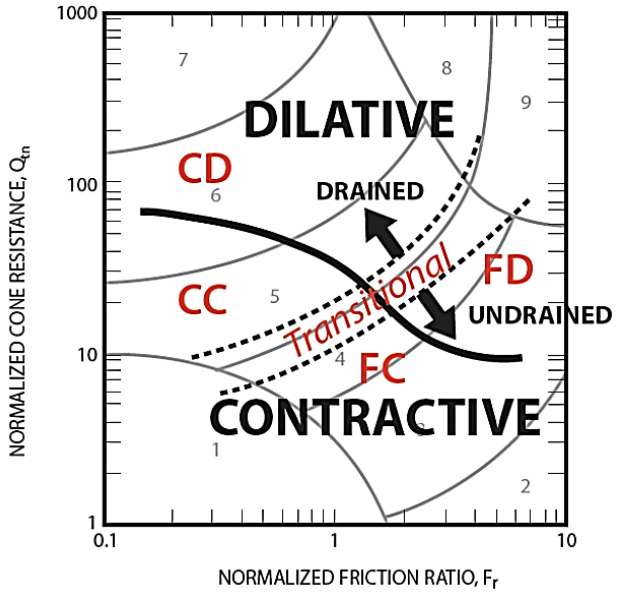

Figure 2.21: Normalized CPT SBT chart (Modified from Robertson, 2012)

Schneider et al. (2012) Chart

Schineder et al. (2012) updated his previous chart (2008) by incorporating Q and u_2 data from PCPT (Figure 2.22). They also included the normalized friction ratio, F_r in this chart. The Q–F_r classification charts are useful when high-quality pore water pressure data are absent.

Robertson (2016) Charts

Robertson (2016) introduced a Q–F_r based soil classification chart that can differentiate ideal soils that are either contractive or dilative (Figure 2.23). The equation for contractive–dilative (*CD*) boundary:

$$CD = 70 = (Q_{tn} - 11)\,(1 + 0.06F_r)^{17} \qquad (2.44)$$

The soils are dilative when $CD > 70$. The lower limit for ideal soil can be defied by:

$$CD\ (lower\ bound) = 60 = (Q_{tn} - 9.5)\,(1 + 0.06F_r)^{17} \qquad (2.45)$$

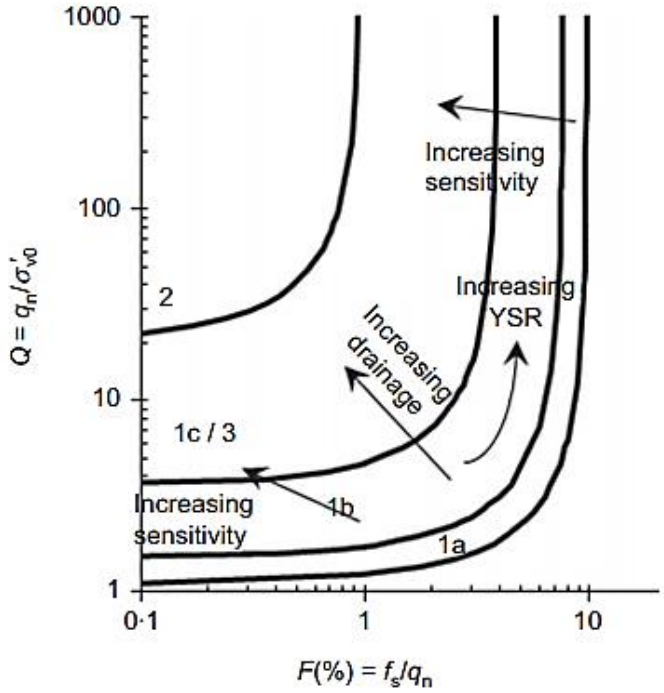

Figure 2.22: *Q–F* classification chart(Robertson et. al, 2012)

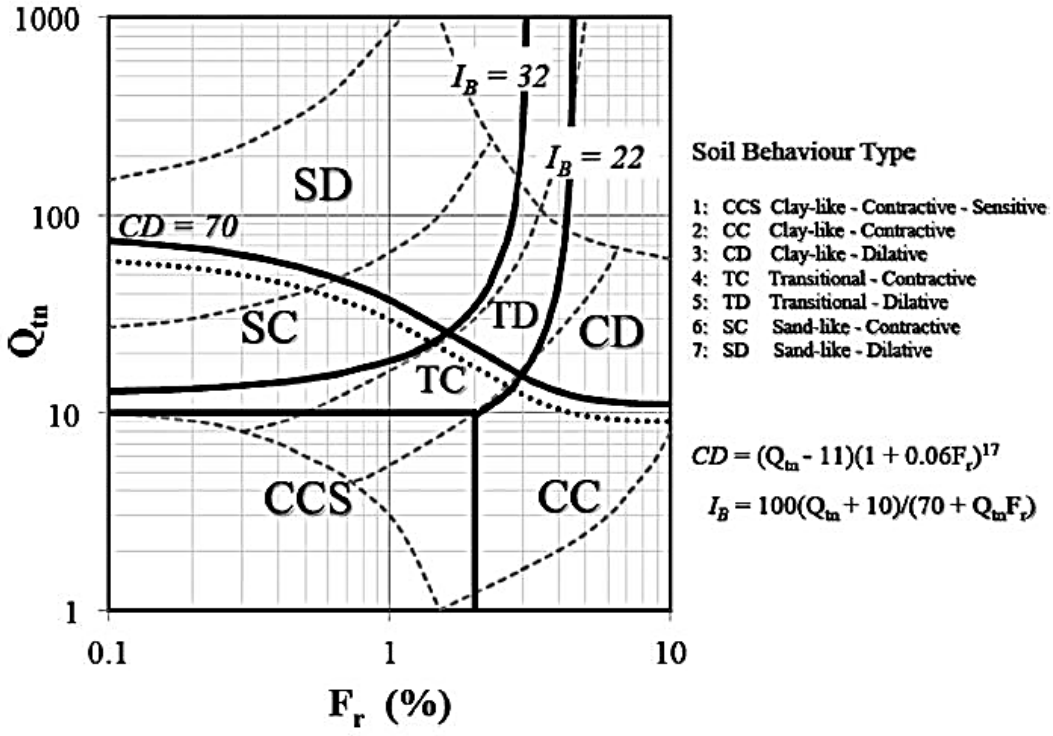

Figure 2.23: Updated SBTn chart based on Q_{tn} - F_r (After Robertson, 2016)

However, according to Robertson and Wride (1998), the simple circular shape of I_c is not always best to define soil zones. To reshape the SBT boundaries, Schneider et al. (2012) had recommended a hyperbolic shape using a modified soil behavior type index, I_B:

$$I_B = 100(Q_{tn} + 10)/(Q_{tn}F_r + 70) \quad (2.46)$$

$I_B = 32$ represents the lower boundary for most sand like ideal soils and $I_B = 22$ represents the upper boundary for most claylike ideal soils. $I_B = 22$ represents the fine-grained ideal soils with $I_p \approx 18\%$. Robertson (2016) updated the Schineder et. al (2012) chart as Q_{tn}–U_2 and it is based on I_B (Figure 2.24). This chart also provides an assessment of possible microstructure.

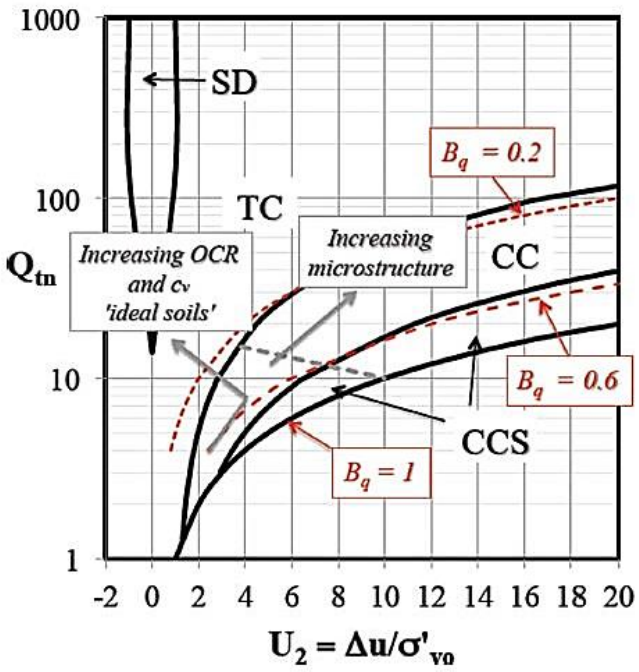

Figure 2.24: Updated Schneider (2008) chart based on $Q_{tn} - U_2$ (After Robertson, 2016)

Saye et al. (2017) Chart

Saye et al. (2017) suggested a soil chart based on Q_t–f_s/σ'_{vo} space (Figure 2.25). They observed a linear relationship with the slope of Δ_Q:

$$\Delta_Q = (Q_t+10)/[(f_s/\sigma'_{vo}) + 0.67] \quad (2.47)$$

The Δ_Q index provides a numerical value that can be linked to soil index and engineering properties. The increasing Δ_Q values indicate the soil as sandy soil. On the other hand, a decreasing trend of Δ_Q indicates the soil as clayey soil.

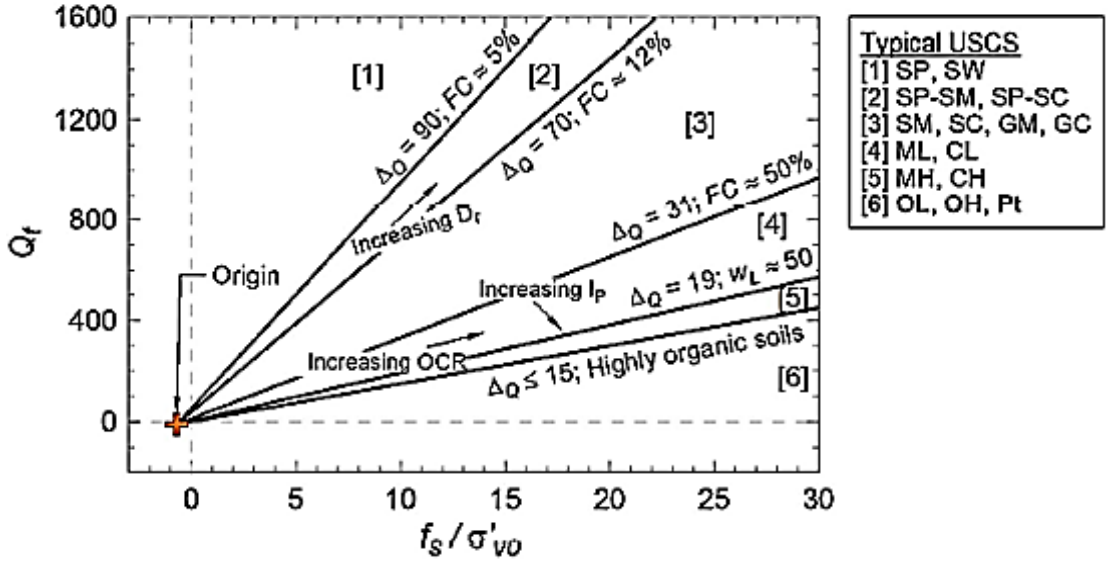

Figure 2.25: Saye et al. (2017) chart based on Q_t–f_s/σ'_{vo}.

2.5.3 Probabilistic Region Estimation Method

Sometimes, the traditional CPT soil classification charts incorrectly identify soil types, especially in transition zones. It encouraged the establishment of the probabilistic region estimation method. The probabilistic method of CPT soil classification addresses the uncertainty of soil types. Conformal mapping was conducted on the Douglas and Olsen (1981) chart. It transformed the chart axis from the CPT data (e.g., q_c, F_r) into the soil classification index (U) by following equations:

$$x = 0.1539\ R_f + 0.8870\ \log q_c - 3.35 \tag{2.48}$$

$$y = -0.2957\ R_f + 0.4617\ \log q_c - 0.37 \tag{2.49}$$

$$U = \frac{(a_1x - a_2y + b_3)\,(c_1x - c_2y + d_3)}{(c_1x - c_2y + d_3)^2 + (c_2x + c_1y + d_2)^2} - \frac{(a_2x + a_1y + b_2)\,(c_2x - c_2y + d_1)}{(c_1x - c_2y + d_1)^2 + (c_2x + c_1y + d_2)^2} \tag{2.50}$$

Then, a statistical correlation was developed between the *U* index and the compositional soil by the USCS (GP, SP, SM, SC, ML, CL, and CH) as shown in Table 2.9. The soil types were again rearranged into three main groups, such as sandy and gravelly soils (GP, SP, and SM), silty soils (SC and ML) and clayey soils (CL and CH) depending on the probability distribution of *U* index (Figure 2.26).

Table 2.9: Soil types from Unified Soil Classification System (Standard 1992)

Symbol	Soil type index (SI)	Typical names
GP	1	Poorly graded gravels, gravel-sand mixtures, little or no fines
SP	2	Poorly graded sands, gravelly sands, little or no fines
SM	3	Silty sands, poorly graded sand-silt mixtures
SC	4	Clayey sands, poorly graded sand-clay mixtures
ML	5	Inorganic silts and very fine sands, rock flour, silty or clayey fine sands with slight plasticity
CL	6	Inorganic clays of low to medium plasticity, gravelly clays, sandy clays, silty clays, lean clays
CH	7	Inorganic clays of high plasticity, fat clays

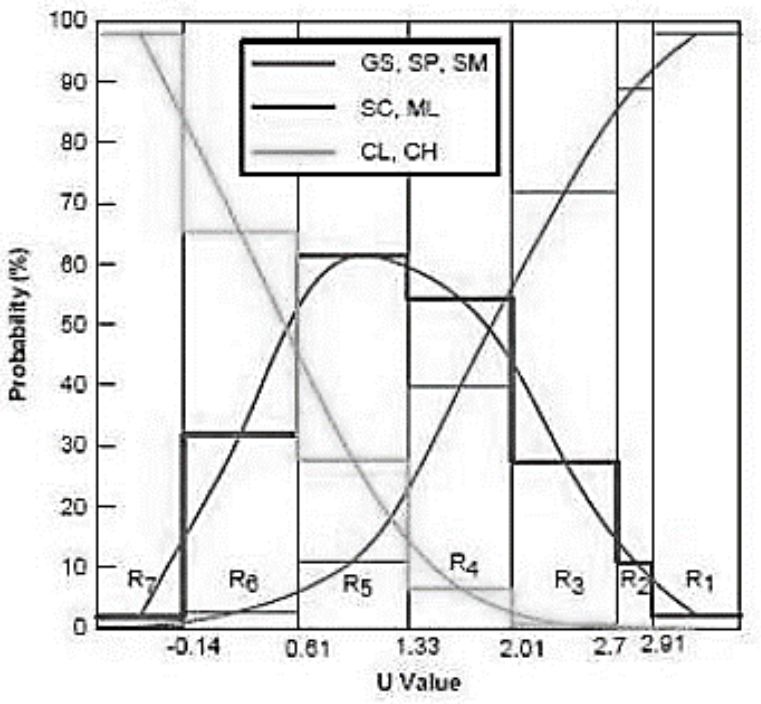

Figure 2.26: Soil groups based on U index value

2.5.4 Fuzzy Approach

Zhang and Tumay (1996) checked the accuracy of CPT classification through probabilistic region estimation method. A fuzzy approach was introduced (Pradhan, 1998; Zhang and Tumay, 1999). Based on fuzzy logic, Zhang and Tumay (1999) introduced a CPT based soil classification method. The results of Zhang and Tumay (1999) method are expressed in percentage probability for sand, silt, or clay. Three soil types are defined in the CPT based fuzzy soil classification system. They are Highly Probable Sandy soil (HPS), Highly Probable Mixed soil (HPM), and Highly Probable Clayey soil (HPC). The fuzzy membership functions are defined as (Zhang, 1994):

$$\mu_C(U) = \begin{cases} exp\left(-\frac{1}{2}\left(\frac{U+0.1775}{0.86332}\right)^2\right) & U \geq -0.1775 \\ 1.0 & U < -0.1775 \end{cases} \quad (2.51)$$

$$\mu_m(U) = exp\left(-\frac{1}{2}\left(\frac{U-1.35}{0.724307}\right)^2\right) \qquad -\infty < U < \infty \quad (2.52)$$

$$\mu_S(U) = \begin{cases} 1.0 & U > 2.6575 \\ exp\left(-\frac{1}{2}\left(\frac{U-2.6575}{0.834586}\right)^2\right) & U \leq 2.6575 \end{cases} \quad (2.53)$$

These equations represent bell-shaped curves with the highest function value of 1.0 for individual soil type (Figure 2.27). These empirical functions reflect an overall perspective of soil properties. This method is similar to the classic soil classification methods and somewhat dependent on soil structure (Zhang and Tumay, 1999).

2.5.5 Other Approaches

Mayne et al. (2002) introduced the rule of thumbs for estimating soil types from CPT. According to Mayne et al. (2002), if $q_t>40$ tsf, it is sand, while for some soft to stiff clays and silts, $q_t<20$ tsf. In fussed clays and silts, the shoulder porewater readings can be zero or negative (≥-1 tsf) (Mayne et al. 1990). Hegazy et al. (2002) suggested a statistical analyses method named cluster analyses

to classify soil. To estimate soil composition from PCPT, Kurup and Griffin (2006) examined the possibilities of regression-based artificial neural network (ANN). Das and Basudhar (2009) suggested their self-developed soil charts and fuzzy clustering method to classify stratified soil from PCPT. Jung et al. (2008) and Cetin and Ozan (2009) also proposed CPT based probabilistic soil classification methods. Abu-Farsakh et al. (2008) introduced CPT-based soil classification system using MS-Windows and Visual Basic operating software.

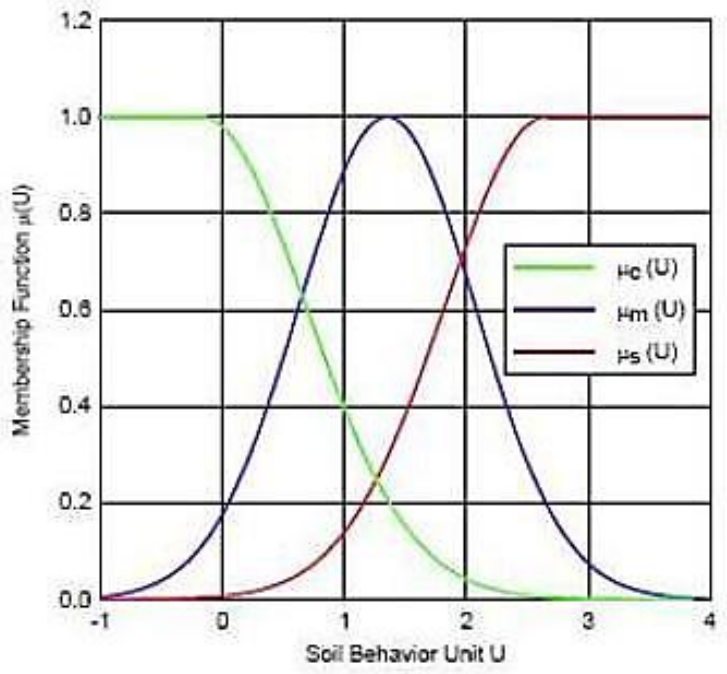

Figure 2.27: CPT Fuzzy classification chart (After Zhang, 1994)

CHAPTER 3
PIEZOCONE AND BORELOG DATABASE

This chapter would provide a brief overview of the piezocone test sites and bore logs. Moreover, this chapter discusses the summary of the in-situ and laboratory test results. 70 test sites were selected in 14 different parishes of Louisiana to conduct in-situ and laboratory tests for the measurement of unconsolidated undrained shear strength and soil classification. Additionally, 11 different PCPT sites were selected to set up a criterion for tip resistance correction where excess pore water pressure measurements were not available with the cone. All the CPT/PCPT and borehole data were collected from the Louisiana Department of Transportation and Development (LADOTD).

3.1 Methodology

The main objective of this study was to estimate the unconsolidated undrained shear strength of the soil layers and to classify the soil type from CPT/PCPT data. Therefore, laboratory tests were performed on the collected Shelby tube soil samples for each site. Besides, in-situ field tests (CPR/PCPT) were conducted to evaluate the soil properties. This section will briefly describe the laboratory and in-situ soil investigation programs.

3.1.1 Laboratory Tests

The laboratory testing program involves retrieving high-quality Shelby tube samples in each site from boreholes at different depths. Basic soil characterization tests such as water content, unit weight, Atterberg limits, grain size distribution and specific gravity were carried out in accordance with ASTM standards D 4643, D 7263, D 4318 and D 422, respectively, to characterize the subsurface soils. In addition, triaxial unconsolidated undrained tests were performed in accordance with ASTM standards D 2850-03a to evaluate the undrained shear strength, s_u, of the soil.

3.1.2 In-Situ Tests

The in-situ test program includes performing cone or piezocone penetration tests (CPT/PCPT). Two types of CPT/PCPT system are available at the Louisiana Transportation Research Centre (LTRC). One is the 20-ton Research Vehicle for Geotechnical in-situ testing and Support (REVEGITS) and the other is the Continuous Intrusion Miniature Cone Penetration test (CIMCPT) system. REVEGITS has hydraulic pushing and levelling arrangement with electronic data acquisition system. Subtraction type Fugro piezocone penetrometer is used in this study.

At each study location, in-situ CPT/PCPT tests were performed around the drilled boreholes, using the 1.55 in^2 (10 cm^2) and 2.33 in^2 (15 cm^2) piezocone penetrometers. During a PCPT test, the piezocone was pushed into the ground at a constant rate of 0.79 in./sec (2 cm/sec). Data was collected every 2 cm (0.79 in.) interval. The 10 cm^2 (1.55 in^2) piezocone provided measurements of the q_c, f_s, and u_2. On the other hand, the 15 cm^2 (2.33 in^2) piezocone measured q_c, f_s, and u_1. In all of the PCPT tests, standard calibration process was followed as suggested by the International Society of Soil Mechanics and Foundation Engineering (ISSMFE). In this study, only 11 sites have PCPT data with pore pressure measurements. Other 70 sites do not have available excess pore water pressure measurements. Figure 3.1 shows photographs of two different CPT sites for this study.

3.2 Description of the Sites

The soil deposits near Baton Rouge zone are of Pleistocene Age terrace deposits. They experienced high desiccation with time (Mayne et al. 1995). Arman and McManis (1977) suggested that these soil deposits are mostly oxidized with a reddish brown color. These deposits contain iron oxide bands (Abu-Farsakh, 2003) with no cementation. Additionally, these soils are weakened by fissure networks and random sand pockets (Mayne et al., 1995).

Figure 3.1: CPT sites

The seventy test sites are located in 14 different parishes of Louisiana, USA. The site locations are represented in Figure 3.2 in a Parish wise manner. Besides, a geologic map of Louisiana is presented in Figure 3.3. It is clear that the soils from Assumption Parish, Iberia Parish, Jefferson Parish, Lafourche Parish, Orleans Parish, Ouachita Parish, St. Mary Parish, Terrebonne Parish, and St. Charles Parish are dominant in alluvium deposits from Holocene age. However, soils from Acadia Parish, Washington Parish, Livingston Parish, Tangipahoa Parish, and Madison Parish are dominant in terraces deposits from Pleistocene age.

A brief overview of seventy investigated test sites and soil laboratory tests result is represented in the following sub-sections. The sub-sections are organized in a location wise (Parish wise) manner. The laboratory soil test data and CPT data are presented in Appendix A.

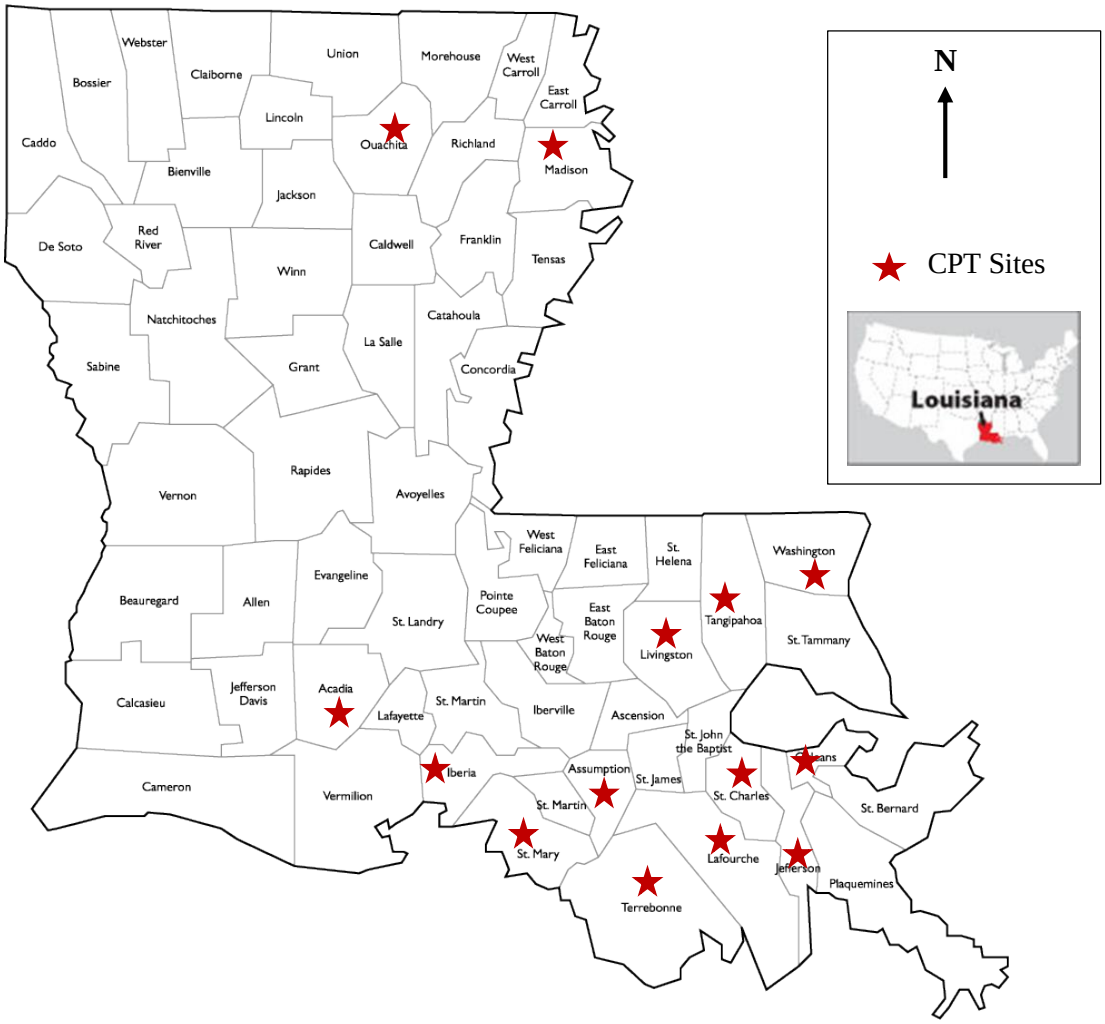

Figure 3.2: Selected CPT locations

3.2.1 Jefferson Parish

The site is located in Jefferson. Bore log and CPT's were done in two different, one in BNSS overpass – Jennings location and another one in I-10 Williams Boulevard Interchange. Three CPT's and adjacent borings were done in I-10 Williams Boulevard Interchange. In contrast, one CPT and boring were done in BNSS overpass - Jennings location. The average drilled depth for borehole for these sites is up to 125 ft. (38 meters) and the water table starts from 5 ft. (1.5 meters) from the ground. Summary of the bore log, laboratory test result and CPT data is presented in Table 3.1.

Table 3.1: Summaries of soil properties for Jefferson Parish

Sites	Unit weight (tsf)	Moisture content (%)	Liquid Limit (%)	Plasticity Index (%)	s_u (tsf)	q_c (tsf)	f_s (tsf)	Cone factor
BNSS Overpass - Jennings	0.053-0.063	23-53	27-92	05-53	0.265-1.75	7.6-24.2	0.2-1.8	5.0-21.8
I-10 Williams Boulevard Interchange TP3A	0.05-0.063	23-69	25-90	05-50	0.165-1.475	1.9-26.1	0.2-1.2	6.7-18.4
I-10 Williams Boulevard Interchange TP4A	0.04-0.065	20-105	40-94	14-53	0.145-1.64	1.0-30.9	0.2-1.3	8.3-24.6
I-10 Williams Boulevard Interchange TP5A	0.035-0.064	22-80	27-93	09-66	0.04-1.21	1.1-41.5	0.1-1.1	10.6-23.9

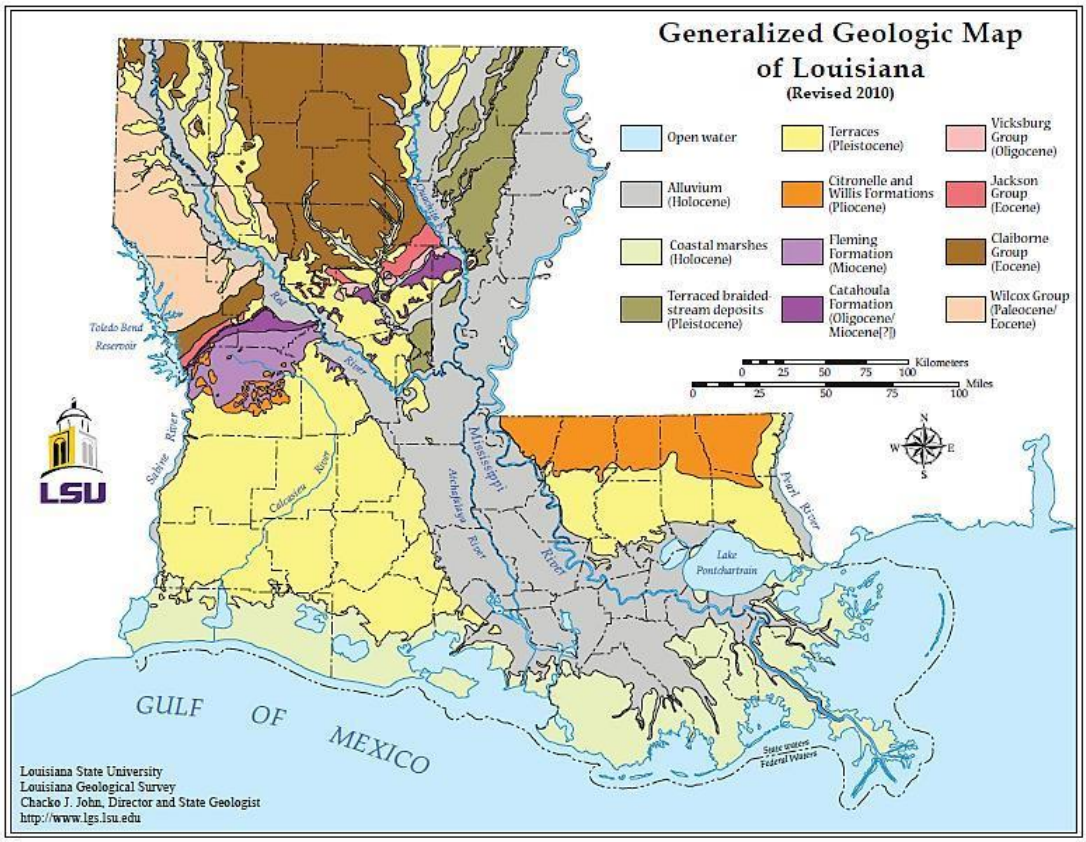

Figure 3.3: Louisiana geologic map (Louisiana Geological Survey, 2010)

3.2.2 Acadia Parish

Three CPT's and boreholes were drilled in Southern Pacific Railroad Overpass location. CPT's and consecutive boreholes were drilled in adjacent locations. The average borehole depth for these sites is 115 ft. (35 meters) and the water table starts from 10 ft. (3 meters) from the ground. Summary of the bore log, laboratory test results with CPT data are represented in Table 3.2.

Table 3.2: Summaries of soil properties for Acadia Parish

Sites	Unit weight (tsf)	Moisture content (%)	Liquid Limit (%)	Plasticity Index (%)	s_u (tsf)	q_c (tsf)	f_s (tsf)	Cone factor
Southern Pacific Railroad Overpass TP1	0.052-0.063	23-60	31-100	08-59	0.49-0.375	14.0-255.0	0.4-2.7	11.3-24.2
Southern Pacific Railroad Overpass TP2	0.05-0.065	18-50	32-82	11-46	0.185-2.205	13.7-106.3	0.3-1.4	5.8-23.6
Southern Pacific Railroad Overpass TP3	0.052-0.064	20-57	06-89	05-51	0.175-1.065	13.7-94.7	0.3-1.4	16.3-24.1

3.2.3 St. Mary Parish

Total fourteen CPT's and boreholes were drilled in St. Mary Parish location. Two CPT's at Southern Pacific railroad overpass, two CPT's at CWW Bridge Approaches, four CPT's Bayou Boeuf Bridge (West Approach) and six CPT's at Morgan City - Gibson Highway. Corresponding boreholes were also drilled in the adjacent location to every CPT's. The average borehole depth for Southern Pacific railroad overpass location is 120 ft. (36.6 meters), with average groundwater table depth of 10 ft. (3 meters). This location has verities of soils, e.g., sandy soils, silty soils, and clayey soils. Summary of the bore log, laboratory test results with CPT data is presented in Table 3.3.

Table 3.3: Summaries of soil properties for St. Mary Parish

Sites	Unit weight (tsf)	Moisture content (%)	Liquid Limit (%)	Plasticity Index (%)	s_u (tsf)	q_c (tsf)	f_s (tsf)	Cone factor
Southern Pacific Railroad Overpass TP1	0.052-0.062	33-50	27-70	6-38	0.23-0.495	6.7-24.6	0.3-0.8	9.7-23.7
Southern Pacific Railroad Overpass TP3	0.052-0.061	25-56	26-91	3-62	0.215-1.035	5.0-105.4	0.3-1.2	7.6-21.0
CWW Bridge Approaches TP3	0.054-0.067	19-74	36-98	14-65	0.229-0.233	3.7-36.1	0.2-1.5	6.4-19.9
CWW Bridge Approaches TP4	0.048-0.064	25-72	25-96	04-67	0.227-1.667	3.4-160.8	0.2-1.6	5.5-25
Bayou Boeuf Bridge (West Approach) TP1	0.05-0.058	34-62	35-105	5-75	0.22-0.47	5.5-151.0	0.3-1.8	14.5-20.7
Bayou Boeuf Bridge (West Approach) TP2	0.055-0.082	31-93	37-89	13-61	0.21-0.35	4.4-55.7	0.3-1.1	10.1-24.2
Bayou Boeuf Bridge (West Approach) TP3	0.055-0.06	29-60	39-70	19-51	0.12-0.47	6.6-13.9	0.2-0.4	14-24.9
Bayou Boeuf Bridge (West Approach) TP4	0.05-0.058	34-62	35-105	5-75	0.22-0.47	5.2-89.6	0.2-1.2	10.2-15.9
Morgan City - Gibson Highway TP1	0.045-0.061	33-97	48-91	17-47	0.205-0.83	5.6-100.6	0.216-2.5	10.5-24.1
Morgan City - Gibson Highway TP2	0.053-0.059	24-60	34-79	8-54	0.105-0.33	4.9-154.4	0.2-2.0	20.4-22.2
Morgan City - Gibson Highway TP3	0.053-0.059	28-46	33-51	10-29	0.36-0.555	8.1-76.8	0.3-1.4	12-18
Morgan City - Gibson Highway TP5	0.043-0.056	47-97	83-133	52-91	0.23-0.575	6.8-180.8	0.2-2.3	14.2-20.8
Morgan City - Gibson Highway TP6	0.043-0.056	27-98	46-65	24-43	0.135-0.395	6.6-221.9	0.2-2.1	20.8-25
Morgan City - Gibson Highway TP7	0.046-0.058	42-74	62-84	39-59	0.25-0.64	8.8-64.1	0.3-1.2	11.4-23.5

3.2.4 Washington Parish

One CPT and borehole was drilled in Bogue Chitto Bridge location. CPT and consecutive borehole was drilled in the adjacent location. The average borehole depth for this site is 75 ft. (22.9 meters). The water table was found 8 ft. (2.4 meters) below the ground. It seems that the clayey type soil layer is hardly found in this region. Most of the soil layers were silts or sands. Table 3.4 demonstrates the summary of the CPT test results, borehole data and laboratory test results for Washington Parish.

Table 3.4: Summaries of soil properties for Washington Parish

Sites	Unit weight (tsf)	Moisture content (%)	Liquid Limit (%)	Plasticity Index (%)	s_u (tsf)	q_c (tsf)	f_s (tsf)	Cone factor
Bogue Chitto Bridge TP3	0.053-0.059	36-57	36-97	13-60	0.25-0.87	32-254	0.4-2.3	16-25

3.2.5 Lafourche Parish

Three CPT's and boreholes were drilled in Lafourche and one PCPT and borehole was drilled near LA1 Improvements Fourchon, LA to Golden Meadow location. Excess porewater measurements were available for LA1 Improvements Fourchon site. The average borehole depth for this location is 160 ft. (48.8 meters) and the average groundwater table depth for this site is 10 ft. (3 meters). The bottom layers of these sites are sands. However, the topsoil layers of these sites are soft clays. Some silts are also found in the mid depths. Table 3.5 represents the summary of the CPT test results, borehole data and laboratory test results for Lafourche Parish.

Table 3.5: Summaries of soil properties for Lafourche Parish

Sites	Unit weight (tsf)	Moisture content (%)	Liquid Limit (%)	Plasticity Index (%)	s_u (tsf)	q_c (tsf)	f_s (tsf)	Cone factor
Bayou Lafourche Bridge and Approach TP1	0.051-0.060	28-47	32-69	9-38	0.190-0.707	2.3-235.5	0.1-2.7	10-21.8
Bayou Lafourche Bridge and Approach TP2	0.045-0.065	28-77	23-86	5-56	0.190-0.955	2.0-222.7	0.1-2.2	8.2-24.8
Bayou Lafourche Bridge and Approach TP3	0.048-0.061	28-75	25-74	9-47	0.21-0.864	2.2-225.6	0.1-2.3	10-22.2
LA1 Improvements Fourchon, LA to Golden Meadow	0.036-0.062	21-99	36-101	6-75	0.04-0.745	0.5-77.0	0.1-1.5	7.3-25.0

3.2.6 Terrebonne Parish

Total nine CPT's and boreholes were drilled in the Terrebonne Parish. Out of these nine sites, six sites are located near Houma I.C.W.W. Bridge, one is near Gibson - Chacahoula - Relocated US 90 location, one site is close to Gibson-Raceland Highway location and another one is near Intercostal Waterway Bridge. The average borehole depth for this location was 150 ft. (45.72 meters) and the average groundwater table depth was about 10 ft. (3 meters). Clayey soil layers are dominant in this region where sandy soil layers are hardly found. Summary of the boreholes, laboratory test and CPT results are presented in Table 3.6.

3.2.7 St. Charles Parish

The test site is located in St. Charles Parish. Four CPT's and boreholes were drilled in Luling Bridge (North Approach)-US61 location. The average drilled borehole depth for this site was 120 ft. (36.6 meters) and the average groundwater table starts from 12 ft. (3.7 meters) from the ground.

All types of soils are available in this location, however, clays are dominant in this region. Summary of the bore log, laboratory test and CPT results are demonstrated in Table 3.7.

Table 3.6: Summaries of soil properties for Terrebonne Parish

Sites	Unit weight (tsf)	Moisture content (%)	Liquid Limit (%)	Plasticity Index (%)	s_u (tsf)	q_c (tsf)	f_s (tsf)	Cone factor
Houma I.C.W.W. Bridges TP1	0.043-0.059	50-112	60-100	31-61	0.225-0.635	5.7-113.8	0.1-1.4	7.2-17.4
Houma I.C.W.W. Bridges TP2	0.045-0.06	31-88	35-95	12-64	0.23-0.7	1.1-58.5	0.1-1.0	9.3-18.5
Houma I.C.W.W. Bridges TP3	0.051-0.061	31-69	29-100	18-66	0.08-0.945	2.9-48.2	0.1-0.9	14.9-16.8
Houma I.C.W.W. Bridges TP4	0.048-0.061	33-81	31-90	6-67	0.125-0.96	2.9-60.3	0.1-1.3	5.9-9.6
Houma I.C.W.W. Bridges TP5	0.045-0.06	29-88	35-95	12-64	0.23-0.7	4.5-109.4	0.1-2.1	8.6-23.6
Houma I.C.W.W. Bridges TP6	0.045-0.06	31-85	32-90	8-60	0.20-0.80	2.9-48.8	0.2-1.2	8-22
Gibson - Chacahoula - Relocated US 90 TP1	0.048-0.058	38-69	35-89	8-57	0.185-0.525	5.2-18.0	0.3-0.7	7.5-24.3
Gibson-Raceland Highway TP4	0.047-0.057	24-81	35-102	10-85	0.13-0.76	3.8-24.2	0.2-0.6	6.1-19.1
Intercostal Waterway Bridge TP1	0.048-0.061	22-86	37-100	15-62	0.13-0.805	3.4-11.5	0.1-0.3	7.6-25

Table 3.7: Summaries of soil properties for St. Charles Parish

Sites	Unit weight (tsf)	Moisture content (%)	Liquid Limit (%)	Plasticity Index (%)	s_u (tsf)	q_c (tsf)	f_s (tsf)	Cone factor
Luling Bridge (North Approach)-US61 TP1	0.054-0.061	25.2-42.1	-	-	0.14-1.095	4.0-108.7	0.1-1.2	7.7-25.0
Luling Bridge (North Approach)-US61 TP2	0.056-0.06	20.2-39.1	37-60	13-39	0.2-1.005	3.6-26.2	0.1-1.3	8.1-25.0
Luling Bridge (North Approach)-US61 TP3	0.054-0.061	30.9-55.2	-	-	0.185-0.495	4.4-213.5	0.2-2.1	10-15.8
Luling Bridge (North Approach)-US61 TP8	0.043-0.065	19-85	25-100	4-68	0.035-1.445	1.5-251.0	0.1-5.2	11.0-25.0

3.2.8 Livingston Parish

Two CPT's and boreholes were performed in Tichfaw River Bridge and approach location. The average drilled depth for boreholes was 95 ft. (29 meters) and the average groundwater table starts from 18 ft. (5.5 meters) from the ground surface. Table 3.8 represents the summary of the CPT test results, bore log data and laboratory test results for Livingston Parish.

Table 3.8: Summaries of soil properties for Livingston Parish

Sites	Unit weight (tsf)	Moisture content (%)	Liquid Limit (%)	Plasticity Index (%)	s_u (tsf)	q_c (tsf)	f_s (tsf)	Cone factor
Tichfaw River Bridge and Approach TP1	0.06-0.067	20-40	26-94	6-55	0.31-2.835	6.9-67.4	0.2-2.7	7.7-19.5
Tichfaw River Bridge and Approach TP3	0.032-0.066	17-36	40-74	17-41	0.03-2.625	0.9-55.0	0.1-1.7	7.6-23.3

3.2.9 Orleans Parish

The site is located near the south-east part of Louisiana. Four CPT's and boreholes were drilled near Rigolets Pass Bridge location and one CPT and borehole was drilled in New Orleans. The average drilled borehole depth for these sites was about 170 ft. (51.8 meters) and the depth of the water table from the ground was about 6 ft. (1.8) from the ground on average. The water table is very near to the ground surface. From laboratory soil tests and CPT, it is clear that the soils of this location are mainly soft clays. However, silts and sands are also present. Table 3.9 represents the summary of the CPT's, borehole data and laboratory test results for Orleans Parish sites.

3.2.10 Iberia Parish

The test sites are located in Iberia Parish. Two CPT's and boreholes were drilled near US 90 Interchange at John Darnell Road. The average borehole depth was 95 ft. (29 meters), with a groundwater table depth of 15 ft. (4.6 meters). CPT's and consecutive boreholes were drilled in

nearby locations. The summary of the CPT's, borehole, and laboratory test results for Iberia Parish is demonstrated in Table 3.10.

Table 3.9: Summaries of soil properties for Orleans Parish

Sites	Unit weight (tsf)	Moisture content (%)	Liquid Limit (%)	Plasticity Index (%)	s_u (tsf)	q_c (tsf)	f_s (tsf)	Cone factor
New Orleans TP1	0.051-0.063	-	33-100	13-84	0.17-1.71	4.9-22.4	0.1-0.3	7.6-19.6
Rigolets Pass Bridge TP1	0.051-0.065	21-58	23-64	5-53	0.1-1.035	5.2-295.2	0.1-3.6	10.3-23.1
Rigolets Pass Bridge TP2	0.051-0.065	20-62	24-97	4-62	0.402-1.942	4.5-184.2	0.1-1.5	10.7-17.7
Rigolets Pass Bridge TP3	0.051-0.064	22-63	24-99	7-62	0.345-1.452	6.9-257.8	0.2-3.5	13.7-23.4
Rigolets Pass Bridge TP4	0.051-0.064	25-54	45-72	23-48	0.397-1.713	10.0-164.7	0.1-2.1	10.2-22.3

Table 3.10: Summaries of soil properties for Iberia Parish

Sites	Unit weight (tsf)	Moisture content (%)	Liquid Limit (%)	Plasticity Index (%)	s_u (tsf)	q_c (tsf)	f_s (tsf)	Cone factor
US 90 Interchange TP1	0.055-0.065	20-45	33-88	9-56	0.11-1.35	0.1-70.8	0.1-2.0	5.7-18
US 90 Interchange TP2	0.056-0.063	22-41	35-84	11-52	0.12-1.29	0.9-65.7	0.1-1.9	7.8-17.8

3.2.11 Assumption Parish

The test sites are located in Assumption Parish. Seven CPT's and boreholes were drilled near Bayou Boeuf Bridge Main Span location. The average depth of drilled boreholes for these sites was 115 ft. (35.1 meters) and the average groundwater table depth was 8 ft. (2.4). It seems that the water table location is near to the ground surface. From borehole data and CPT's, it can be predicted that the soils of Assumption Parish are mainly soft clays. Table 3.11 represents the summary of the CPT's, boreholes and laboratory test results for Assumption Parish.

Table 3.11: Summaries of soil properties for Assumption Parish

Sites	Unit weight (tsf)	Moisture content (%)	Liquid Limit (%)	Plasticity Index (%)	s_u (tsf)	q_c (tsf)	f_s (tsf)	Cone factor
Bayou Boeuf Bridge Main Span TP1	0.052-0.06	28-37	33-54	9-33	0.175-0.37	6.7-78.3	0.2-1.1	18.3-20.1
Bayou Boeuf Bridge Main Span TP2	0.053-0.059	27-40	36-68	08-45	0.145-0.785	3.4-18.6	0.1-0.3	9.4-23.5
Bayou Boeuf Bridge Main Span TP3	0.053-0.06	26-50	43-73	21-49	0.225-0.745	5.7-91.3	0.2-1.1	10.2-24.4
Bayou Boeuf Bridge Main Span TP4	0.053-0.06	30-72	38-89	15-59	0.24-0.93	6.1-62.0	0.3-1.2	12.4-24.9
Bayou Boeuf Bridge Main Span TP5	0.052-0.062	30-72	39-72	14-50	0.155-0.58	3.8-80.0	0.2-1.3	9.5-22.9
Bayou Boeuf Bridge Main Span TP6	0.057-0.059	33-44	37-76	11-40	0.22-0.545	5.4-8.1	0.3-0.4	10.8-22.7
Bayou Boeuf Bridge Main Span TP7	0.053-0.059	31-72	42-85	20-57	0.175-0.6	1.5-12.6	0.1-1.1	5.2-25.0

3.2.12 Tangipahoa Parish

One CPT and borehole was drilled near Wardline Road Interchange Route I-55 location. The average borehole depth was 90 ft. (27.4 meters) with an average groundwater table depth of 15 ft. (4.6 meters). CPT and consecutive borehole were drilled in the adjacent location. The summary of the CPT, borehole and laboratory test results for Tangipahoa Parish is presented in Table 3.12.

Table 3.12: Summaries of soil properties for Tangipahoa Parish

Sites	Unit weight (tsf)	Moisture content (%)	Liquid Limit (%)	Plasticity Index (%)	s_u (tsf)	q_c (tsf)	f_s (tsf)	Cone factor
Wardline Road Interchange Route I-55 TP1	0.055-0.060	10-26	22-61	12-38	0.385-1.59	14.6-118.3	0.2-4.4	13.1-18.6
Wardline Road Interchange Route I-55 TP2	0.056-0.060	12-23	24-58	15-35	0.412-1.48	15.3-110.5	0.2-4.0	13.3-18.5

3.2.13 Madison Parish

The sites are located in Madison Parish. Two CPT's and boreholes were drilled near Bayou Macon Bridge location. The average borehole depth for these sites was 90 ft. (27.4 meters) and the average water table depth from the ground surface is nearly 7 ft. (2.1 meters). Thus, the groundwater table location is very close to the surface. Table 3.13 shows the summary of the CPT's, boreholes and laboratory test results for Madison Parish.

Table 3.13: Summaries of soil properties for Madison Parish

Sites	Unit weight (tsf)	Moisture content (%)	Liquid Limit (%)	Plasticity Index (%)	s_u (tsf)	q_c (tsf)	f_s (tsf)	Cone factor
Bayou Macon Bridge CPT1	0.055-0.065	24-39	30-54	7-26	0.3-1.445	6.7-285.5	0.2-2.5	5.2-20.5
Bayou Macon Bridge CPT2	0.055-0.065	17-39	30-56	8-24	0.36-1.31	7.0-246.1	0.3-2.3	8.6-19.2

3.2.14 Ouachita Parish

The sites are located in Ouachita Parish near Monroe. Seven CPT's and boreholes were drilled in North Eighteen Street Ext. - Segment 2 location. The borehole and consecutive CPT was done in the adjacent location. The average depth of boreholes was 85 ft. (25.9 meters) and the average groundwater table depth was 10 ft. (3 meters). Table 3.14 shows the summary of the CPT's, boreholes, and laboratory test results for the test sites of Ouachita Parish.

3.3 Corrected Tip Resistance

Due to the geometric design of the cone, ambient pore water pressure will act on the shoulder area behind the cone and on the ends of the friction sleeve, which is known as unequal area effect. Thus, the total stress measured from cone and sleeve friction has to be corrected for this unequal area effect. The corrected cone tip resistance (q_t) is calculated from equation (2.10).

Table 3.14: Summaries of soil properties for Ouachita Parish

Sites	Unit weight (tsf)	Moisture content (%)	Liquid Limit (%)	Plasticity Index (%)	s_u (tsf)	q_c (tsf)	f_s (tsf)	Cone factor
North Eighteen Street Ext. - Segment Bent2	0.051-0.068	19-59	31-103	10-57	0.28-2.35	7.7-26.4	0.3-1.4	13.7-25.0
North Eighteen Street Ext. - Segment Bent9	0.052-0.063	21-57	32-85	6-58	0.27-0.69	8.1-19.2	0.3-1.3	16-23.5
North Eighteen Street Ext. - Segment Bent13	0.052-0.063	23-52	36-78	7-56	0.29-0.63	8-16.5	0.3-1.1	15-22.1
North Eighteen Street Ext. - Segment Bent14	0.052-0.063	25-56	35-79	8-60	0.29-0.72	8.5-19.4	0.2-1.0	14.4-20.2
North Eighteen Street Ext. - Segment Bent27	0.052-0.066	24-68	31-88	9-47	0.215-2.23	7.9-28.7	0.3-1.3	9.4-17.5
North Eighteen Street Ext. - Segment TP1	0.052-0.063	22-54	41-93	15-52	0.294-0.85	10.8-23.4	0.3-1.0	13.2-24.6
North Eighteen Street Ext. - Segment TP2	0.055-0.065	10-55	18-88	10-59	0.225-2.16	10.2-32.3	0.5-1.3	13.5-15.7

Most of the CPT data collected for this study are from the Louisiana Department of Transportation and Development (LADOTD). Pore-water pressure measurements (u_1 or u_2) are not available for most of the database. Therefore, correction of tip resistance is difficult for those datasets. However, some researchers used uncorrected tip resistance values (q_c) in their calculations (eg., Schmertmann, 1978; Zhang and Tumay, 1999). On the other hand, some researchers (eg., Robertson, 1990; Olsen and Mitchell, 1995) made a case for the adjustment of the tip resistance values (q_t) using the pore water pressure and the effective area ratio. Nowadays, most of the researchers use corrected cone tip resistance q_t values for their analyses. Therefore, it is very important to develop a criterion to estimate q_t where pore water pressure measurements are not available.

Previously, some researchers suggested some guidelines to estimate q_t where pore pressure measurements were not available. For example, Tumay and Hatipkarasulu (2011) suggested the difference between q_t and q_c to be below 10%, though it is not very reliable because they analyzed

data from two sites only. According to Mayne (2007), for dense granular soils and clean sands, there are no differences between q_t and q_c. But, for soft to stiff clayey soils, high pore-water pressures are produced and the correction may be very significant, from 20% to 70% in some cases (Robertson, 1988). Perhaps, even with standard friction-type cones that do not measure pore water pressures, the correction is still needed. A survey result indicates that only 48% of DOTs are using the q_t (Mayne, 2007). However, without using the corrected tip resistance, the interpretations of soil parameters and application of direct CPT methodologies may not be reliable (Mayne, 2007).

11 different sites were selected from all over Louisiana in order to set up a criterion for estimating q_t from q_c data where pore water pressure measurements are not available (Figure 3.4). These 11 sites have PCPT data with available pore water pressure measurements. Form PCPT and laboratory test results, one can say that Louisiana soil is a mixture of all types of soils- from soft clay to stiff clays to silty to sandy soil layers. PCPT data from 11 sites were analyzed to observe the variation from q_t to q_c. Example of one test site with pore water pressure measurements- the LA1 site is shown in Figure 3.5, which represents both uncorrected and corrected tip resistance (q_c, q_t).

By observing the PCPT profile in Figure 3.5, it was assumed that the range of q_c, friction ratio ($FR=f_s*100/q_c$) and depth has effects on the relationship between q_t and q_c. From Figure 3.5, it is clear that the difference between q_t and q_c is greater for increased depth, but for greater cone tip resistance the difference is negligible. It is because, soft soil has very low tip resistance values, but very high pore pressure (u_2) values. Thus, according to equation (2.10) the difference between corrected and uncorrected tip resistances (q_t, q_c) becomes more significant with depth. On the other hand, if the soil is cohesionless soil (sandy), then the pore pressure (u_2) value becomes very low to zero. Therefore, the later part of equation (2.10) becomes insignificant. As a result, the

difference between corrected and uncorrected cone tip resistances for sandy soils becomes negligible. From Figure 3.5 and equation (2.10), it is clear that higher pore pressure causes a higher difference between q_t and q_c. Thus, it was assumed here that the value of cone tip resistance, the depth and maybe the friction ratio plays an important role in the difference between q_t and q_c.

Figure 3.4: Selected PCPT sites for tip resistance correction

After analyzing data from the 11 different sites, it was seen that q_t/q_c increases with depth. For low q_c values, the difference between q_t and q_c is significant. For q_t>50 tsf, the difference between q_t and q_c becomes negligible. Based on the results of data analyses, a chart was proposed

(Figure 3, where z = depth of soil layer) for predicting corrected tip resistance, q_t from uncorrected tip resistance, q_c where pore water pressure measurements are not available.

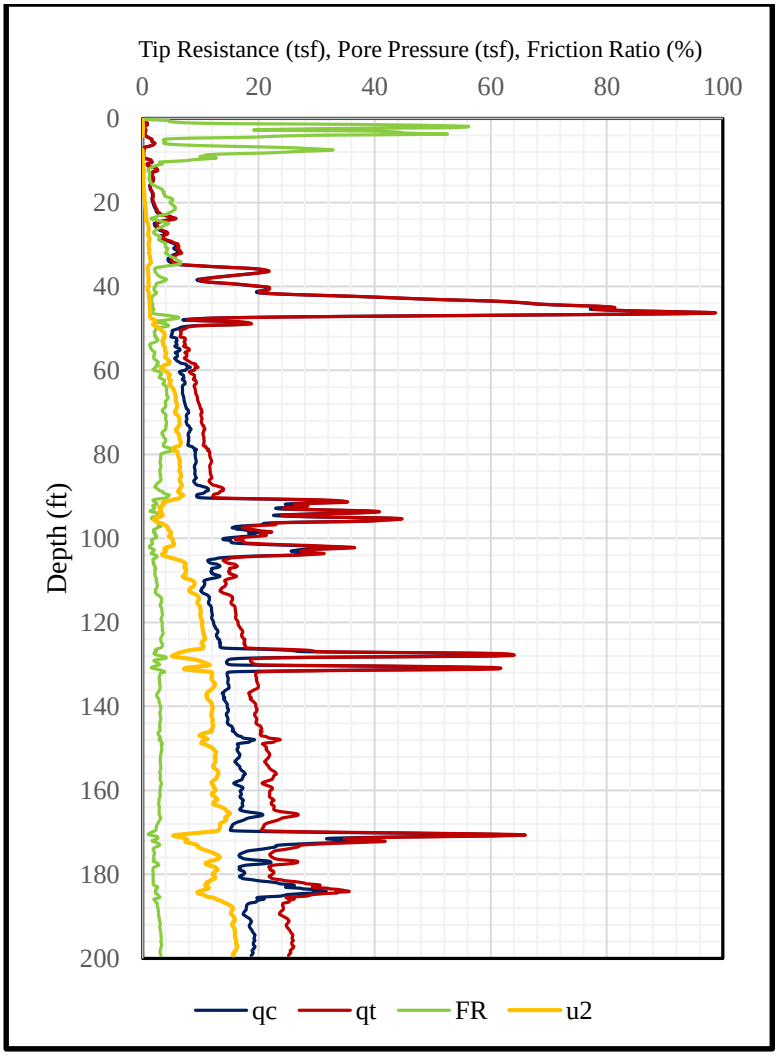

Figure 3.5: PCPT measurements of LA1 site

For analysis, four q_c rages were selected; q_c<10 tsf, 10 tsf<q_c<25 tsf, 25 tsf<q_c<50 tsf, and q_c>50 tsf. The q_c ranges were selected since there is a thumb rule about q_c values, such that if q_c<10 tsf, it can be soft clay and if q_c>50 tsf, it can be stiff clay. Additionally, four different soil depths were selected; depth<40 ft, 40 ft<depth<80 ft, 80 ft<depth<120 ft and depth>120 ft. Six different friction ratios were also considered; *FR*<1%, 1%< *FR* <3%, 3%< *FR* <5%, 5%< *FR* <10%, 10%<

FR <15% and *FR* >15%. However, later it was observed that the friction ratio does not have a significant effect on the correction of cone tip resistance. Therefore, only the cone tip resistance and the depth have a significant effect on the correction of tip resistance. From these different sets of data ranges, criteria are set for correction of tip resistance (Figure 3.6).

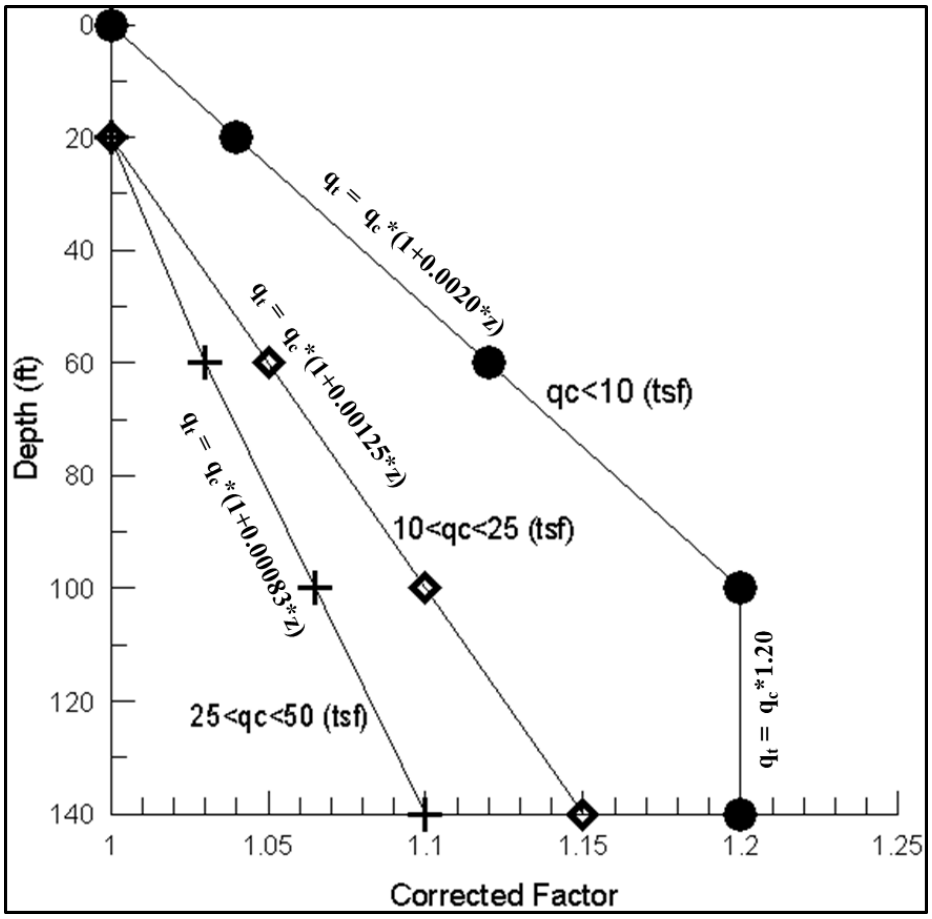

where, z = depth of soil layer

Figure 3.6: Proposed chart for tip resistance correction

Throughout our entire analyses, we used the guideline presented in Figure 3.6 to estimate q_t values where the pore water pressure measurements are not available. This chart gives quite good predictions for measuring q_t values for CPT. Figure 3.7 presents an example of accurateness

of using Figure 3.6 guidelines for predicting q_t which shows good agreement between measured and predicted corrected tip resistance, q_t.

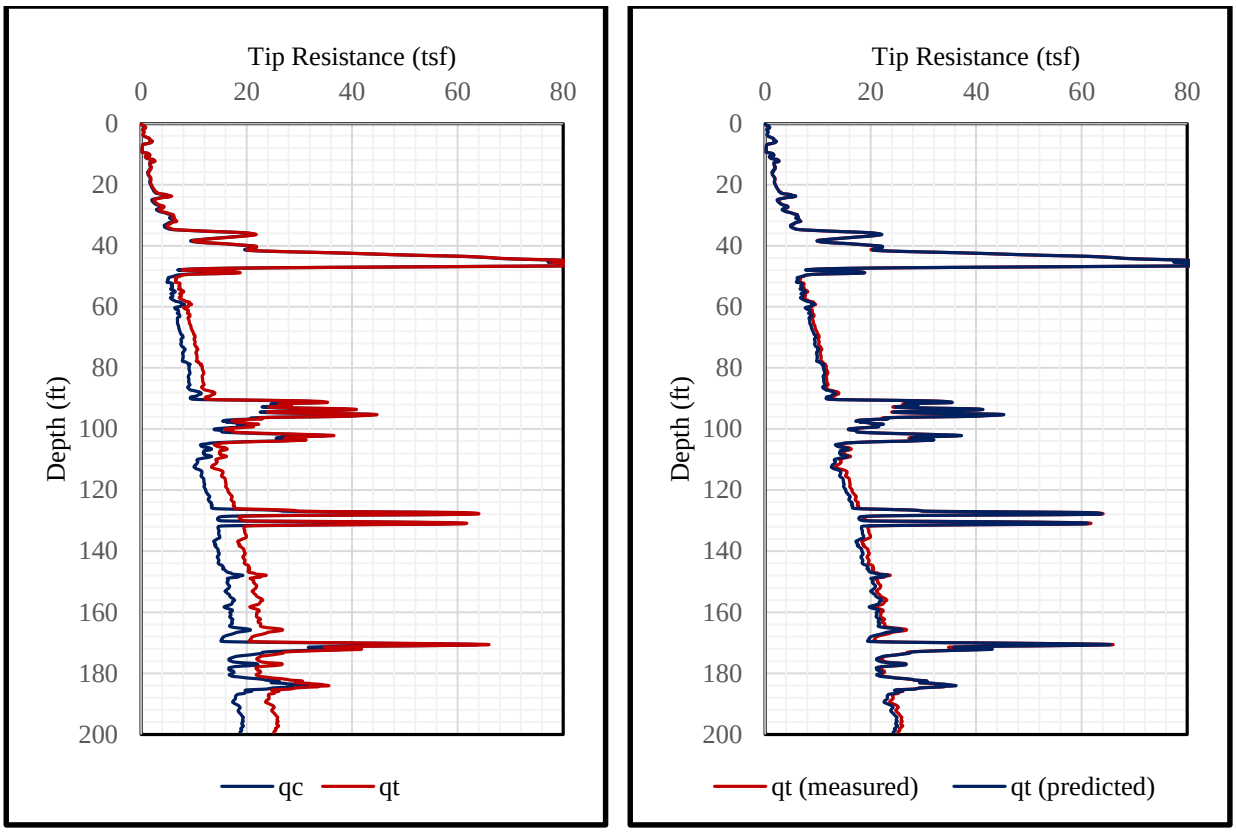

(a) (b)

Figure 3.7: (a) Measured and (b) predicted corrected tip resistance profile for LA1 site

3.4 Undrained Shear Strength

Based on CPT/PCPT data, laboratory test results and soil borehole data, statistical correlations were developed to estimate the unconsolidated undrained shear strength (s_u). Using the statistical regression models, the s_u could be estimated without doing any shear strength tests in the laboratory. The average q_t and f_s value of any specific soil layer was used to develop the regression models. The graphical representation of the data collection procedure is presented in Figure 3.8. For example, for soil layer 2, the σ_{vo} was calculated up to point B. Besides, the average q_t value of total 3′ of soil was collected for soil layer 2. Similarly, the average f_s value was collected for soil

layer 2. For this specific soil layer, other necessary parameters (e.g., *LL*, I_p, *MC*) will be determined from laboratory tests.

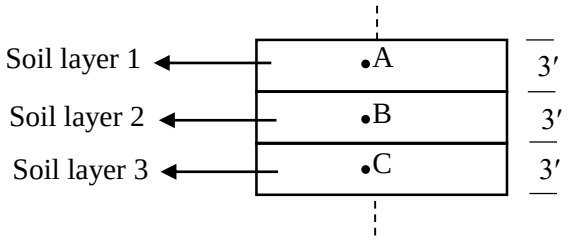

Figure 3.8: Data points selection system

3.5 Soil Classification

Some CPT/PCPT soil classification charts were analyzed for this study, e.g., Douglas and Olsen chart (1981), modified Shmertmann chart by Tumay (1985), Robertson (1990, 2009 and 2010) charts, Zhang and Tumay (1999) probability method, and Saye et at. (2017) chart. In this study, we fitted the CPT/PCPT data in these charts based on USCS soil classification system. Only three basic type of soils were considered, e.g., clayey, silty and sandy. Then, the existing soil classification charts were modified/adjusted based on the CPT/PCPT and laboratory test.

3.6 Model Verification Data

Total 455 data points were collected from all study locations. Out of 455 points, 1/3rd of the data points (133 data points) were randomly selected for the verification of statistical regression modes. These 133 points were not used to develop the s_u models. Model verification parameters will be briefly discussed in the following chapter.

3.7 Conclusion

Seventy CPT's and consecutive bore logs were selected from 14 parishes throughout Louisiana. Laboratory tests were performed to determine some basic soil parameters. Total 455 data points were collected from these in-situ and laboratory tests. Then, 133 pots were selected randomly for

verification of the models. The remaining 322 points were used for model development. Additionally, CPT/PCPT and soil borehole data were used to adjust/modify the existing CPT soil classification charts. Furthermore, 11 different PCPT test sites were selected for developing the tip resistance correction guideline, where pore pressure measurements are not available.

CHAPTER 4
STATISTICAL ANALYSIS

This chapter would provide a detailed overview of statistical analyses, regression models, limitations, assumptions, and practical considerations for model development. Multiple linear and non-linear regression analyses of the unconsolidated undrained shear strength, s_u, would be discussed in this study. To identify the potential significant parameters for s_u model development, a parametric statistical analysis was conducted. All statistical analyses were performed by the Statistical Analysis Software (SAS®) package. Results from statistical analyses are presented in details here to modify existing correlations and to develop new s_u models.

4.1 Statistical Approaches

A statistical model is basically a mathematical model. It represents some statistical assumptions about the generation of some sample data and similar data from a huge population. For example, a simple statistical model is a relation between two variables with a straight line:

$$Y = m * X + \varepsilon \tag{4.1}$$

where m is the slope, X is the independent variable, Y is the dependent variable and ε is intercept (Figure 4.1).

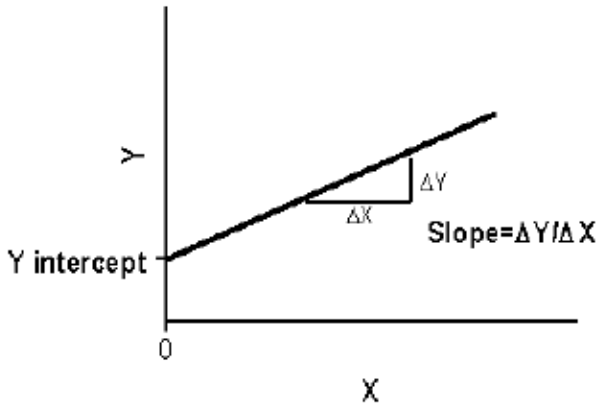

Figure 4.1: Simple linear relation

The relation between the dependent and independent variables can be determined from the statistical analyses of the measured set of *X* and *Y* using standard techniques, e.g., curve fitting or regression method.

4.1.1 Regression Analysis

Regression analysis method examines the relationship between the dependent and a number of independent variables. There are two approaches, linear and nonlinear regression analysis. Linear regression analysis is of two types, simple linear regression (SLR) analysis and multiple linear regression (MLR) analysis. SLR analysis is a relation between two variables, where the best fit straight line passes through the dataset. The objective of SLR analysis is to find the optimum line that best fits *Y* from *X*. In other words, SLR minimizes the sum of the squares (SS) of the vertical distances (errors) of the points from the best fit line. The SLR line can then be defined as:

$$Y = \beta_0 + \beta_1 * X + \varepsilon \tag{4.2}$$

where β_0 is the intercept, β_1 is the slope and ε is the error. An error exists in the model because with a large number of datasets, a model hardly fits perfectly.

MLR analysis is an extension of SLR, where the dependent variables are influenced by multiple variables. Thus, the regression equations can be visualized as a plane rather than straight lines. The MLR analysis has the following form:

$$Y_i = \beta_0 + \beta_1 * X_{i1} + \beta_2 * X_{i2} + \ldots\ldots\ldots + \beta_n * X_{in} + \varepsilon_i \tag{4.3}$$

where $i=1, 2, 3, \ldots, n$, n is the total observation numbers, Y_i is the dependent variable, X_{i1}, X_{i2}, X_{i3}, …. , X_{in} are the independent variables, $\beta_0, \beta_1, \beta_2, \ldots, \beta_n$ are the unknown parameters, and ε_i is the error. The relationship can also be expressed in matrix form like this:

$$[Y] = [X] * [\beta] + [\varepsilon] \tag{4.4}$$

$$\begin{Bmatrix} Y_1 \\ Y_2 \\ . \\ . \\ Y_n \end{Bmatrix} = \begin{Bmatrix} X_1 \\ X_2 \\ . \\ . \\ X_n \end{Bmatrix} * \begin{Bmatrix} \beta_1 \\ \beta_2 \\ . \\ . \\ \beta_n \end{Bmatrix} + \begin{Bmatrix} \varepsilon_1 \\ \varepsilon_2 \\ . \\ . \\ \varepsilon_n \end{Bmatrix} \quad (4.5)$$

where Y is $n \times 1$ vector of observation, X is a matrix of $n \times p$, p is the number of independent variables, β is $p \times 1$ vector of unknown parameters and ε is $n \times 1$ vector of observation. On the other hand, nonlinear regression is a regression analysis where observational data are modelled by a function which is a nonlinear combination of the model parameters. It depends on one or more independent variables. Successive approximation technique is used to fit the data. Nonlinear regression analysis can be expressed as:

$$Y = \alpha X_{1i}^{\beta} * X_{2i}^{\beta} + \varepsilon_i \quad (4.6)$$

where Y is the output (dependent variable), X_{1i} and X_{2i} are the independent variables or input parameters. A nonlinear regression model is preferred over regression analyses (SAS® Manual). Generally, nonlinear models can accommodate a wide range of functions and can incorporate each variable with a meaningful interpretation. Moreover, different functions, e.g., exponential decay, exponential rise, the sigmoidal function, logarithmic function, bell curve, and others can be incorporated in one regression model. Finally, one final dependent variable can be estimated or calculated.

4.1.2 Model Assessment Criteria

Several methods are used to explain the relationship between dependent and independent variables and to evaluate the "goodness" of the regression models. Most popular methods are summarized in the sub-sections:

4.1.2.1 Scatter Plot

Examining the relationship between different dependent variables and predictors is the first step in developing regression models. Additionally, the existing theoretical or empirical models are used to explore correlation which correlates different variables in simple graphical displays. One such method is the scatter plot method and it is the graphical representation of two quantitative variables out of the multidimensional dataset. It demonstrates the shape, strength, and direction of the relationship between the two variables. If the curvature is observed from scatter plots, a nonlinear relationship is recommended. Sometimes, outliers can be selected by observing the scatter plot.

4.1.2.2 Outlier Removal

Compared to a large number of a dataset, an outlier is an observation which appears too large or too small to the average value. An outlier may result from an incorrect experimental procedure or calculation, and sampling. The observation may be correct in times, however, it is necessary to omit the data points statistically to get a good correlation.

4.1.2.3 Residual Variance and Coefficient of Determination

The deviation of a particular point from its predicted value is called the residual value. The prediction is better when the variability of the residual values around the regression line is smaller compared to the overall variability. If there is no relationship between the *X* and *Y* variables, then the ratio of the residual variability of the *Y* variable to the original variance is equal to 1.0. If *X* and *Y* are perfectly related, then there is no residual variance and the ratio of variance would be 0.0. The coefficient of determination *(R^2)* is defined as:

$$R^2 = 1 - \frac{SSE}{SST} \tag{4.7}$$

where $SSE = \sum (y_i - y_i)^2$ is the residual sum of square and SST is the total sum of squares, $\sum y_i^2$. The R^2 value is an indicator of goodness of fit. For example, if the R^2 is close to 1.0, it indicates that we have considered almost all of the variability with the variables specified in the model. However, R^2 increases with the number of the predictor in the model. Thus, alternative statistics is defined as adjusted R^2. When there are multiple predictors are present in the database it is better to use adjusted R^2.

$$R_{adj}{}^2 = 1 - \frac{SSE}{SST}\left(\frac{n-1}{n-p}\right) \tag{4.8}$$

where *n* is the total observation number and *p* is the total independent variables present in the model.

4.1.2.3 Collinearity Test

Collinearity or multi-collinearity can be problematic in regression analysis. because linearly correlated independent variables can increase the variance of the predicted regression coefficients, which make them unstable and difficult to interpret. The Pearson's correlation coefficient or the linear correlation coefficient, *r*, is a measure of strength and direction of the linear relationship between the selected variables. *r* can be represented by the following relationship:

$$r = \frac{n(\sum xy) - (\sum x)(\sum y)}{\sqrt{[n(\sum x^2) - (\sum x)^2][n(\sum y^2) - (\sum y)^2]}} \tag{4.9}$$

where x and y are variables and n is the number of variables. The maximum *r*-value varies from -1 to +1 and a value of zero indicates no relationship between the variables. The sign of *r* demonstrates the positive or negative relationship between two variables. Generally, a large absolute value of the *r* indicates a potential multi-collinearity problem. For this study, a Pearson's coefficient value greater than 0.80 was considered highly collinear. However, sometimes, it is possible to determine no pairwise correlation in multiple regression analysis. The variance

inflation factor (VIF) is the most common method to address the multi-collinearity problem in this situation. VIF is a measure of the inflation in the standard error associated with a particular weight due to multi-collinearity. E.g., a VIF of 8 indicates that the standard errors are larger by a factor of 8. Several recommendations for acceptable levels of VIF have been published in the previous literature. However, a value of 5 or 10 has been recommended as the maximum level of VIF. For this study, a value of 5 was used.

4.1.3 Model Selection Criteria

The significance test is performed to evaluate the effectiveness of the overall model. It is a good way to measure whether the relationship exists between the variables. This is usually done by testing the null hypothesis, H_0, against the alternative hypothesis, H_1. H_0 denotes that none of the independent variables is linearly correlated to the dependent variable in the assumed multiple regression equation. Conversely, H_1 implies at least one of the independent variables is linearly related to the dependent variable. This hypothesis can be tested by a comparison of Mean Square Regression (MSR) and Mean Square Error (MSE). This test is an *F* statistic. The best way for this test is to use Analysis of Variance (ANOVA). An example of an ANOVA table is presented in Table 4.1. For this study, 95% significance level was assumed.

Table 4.1: ANOVA table format

	Degrees of Freedom	**Sum of Squares**	**Mean Square**	**F**
Regression	k	SSR	MSR	MSR/MSE
Error	n-k-1	SSE	MSE	
Total	n-1	SST		

where SST = $\sum_{i=1}^{n}(y_i - \bar{y})^2$ total sum of squares

SSE = $\sum_{i=1}^{n}(y_i - \hat{y}_i)^2$ sum of squares due to error

SSR = $\sum_{i=1}^{n}(\hat{y}_i - \bar{y})^2$ sum of squares due to regression

MSE = $\frac{SSE}{n-k-1}$ mean square due to error

MSR = $\frac{SSR}{k}$ mean square due to regression

where $\bar{y}_i$ are the predicted values, and $\bar{y}$ is the mean input parameters. SST can be alternatively calculated by adding SSR and SSE. If H_0 is rejected, then additional tests are required. Significance tests for individual regression coefficients would be suitable in this situation. This is generally done by testing the H_0. If H_0 is not rejected, it indicates the independent variable can be removed from the regression model. This test is called the *t* statistic test.

$$t = \frac{\hat{\beta}_j}{SE_{\hat{\beta}_j}} \tag{4.10}$$

where $SE_{\hat{\beta}_j}$ is the standard error of the regression coefficient $\hat{\beta}_j$. Finally, model significance was checked by the goodness of fit, bias, the coefficient of variation (COV). The goodness of fit may be evaluated by a quick visual and numerical assessment. The numerical statistical indices for the goodness of fit test are R^2, adjusted R^2, SS, SST, MSE, root mean square error (RMSE) and others. RMSE is the square root of the SSE (RMSE= √SSE). It signifies how close the observed data points are to the model's predicted values. For any regression model, smaller RMSE value is preferred. COV is a measure of relative variability. It is the ratio of the standard deviation to the mean.

$$\text{COV} = \frac{SD}{\bar{x}} \tag{4.11}$$

where $\bar{x}$ is the mean of depended variables, *SD* is the standard deviation and it is a measure that is used to quantify the amount of variation or dispersion of a set of data values :

$$\mathrm{SD} = \sqrt{\frac{(x_i - \bar{x})^2}{(n-1)}} \tag{4.12}$$

where x_i is the observed values and n is the number of observations. The smaller COV indicates smaller dispersion around the mean.

4.2 Statistical Analysis for Undrained Shear Strength (s_u)

4.2.1 Variables in the Statistical Analysis

Unconsolidated undrained triaxial tests were performed on high quality Shelby tube samples obtained from the field to evaluate the unconsolidated undrained shear strength, s_u. Cone penetration test data compiled included uncorrected and corrected cone tip resistance (q_c, q_t), sleeve friction (f_s), and for piezocone the pore pressure measured at u_2 location. Also, the soil information was collected on the index properties: moisture content (*MC*), liquid limit (*LL*), plastic limit (*PL*), plasticity index (I_p). Average total overburden pressure (σ_{vo}), and hydrostatic pressure (u_0) were estimated for different soil layers based on bore log information.

Plots of undrained shear strength (s_u) and the CPT parameters (q_t, f_s) are presented in Figure 4.2 and Figure 4.3. Direct linear increasing trend is evident from the scatter plot between s_u versus f_s as shown in Figure 4.3. Moreover, Figure 4.2 reveals increase in s_u with increasing q_t, though data are relatively less scattered than in the plot against s_u versus f_s. However, data shows slight scattering at higher value of q_t and suggest bi-linear or nonlinear relationship. Very weak trend was observed between s_u and σ_{vo}, as shown in Figure 4.4. Data are highly scattered in the plot between s_u versus σ_{vo}. It demonstrates that s_u does not have direct correlation with σ_{vo}. On the other hand, data are highly scattered in the plot between s_u versus *LL* as shown in Figure 4.5. Similarly, plot of s_u versus I_p shows highly scattered data as shown in Figure 4.6. Finally, Figure 4.7 shows a decreasing trend of s_u with *MC* with high scatter.

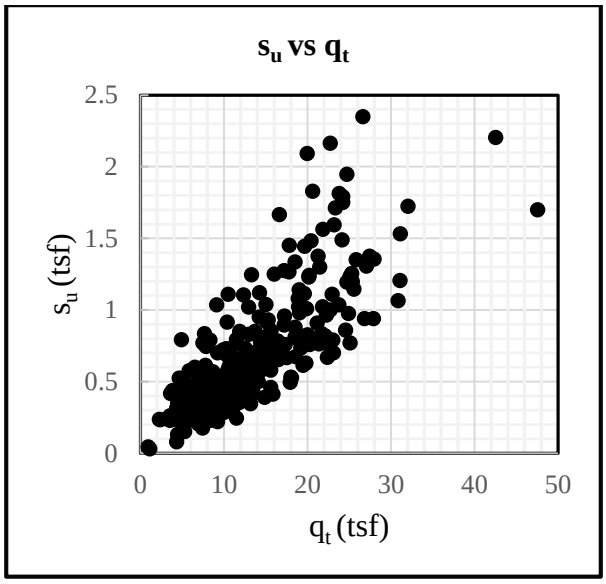

Figure 4.2: Plot of s_u vs q_t

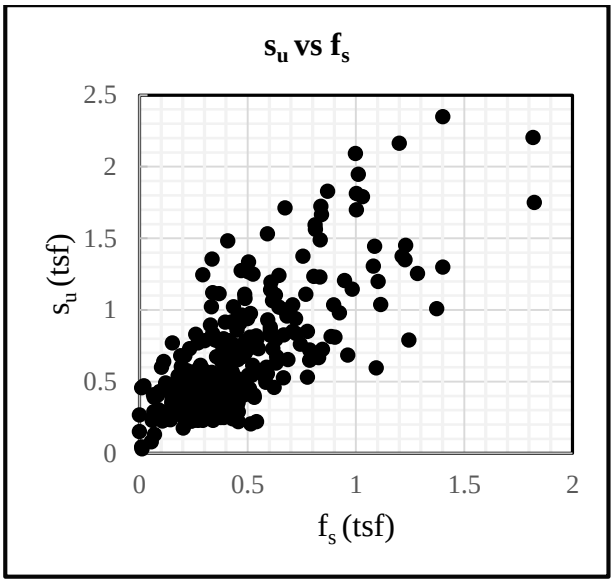

Figure 4.3: Plot of s_u vs f_s

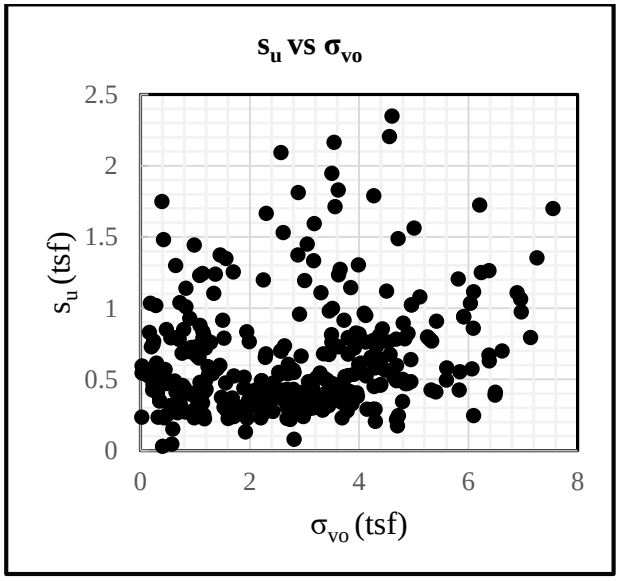

Figure 4.4: Plot of s_u vs σ_{vo}

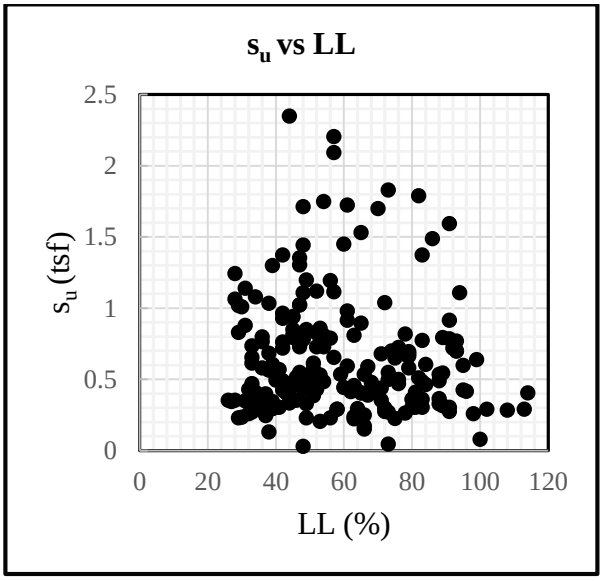

Figure 4.5: P plot of s_u vs LL

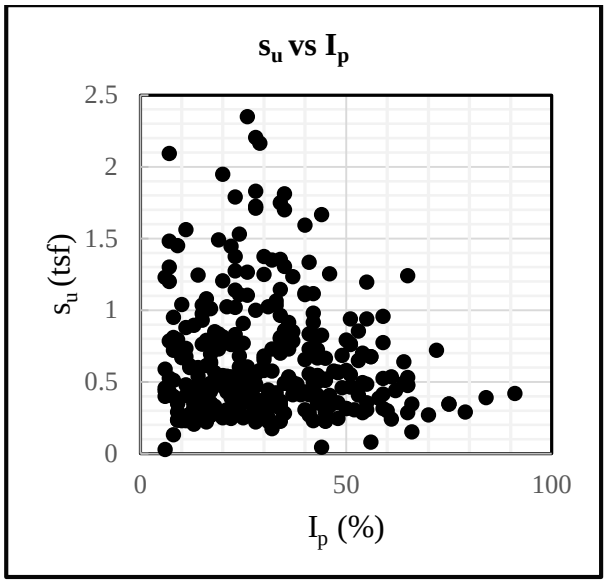

Figure 4.6: Plot of s_u vs I_p

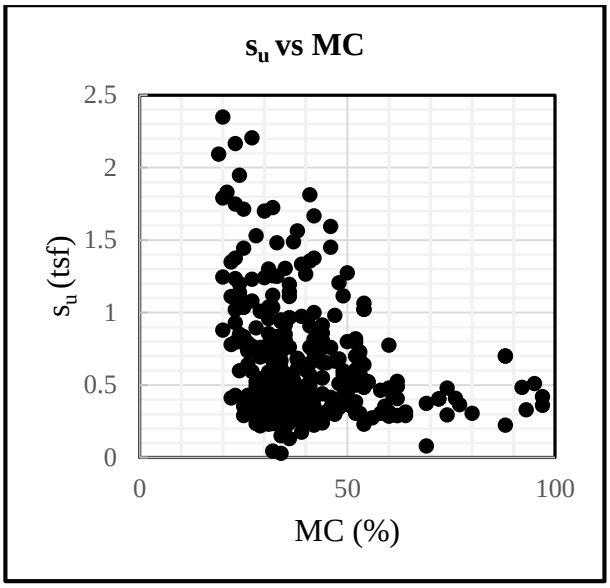

Figure 4.7: Plot of s_u vs MC

4.2.2 Regression Analysis

To assess the significance of the independent variables (i.e., q_c, q_t, f_s, σ_{vo}, *MC*, *LL* and I_p) on the prediction of the dependent variable (s_u), linear and non-linear regression analyses were conducted. At first, the Analysis of Variance (ANOVA) between the dependent variables, and the independent variables were conducted using the Statistical Analysis System (SAS®) software. Independent variables that were not statistically significant in the model were removed and this procedure was repeated until only the significant variables were present in the s_u model.

Table 4.2 summarizes the results of the Analysis of Variance (ANOVA) analysis. It was observed that three independent variables (e.g., *LL*, I_p and *MC*) were not statistically significant at a 5% significance level, and therefore they were removed from consideration in developing the s_u model. SAS codes and sample outputs for regression analyses are represented in Appendix B.

Multi-collinearity tests were also conducted between the variables. Table 4.3 depicts the summary of the Pearson correlation coefficients for all variables considered in developing s_u models which shows that q_t, f_s and σ_{vo} does not have multi-collinearity with each other. Therefore,

these three parameters would be necessary in the development of s_u prediction models. To further filter out the multi-collinear independent variables, a second statistical factor VIF was used. In this study, the VIF values for the selected independent variables were within the acceptable range (Table 4.3), which indicates that no multi-collinear independent variables have been included in the s_u model.

Table 4.2: Summary of ANOVA Analysis

Parameter	Estimate	Standard Error	F value	P value
With all independent parameters				
q_t	-0.037372722	0.02212901	3.85	0.0428
f_s	1.207793222	0.19539001	38.21	<0.0001
σ_{vo}	0.095054377	0.01308211	52.79	<0.0001
LL	-0.014888379	0.00865776	2.96	0.0871
PI	0.001903961	0.01064272	0.03	0.8582
MC	-0.023902493	0.01199017	3.17	0.0676
With independent significant parameters only				
q_t	0.04099	0.00372	11.00	<.0001
f_s	0.35867	0.07601	4.72	<.0001
σ_{vo}	-0.03231	0.01000	-3.23	0.0014

Additionally, to assess the statistical significance of the model and predictor influence, choice and suitability of model, some practical consideration are taken into account. Some of these practical considerations are time and convenience of obtaining predictor variable in the field, repeatability and reliability of such test and theoretical or empirical models based on past experience.

In this study, statistical regression correlation models were divided into two categories: direct and the indirect models. In the direct methods, correlations are formed using the parameters that are measured directly from CPT tests such as q_c, q_t and f_s. Indirect models incorporated total overburden pressure, σ_{vo} in addition to CPT data. Summary of the significant models based on this study is presented in Table 4.4.

Models presented in Table 4.4 are based on n = 322 (i.e., 2/3rd of the database) data points that are randomly selected from a total 455 collected data points all over Louisiana. These models are valid within certain ranges.

Table 4.3: Summary of multi-collinearity tests

Summary of Pearson's correlation analyses				
	s_u	q_t	f_s	σ_{vo}
s_u	1.00000	0.78045	0.75287	0.22104
q_t	0.78045	1.00000	0.71724	0.49999
f_s	0.75287	0.71724	1.00000	0.10333
σ_{vo}	0.22104	0.49999	0.10333	1.00000

Summary of VIF analyses							
Variable	**DF**	**Parameter Estimate**	**Standard Error**	**t Value**	**Pr > |t|**	**Tolerance**	**Variance Inflation**
Intercept	1	0.06348	0.03177	2.00	0.0466	-	0
q_t	1	0.04099	0.00372	11.00	<.0001	0.28714	3.48257
f_s	1	0.35867	0.07601	4.72	<.0001	0.39245	2.54810
σ_{vo}	1	-0.03231	0.01000	-3.23	0.0014	0.56504	1.76979

Table 4.4: Regression Models for s_u

RM	Parameters	Model	R^2	Adj. R^2	RMSE	Cone Factor
Models using only CPT data						
1	q_t	$s_u=0.061*q_t^{0.935}$	0.67	0.67	0.23	-
2		$s_u=0.05*q_t$	0.64	0.64	0.25	-
3		$s_u=0.225*\exp^{(0.069*qt)}$	0.61	0.62	0.25	-
4		$s_u=0.549*\ln(q_t)-0.666$	0.56	0.56	0.27	-
5	f_s	$s_u=1.057*f_s+0.181$	0.57	0.58	0.28	-
6		$s_u=0.284*\exp^{(1.458*fs)}$	0.48	0.49	0.28	-
7		$s_u=0.807*f_s^{0.368}$	0.35	0.34	0.33	-

Table 4.4 (Cont.)

RM	Parameters	Model	R^2	Adj. R^2	RMSE	Cone Factor
8	q_t, f_s	$s_u=0.033*q_t+0.513*f_s$	0.71	0.70	0.22	-
9		$s_u=0.032*q_t^{1.004}+0.509*f_s+0.016$	0.69	0.70	0.22	-
10		$s_u=0.035*q_t+0.108*\exp^{(1.296*fs)}$	0.67	0.67	0.24	-
11		$s_u=0.049*(q_t+f_s)$	0.66	0.65	0.25	20.4
12		$s_u=1.151*f_s-2.1*(f_s/q_t)+0.227$	0.55	0.56	0.26	-
Models using CPT and laboratory soil data						
13	q_t, σ_{v0}	$s_u=0.063*(q_t-\sigma_{v0})$	0.70	0.71	0.23	16
14		$s_u=0.092*(q_t-\sigma_{v0})^{0.853}-0.012$	0.68	0.68	0.24	-
15		$s_u=0.093*q_t^{0.861}-0.059*\sigma_{v0}$	0.67	0.68	0.24	-
16		$s_u=0.055*q_t-0.059*\sigma_{v0}^{0.971}+0.116$	0.67	0.68	0.25	-
17		$s_u=0.109*q_t^{0.809}-0.091*\ln(\sigma_{v0})-0.118$	0.66	0.66	0.26	-
18		$s_u=0.057*q_t-0.017*\exp^{(0.463*\sigma v0)}$	0.65	0.66	0.27	-
19	q_c, σ_{v0}	$s_u = 0.067*(q_c-\sigma_{v0})$	0.67	0.67	0.26	15
20	q_t, σ_{oct}	$s_u = 0.059*(q_t-\sigma_{oct})$	0.66	0.66	0.26	17
21	q_t, σ_{ho}	$s_u = 0.056*(q_t-\sigma_{ho})$	0.65	0.66	0.27	18

Table 4.4 (Cont.)

RM	Parameters	Model	R^2	Adj. R^2	RMSE	Cone Factor
22	q_t, f_s, σ_{v0}	$s_u=0.070*(q_t-\sigma_{v0})^{0.846}+0.390*f_s$	0.74	0.75	0.20	-
23		$s_u=0.040*q_t+0.402*f_s-0.033*\sigma_{v0}+0.061$	0.71	0.71	0.23	-
24		$s_u=0.041*(q_t-\sigma_{v0})+0.368*f_s^{1.151}+0.099$	0.69	0.69	0.25	-
25		$s_u=0.041(q_t-\sigma_{v0})+0.392*f_s+0.075$	0.68	0.69	0.26	-
26		$s_u=0.040*q_t+0.402*f_s-7.444*\exp^{(0.004*\sigma v0)}+7.505$	0.67	0.68	0.26	-
27		$s_u=0.063q_t^{0.880}+0.393*f_s-0.054*\sigma_{v0}^{0.792}+0.012$	0.67	0.67	0.26	-
28		$s_u=0.053*(q_t+f_s)-0.052*\sigma_{v0}+0.103$	0.66	0.67	0.27	-
29		$s_u=0.060*(q_t+f_s-\sigma_{v0})$	0.66	0.66	0.27	16.7
30		$s_u=0.384*\ln(q_t)+0.572*f_s-0.023*\sigma_{v0}-0.461$	0.65	0.66	0.28	-

4.2.3 s_u Models Based on Cone Tip Resistance

In this study, a non-linear trend of s_u and cone tip resistance q_t is observed (Figure 4.2), and therefore, a nonlinear regression analysis was performed to explore the relation between s_u and q_t. The developed regression models RM 1, RM 2, RM 3 and RM 4 from Table 4.4 are verified by comparing the predicted results of regression models with 133 randomly selected data points ($1/3^{th}$ of the total dataset) that were not used to develop the s_u models. The prediction accuracy of the nonlinear model from RM-1 in Table 4.4 is quite acceptable. According to Figure 4.8, the verification of this model also indicates a satisfactory prediction of s_u. However, the performance of linear model RM 2 in Table 4.4 is not satisfactory as $R^2 = 0.64$ is lower and RMSE = 0.25 is

higher than the non-linear model. Similarly, the other regression models RM 3 and RM 4 in Table 4.4 are not satisfactory. On the basis of the results of statistical analysis, the authors recommend using the correlation presented in Equation 4.13 to estimate the s_u of clayey soil directly from q_t data as:

$$s_u = 0.061 * q_t^{0.935} \quad (R^2 = 0.67) \qquad (4.13)$$

4.2.4 s_u Models Based on Sleeve Friction

Different linear and non-linear regression analyses were performed to explore the relation between s_u and f_s. As evident from the scatter plot (Figure 4.3), a direct linear trend does exist between s_u and f_s for the total the dataset. However, the value of R^2 is 0.57 and the RMSE value is 0.28 for the linear regression model RM 5 in Table 4.4, which is not good for s_u prediction. The other regression models RM 6 and RM 7 in Table 4.4 are not suitable as they have low R^2 and RMSE values. The verification plots of these models are not satisfactory as well (Figure 4.12-4.14). On the basis of the results of statistical analysis, it was not recommended to use f_s alone for determination of s_u of clayey soil.

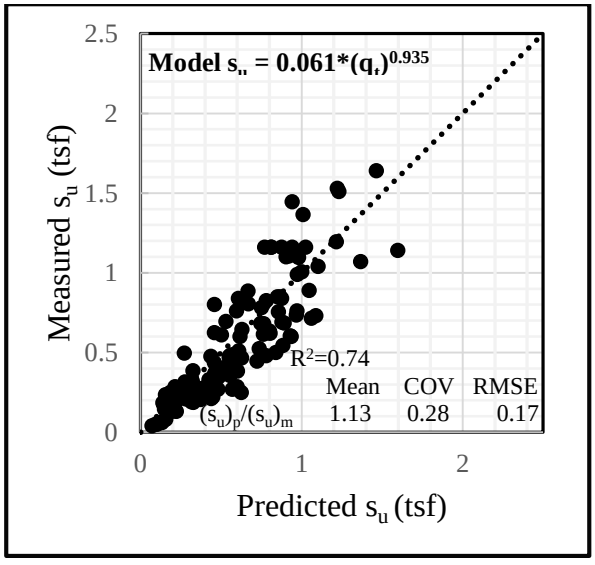

Figure 4.8: Verification of s_u model for q_t

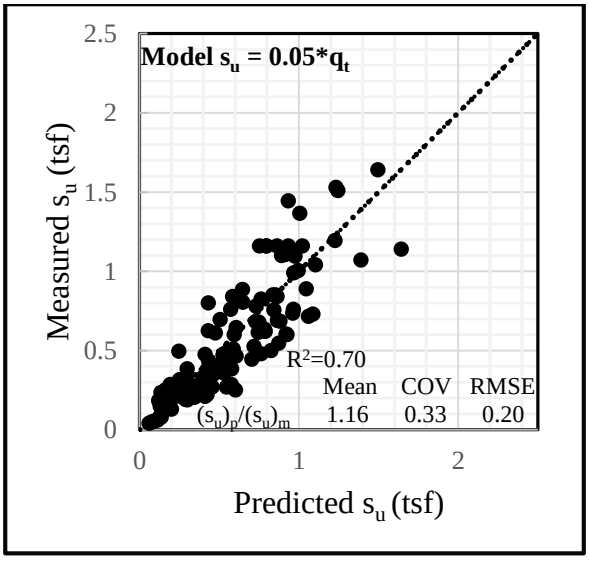

Figure 4.9: Verification of s_u model for q_t

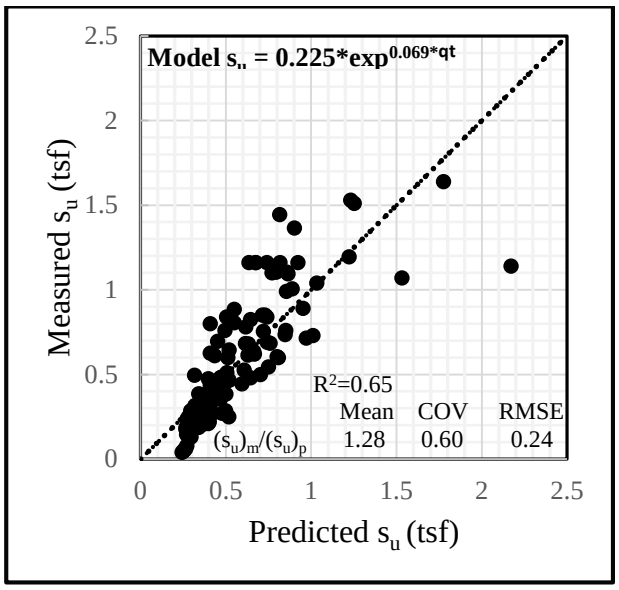

Figure 4.10: Verification of s_u model for q_t

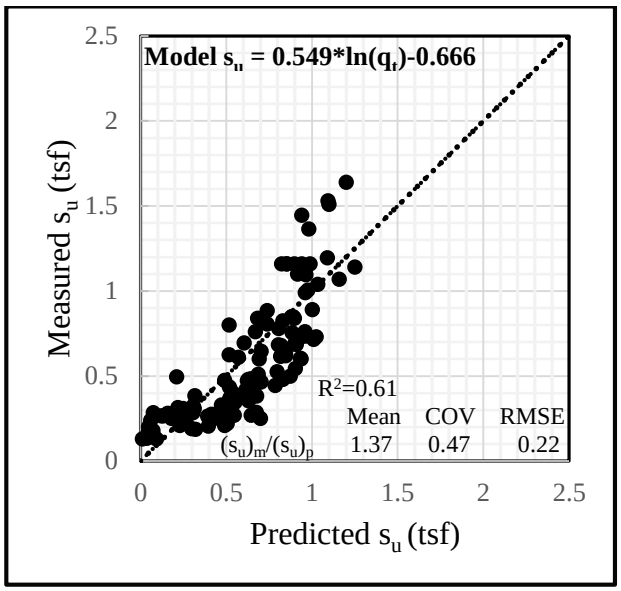

Figure 4.11: Verification of s_u model for q_t

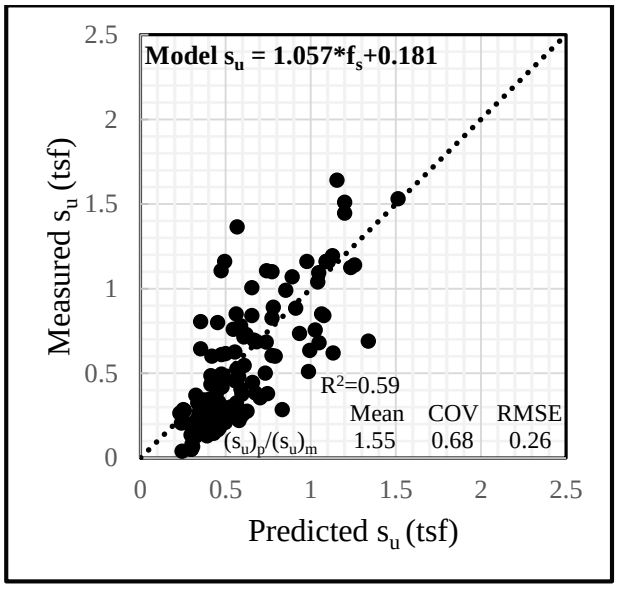

Figure 4.12: Verification of s_u model for f_s

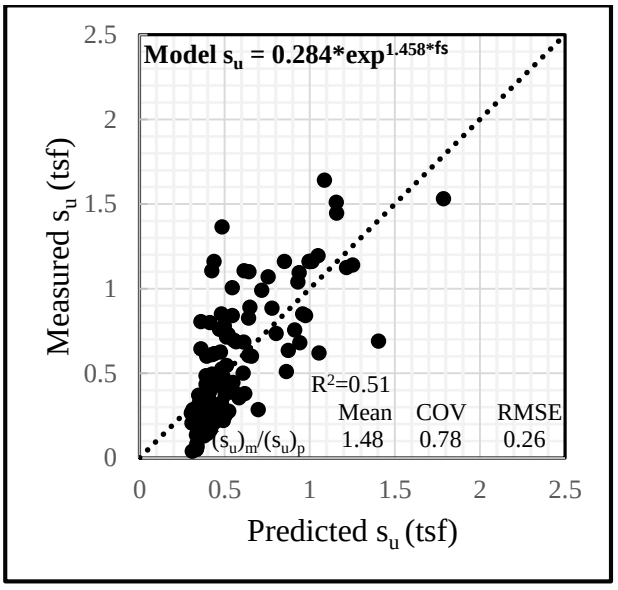

Figure 4.13: Verification of s_u model for f_s

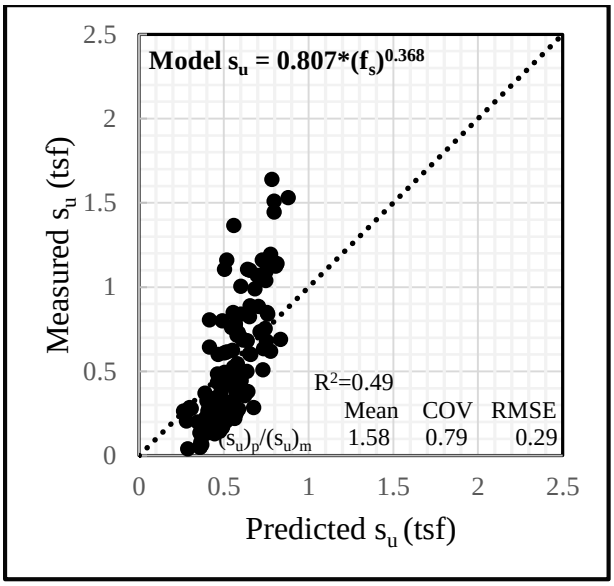

Figure 4.14: Verification of s_u model for f_s

4.2.5 s_u Models Based on Cone Tip Resistance and Sleeve Friction

The overall effectiveness of s_u model increases with using q_t and f_s together in the regression analysis. In this study, we found that both the linear and nonlinear models can significantly predict s_u of soil that comprises both q_t and f_s. Though, the value of R^2 was found to be slightly higher (0.71) for the linear regression model than the nonlinear model (R^2=0.69) as shown in RM 8 and RM 9 in Table 4.4. The other regression models RM 10, RM 11 and RM 12 in Table 4.4 is not suitable as they have low R^2 and RMSE values. However, after performing all the detailed statistical analyses and verification for the rest 133 data points (Figure 4.15- 4.19), the authors suggest that the linear model (Equation 4.14) may be considered as the best predictor of s_u (Figure 4.15).

$$s_u=0.033*q_t+0.513*f_s \quad (R^2=0.71) \qquad (4.14)$$

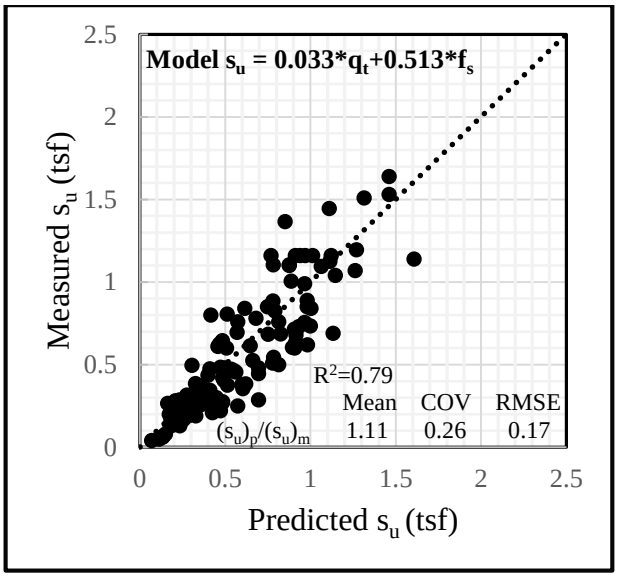

Figure 4.15: Verification of s_u model for q_t and f_s

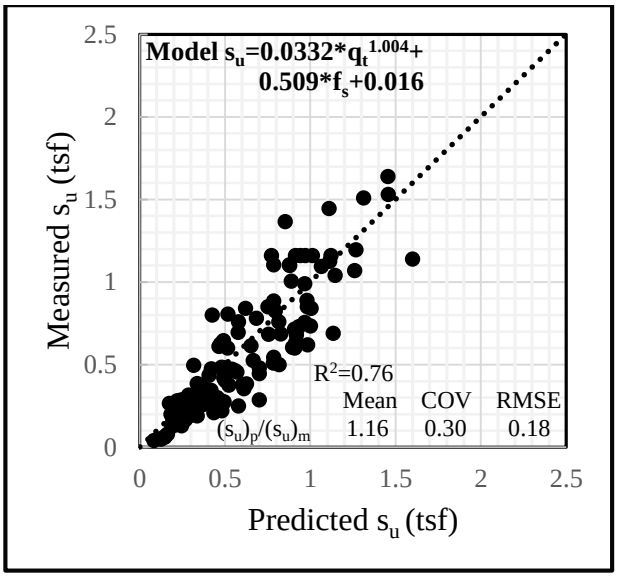

Figure 4.16: Verification of s_u model for q_t and f_s

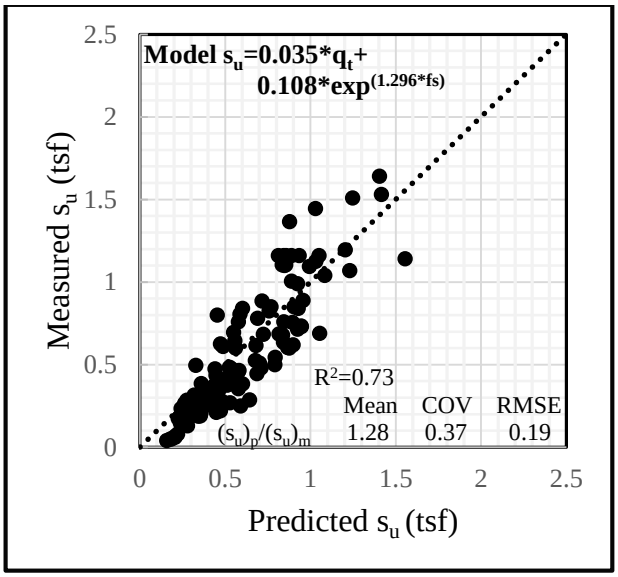

Figure 4.17: Verification of s_u model for q_t and f_s

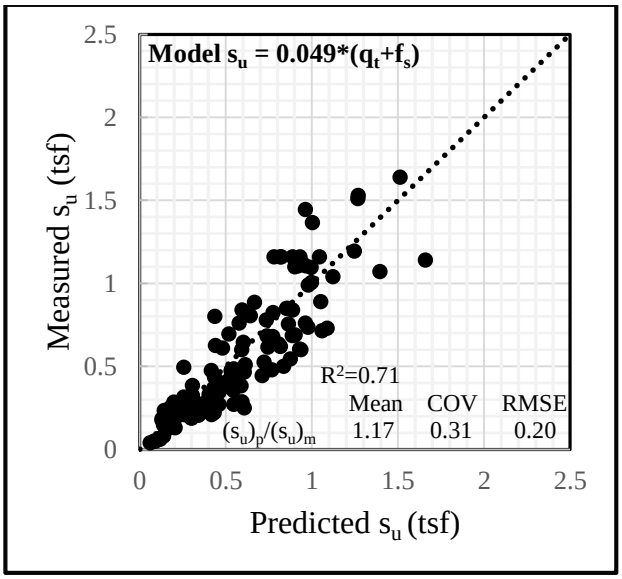

Figure 4.18: Verification of s_u model for q_t and f_s

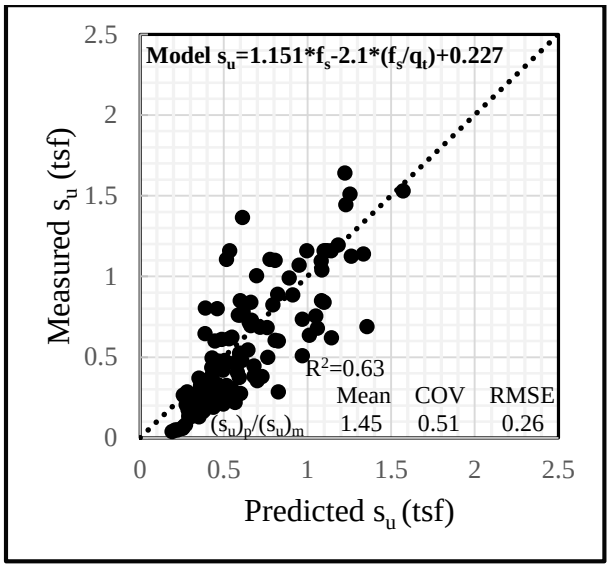

Figure 4.19: Verification of s_u model for q_t and f_s

4.2.6 s_u Models Based on Cone Tip Resistance and Overburden Pressure

According to previous studies (e.g., Mayne, 2007; Robertson, 2009), including the parameters, q_t and σ_{vo} give the best estimate of s_u for clayey soils. Some researchers (e.g., Senneset, 1982; Roberson, 2012) showed that a linear correlation exists between s_u and both q_t and σ_{vo}. Our regression analysis also shows the similar trend. The cone factor, N_{kt} for our model is 16, which lies within the suggested cone factors in previous studies (e.g., Mayne, 2007; Robertson, 2009). The $R^2 = 0.70$ is also acceptable for this model. The verification of model (Figure 4.25) also shows acceptable $R^2 = 0.79$ with mean of proposed/measured $s_u = 1.02$ with RMSE = 0.16 and COV = 0.16. However, if we consider uncorrected cone tip resistance, q_c, instead of q_t, we get a cone factor $N_k = 15$ with a lower $R^2 = 0.67$ (RM 19 in Table 4.4). The verification of $s_u - q_c, \sigma_{vo}$ model (Figure 4.26) also shows less effective than the $s_u - q_t, \sigma_{vo}$ model. That demonstrates the importance of tip resistance correction and the development of q_t versus q_c chart in Figure 3.6.

With the available database, it is not possible to measure the *OCR* and the earth pressure coefficients. However, for a rough estimation, earth pressure coefficient at rest (k_o) was assumed 0.50 for this study. An assumption was made that the angle of internal friction, ϕ, for this clayey soil equals 30°. Then, the horizontal overburden pressure, σ_{ho}, was calculated. A model was developed (Figure 4.27) with q_t to estimate s_u. The measured cone factor was 16. Though, the R^2=0.65 is too low to accept the model. Similarly, the octahedral stress (σ_{oct}= *[2*σ_{ho}+σ_{vo}]/3*) was calculated with the previously calculated σ_{ho} and σ_{vo} values. A model was developed (Figure 4.26) with q_t and σ_{oct} to estimate the s_u. Though many researchers believe that octahedral stress is dominant at cone tip, however, octahedral stress model found insignificant as R^2=0.67 low and RMSE=0.26 is high. The measured cone factor was 15. Based on regression analysis (RM 13-21) and model verification (Figure 4.20-4.28), the following equation (4.15) is proposed:

$$s_u = 0.063*(q_t-\sigma_{v0}) = \frac{q_t-\sigma_{vo}}{N_{kt}},\ N_{kt} = 16 \quad (R^2=0.70) \qquad (4.15)$$

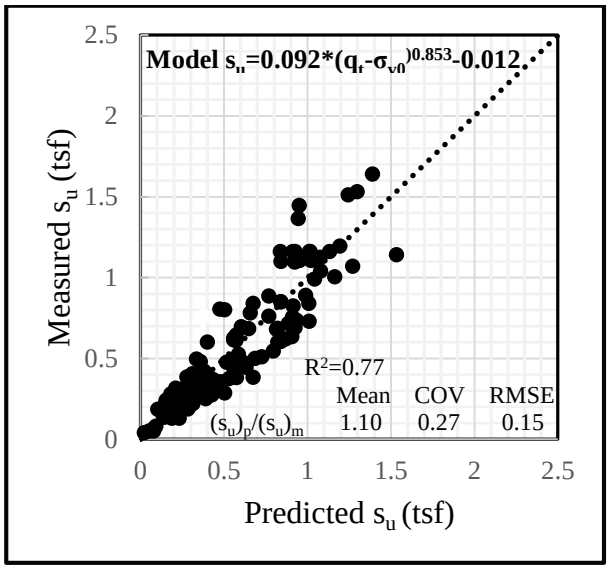

Figure 4.20: Verification of s_u model for q_t and σ_{vo}

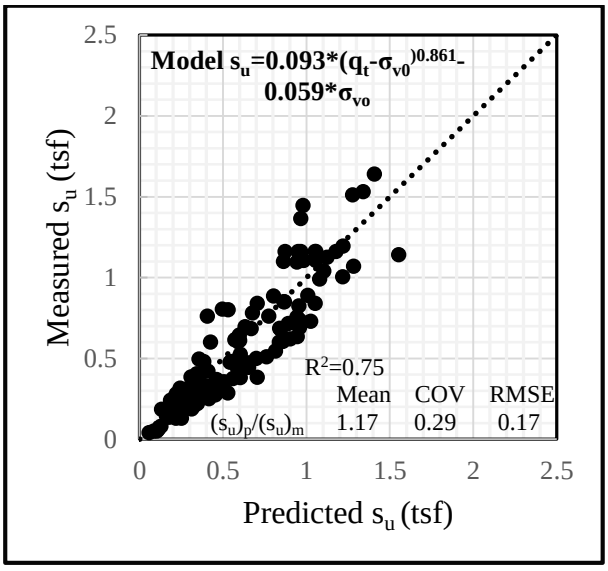

Figure 4.21: Verification of s_u model for q_t and σ_{vo}

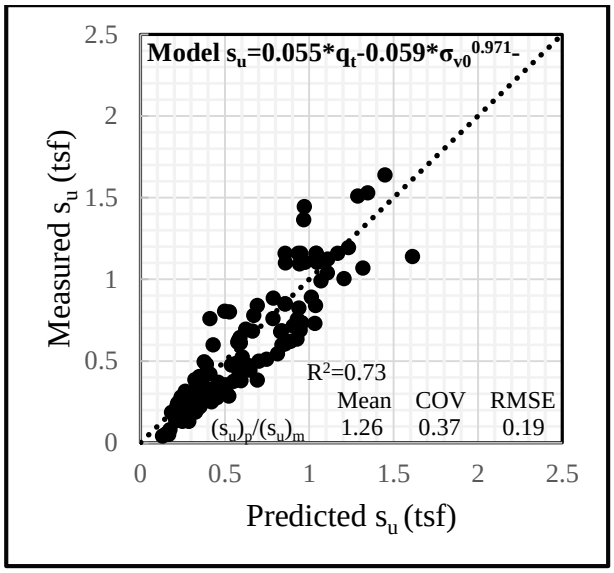

Figure 4.22: Verification of s_u model for q_t and σ_{vo}

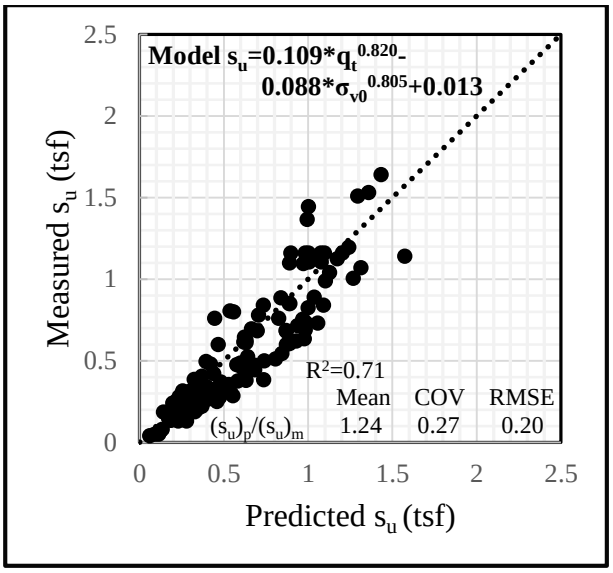

Figure 4.23: Verification of s_u model for q_t and σ_{vo}

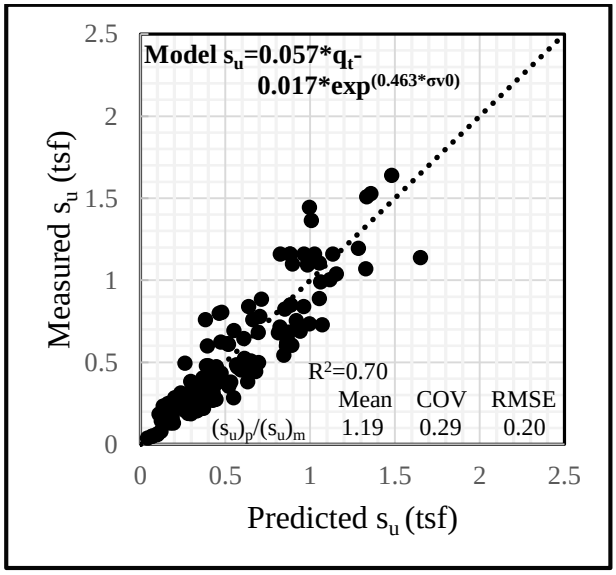

Figure 4.24: Verification of s_u model for q_t and σ_{vo}

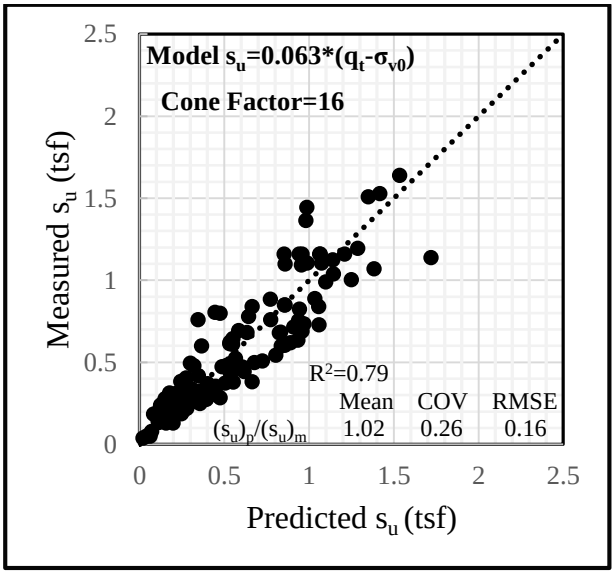

Figure 4.25: Verification of s_u model for q_t and σ_{vo}

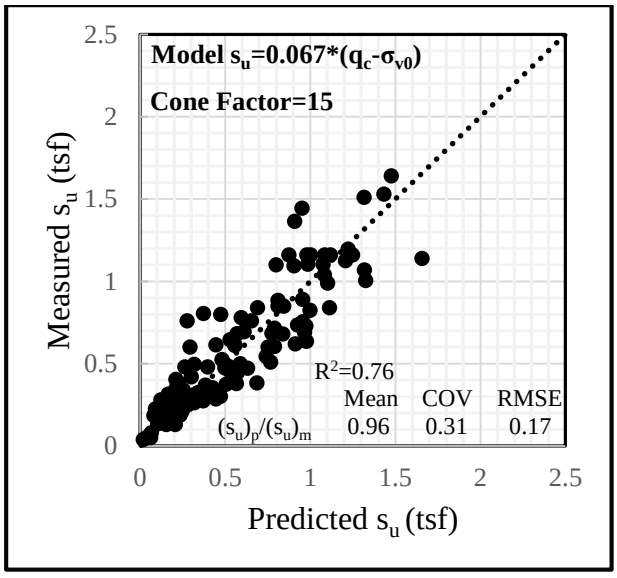

Figure 4.26: Verification of s_u model for q_t and σ_{vo}

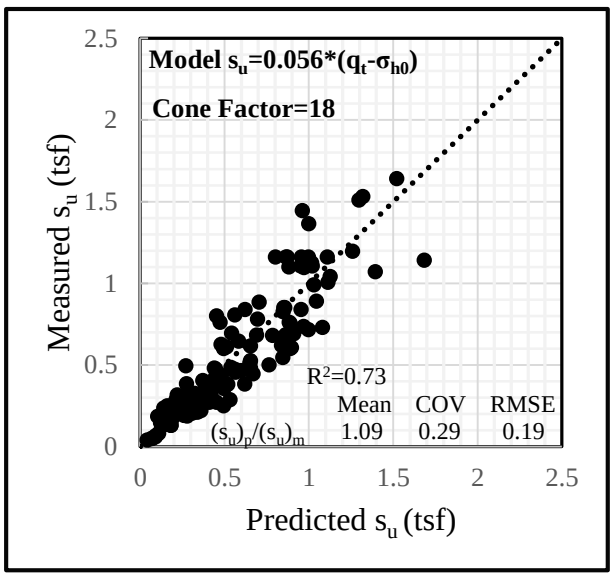

Figure 4.27: Verification of s_u model for q_c and σ_{ho}

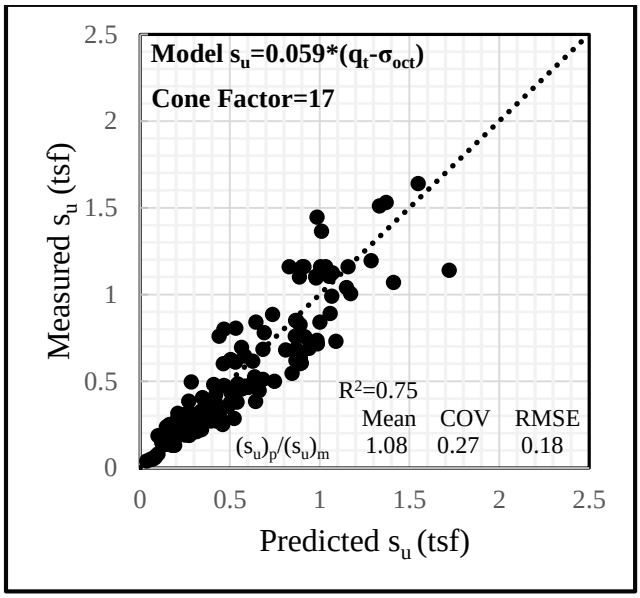

Figure 4.28: Verification of s_u model for q_t and σ_{oct}

4.2.6 s_u Models Based on Combination of Tip Resistance, Sleeve Friction and Overburden Pressure

In this study, a good correlation was obtained between s_u and q_t, f_s and σ_{vo} together. Both the linear and nonlinear regression models give good predictions as shown in RM 23 and RM 22 in Table 4.4. But the nonlinear model gives better predictions with R^2 = 0.74 and RMSE = 0.20 than the linear model. From model verifications (Figure 4.29 to Figure 4.37), it is clear that the nonlinear model RM 22 in Table 4.4 gives the best prediction with the ratio of predicted/measured mean s_u = 1.07 and COV = 0.20. Therefore, based on statistical regression analysis and model verification, the following equation (4.16) is proposed to evaluate s_u from q_t, f_s and σ_{vo}:

$$s_u = 0.070*(q_t-\sigma_{v0})^{0.846} + 0.390*f_s \quad (R^2=0.74) \qquad (4.16)$$

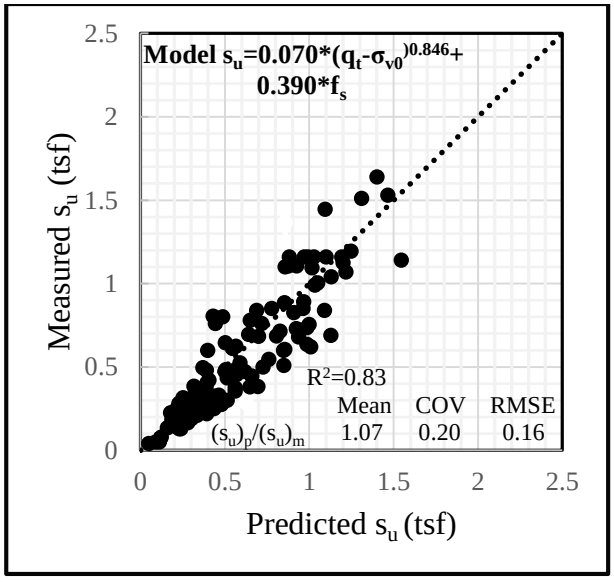

Figure 4.29: Verification of s_u model for q_t, f_s and σ_{vo}

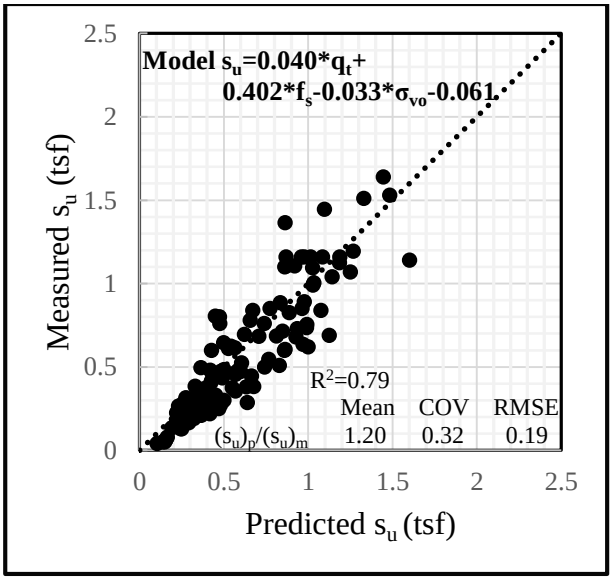

Figure 4.30: Verification of s_u model for q_t, f_s and σ_{vo}

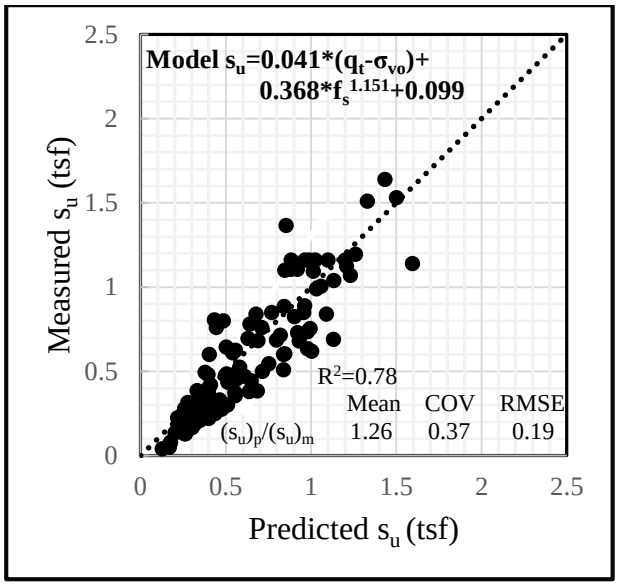

Figure 4.31: Verification of s_u model for q_t, f_s and σ_{vo}

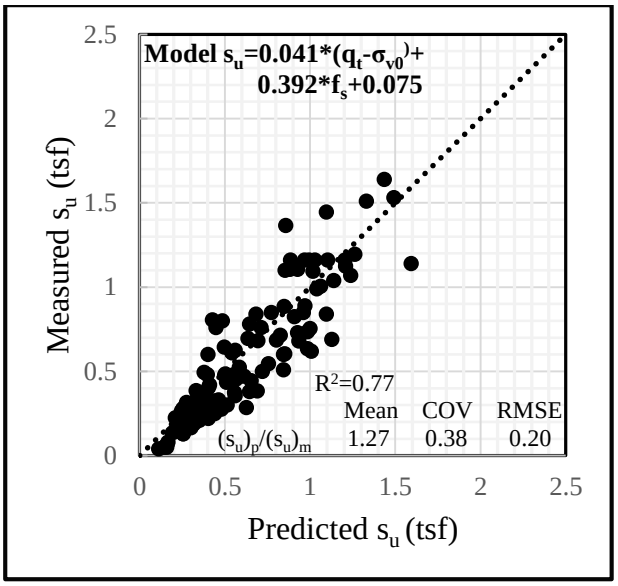

Figure 4.32: Verification of s_u model for q_t, f_s and σ_{vo}

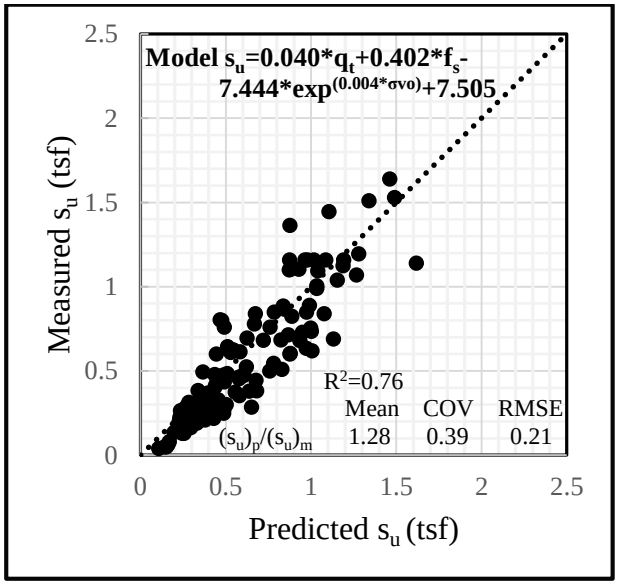

Figure 4.33: Verification of s_u model for q_t, f_s and σ_{vo}

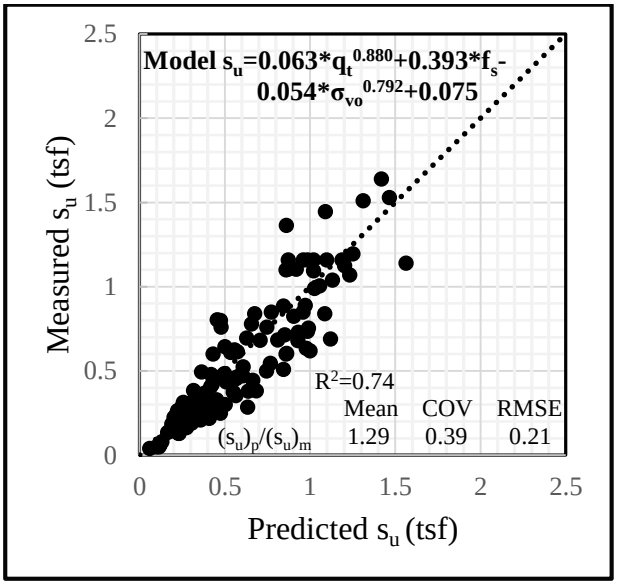

Figure 4.34: Verification of s_u model for q_t, f_s and σ_{vo}

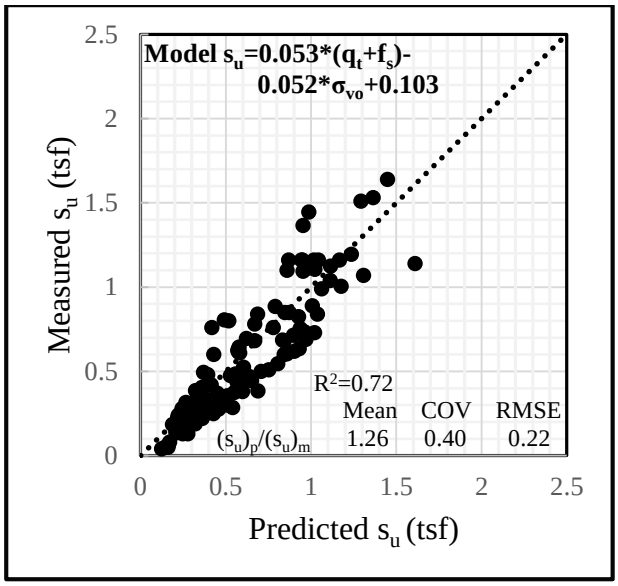

Figure 4.35: Verification of s_u model for q_t, f_s and σ_{vo}

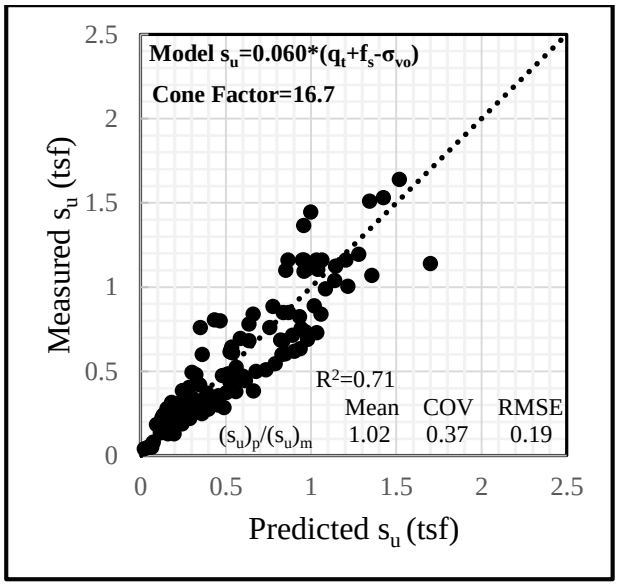

Figure 4.36: Verification of s_u model for q_t, f_s and σ_{vo}

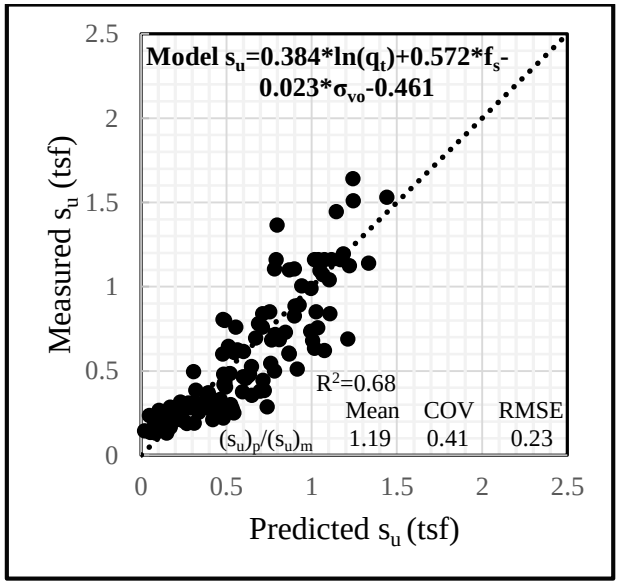

Figure 4.37: Verification of s_u model for q_t, f_s and σ_{vo}

4.3 s_u Profiles from Proposed Models

Two test sites (Bayou Boeuf Bridge and Williams Boulevard Interchange) were randomly selected that were not used for model development to draw s_u profiles from our proposed models. Then,

these s_u profiles were compared with laboratory s_u (measured) profiles (Figure 4.38 a, Figure 4.38 b). The figures clearly demonstrate that the proposed models can predict the unconsolidated undrained shear strength with good accuracy. Though, model based on the combination of cone tip resistance, sleeve friction and overburden pressure (equation 4.16) gives better s_u prediction than the other proposed.

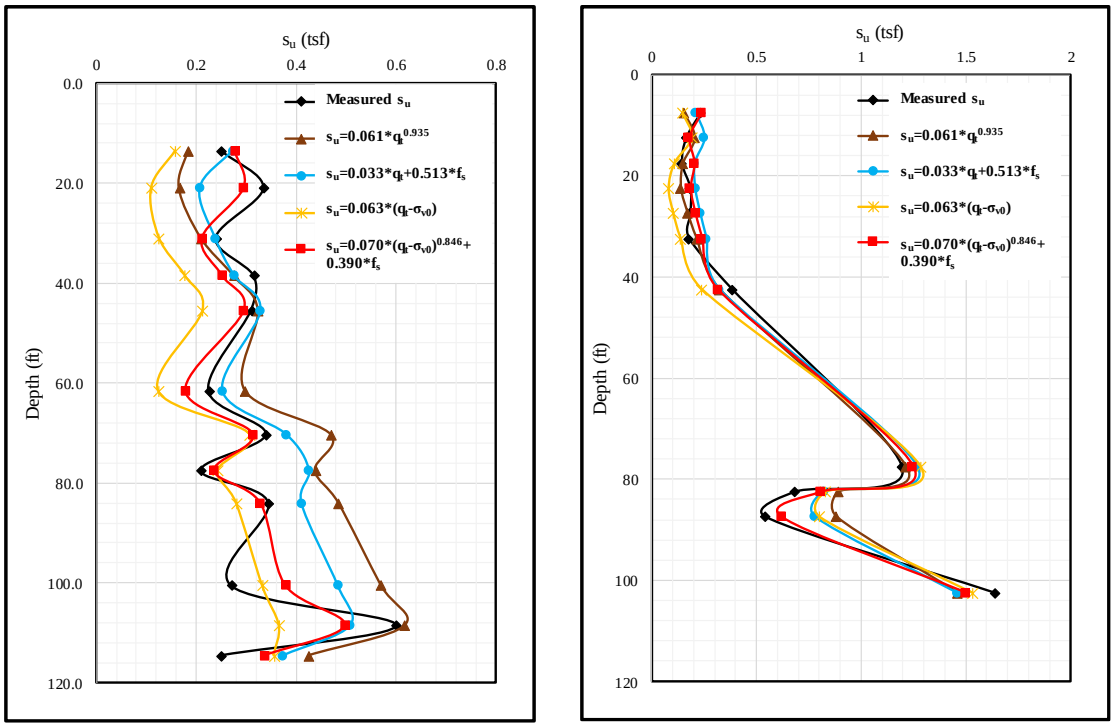

(a) (b)

Figure 4.38*:* s_u profiles from proposed models: (a) Bayou Boeuf Bridge and (b) Williams Boulevard Interchange

4.4 Possible Correlation between Cone Tip Factor and Soil Properties

The cone tip factor, N_{kt} is an indirect method for calculating the undrained shear strength of soil using equation (4.15). The cone tip factor is inversely proportional with soil shear strength. In this study, the cone tip factors were calculated for all available database. Then, an attempt was made to develop a correlation between the cone tip factor, N_{kt} and some selected soil parameters: I_p, *MC*

and *LL* for using in equation (4.15) to estimate s_u. The plot of N_{kt} with different soil parameters (*LL*, I_p, *MC*) are presented in Figure 4.39 to Figure 4.41. The plots show high scattered data with no clear trend. This means it is unlikely to have a linear or nonlinear relationship between N_{kt} and either *LL*, I_p, *MC*.

ANOVA analyses between the dependent variable (N_{kt}), and the independent variables (*LL*, I_p, *MC*) was conducted using the SAS® software. The independent variable that was not statistically significant in the model was removed, and this procedure was repeated until only significant variables were present in the model. Table 4.5 summarizes the results of the ANOVA analyses. It can be observed that the two independent variables, *LL* and *MC* were not statistically significant at a 5% significance level, and therefore they were removed from the developed N_{kt} model. Although the *P valu*e of plasticity index was significant, the high scatter plot of I_p with cone factor does not suggest a potential trend for developing acceptable N_{kt} model. Perhaps, adding another parameter like OCR (data is not available for this study) with I_p may improve the chance of obtaining a good model to predict N_{kt}.

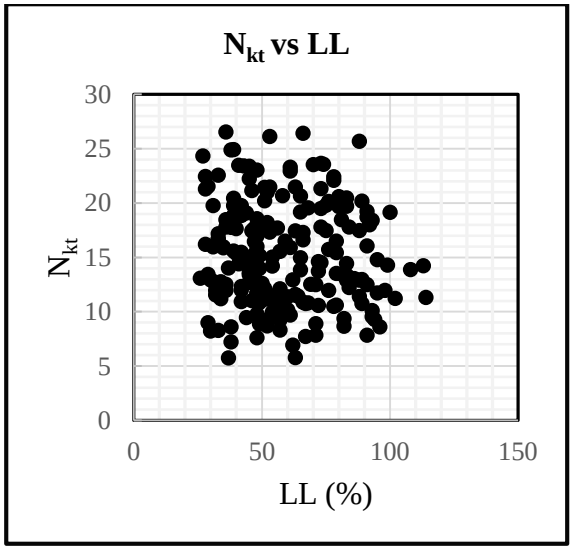

Figure 4.39: Plot of N_{kt} vs. LL

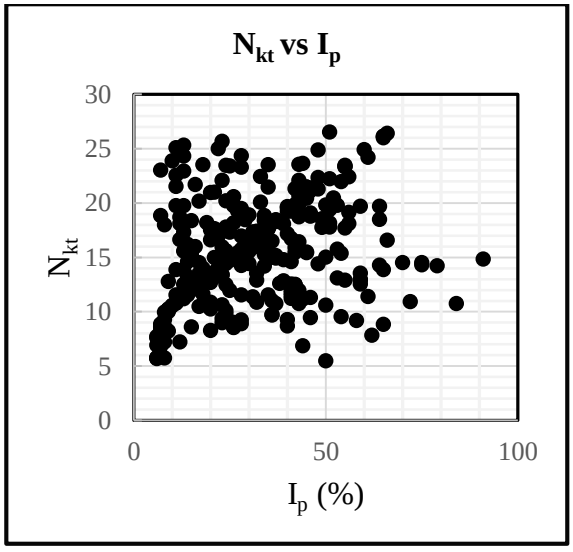

Figure 4.40: Plot of N_{kt} vs. I_p

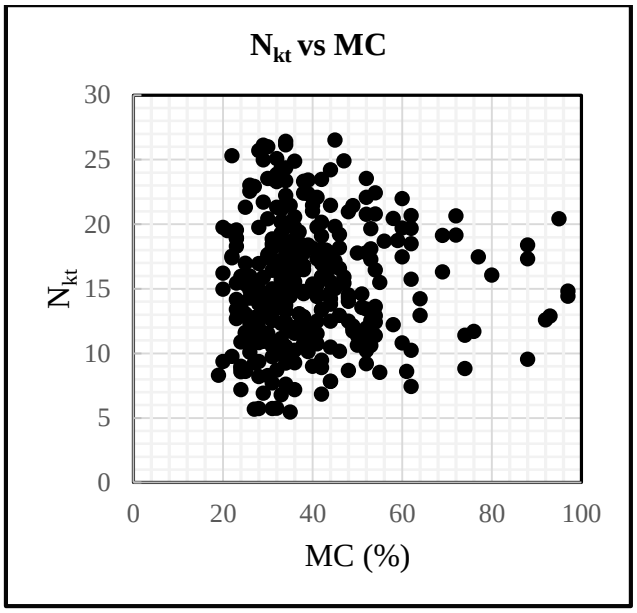

Figure 4.41: Plot of N_{kt} vs. MC

Table 4.5: Summary of ANOVA Analysis

Parameter	Estimate	Standard Error	F value	P value
LL	-0.037372722	0.02212901	3.19	0.0536
I_p	1.207793222	0.19539001	23.55	<.0001
MC	0.095054377	0.01308211	0.01	0.9033

4.5 Guidelines to Estimate Mobilized Unconsolidated Undrained Shear Strength

Previous researchers indicate that undrained shear strength tests, e.g., triaxial test or vane shear test are not always equal to mobilized shear strength ($s_{u(mob)}$) in practical failure situations (e.g., Mesri, 2001; Mesri & Huvaj, 2007). This is because undrained shear strength is usually determined by mineralogical structure, composition, and previous consolidation history, and generally influenced by mode of shear, failure time during shear, progressive yielding, and soil disturbance (Bjerrum 1973, Terzaghi et al. 1996). Therefore, the laboratory and in-situ shear strength measurements should be adjusted before they are used for foundation and stability analyses.

According to Terzaghi et al. (1996), for A quality saturated soft soils, the difference between unconfined compression shear strength ($s_{u(UC)}$) and triaxial compression shear strength $s_{u(TC)}$ can be ignored. Moreover, the UC test is a special case of the UU test. For saturated soft clays and silts, the increase in porewater pressure results from the equal increases in all-around pressure. Thus, for A quality saturated soft clays, there are no significant differences in shear strength for UC tests or UU tests (Terzaghi et al. 1996). Terzaghi et al. (1996) suggested for inorganic soft clay and silt deposits from A quality samples:

$$\frac{s_{u(TC)}}{\sigma'_p} = \frac{s_{u(UC)}}{\sigma'_p} = \frac{s_{u(UU)}}{\sigma'_p} = 0.32 \qquad (4.17)$$

where σ'_p is the pre-consolidation pressure. For UU or UC tests, the soil samples are of C to D quality as they are carried out from boreholes on Shelby tube samples. Therefore, a reduction of 70% of $s_{u(TC)}/\sigma'_p = 0.32$ equals approximately 0.22 (0.32*0.70). The 0.22 value is an estimate for the average mobilized undrained shear strength ratio for soil stability analysis (Terzaghi et al. 1996). Thus, for inorganic soft clay and silts:

$$\frac{s_{u(mob)}}{\sigma'_p} = 0.22 \qquad (4.18)$$

To compute $s_{u(mob)}$ from cone penetration test, Mesri (2001) assumed: (a) the mode of shear for cone penetration is same as triaxial compression, (b) $s_{u(cone)}$ is mobilized in around 2 seconds, (c) the degree of soil disturbance ahead of cone for in-situ CPT and for triaxial compression strength test are identical, (d) plasticity index is independent, and (e) undrained shear strength increases by 7% for each ten times decrease in time to failure. With these assumptions and using equation (4.17), Mesri & Huvaj (2007) proposed the following equation for inorganic soft clay and silt deposits:

$$N_{kt(test)} = \frac{3.57}{s_{u(test)}/\sigma'_p} \qquad (4.19)$$

Now, substituting equation (4.18) into equation (4.19): $N_{kt(mob)} = 16$. For organic soft clay and silt deposits, a similar approach form Mesri (1993) leads to the mobilized cone factor value, $N_{kt(mob)} = 16$ (Mesri & Huvaj, 2007). Thus, $s_{u(mob)}$ for stability and foundation analyses of both inorganic and organic soft clay and silt soils can be predicted from:

$$s_{u(mob)} = \frac{q_t - \sigma_{vo}}{16} \quad (4.20)$$

Equation (4.20) is identical to the developed equation from this study (Table 4.4, RM 13). In both cases, the cone factor value is 16. Therefore, by adapting Mesri (2001) assumptions, RM 13 in Table 4.4 can be used to estimate $s_{u(mob)}$ of soft clay and silt deposits for stability analyses of slopes and foundations from CPT.

4.6 Limitations of Regression Models

The regression models were developed from a database collected from DOTD. The database of this study mostly represents clayey soils in Louisiana. Thus, the proposed regression models should perform well for clayey soils of Louisiana, and other locations with similar geological conditions. However, it is recommended to follow the following guidelines at the time of using the regression models:

a) The range of q_t should be ≤50 tsf (100000 psf, 4788 kPa), the range of f_s should be ≤2 tsf (4000 psf, 191.5 kPa) and the range of σ_{vo} should be ≤9 tsf (18000 psf, 861.8 kPa), and the range of soil collection depth should be between 4 feet (1.2 meters) to 110 feet (33.5 meters).

b) Regression models should perform well for the Holocene age alluvium soil deposits. However, the regression models should provide a satisfactory estimation of s_u for Pleistocene age terraces soil deposits.

c) The regression models are developed from all types of clayey soil layers in Louisiana. Therefore, a wide range of cone factor value is observed for RM 13 in Table 4.4 with N_{kt} = 16±6, where the average N_{kt} = 16. Hence, this regression model can over predict and under predict cone factor values for some soils at a specific location. Thus, a further study is needed to classify the cone factor based on geologic history and soil classification, e.g., high plastic clays, organic clays, and fissured clays. Local correlations based on geology is preferred for estimating cone factor on specific soil types.

d) While an agreement was observed when the regression models were applied to the validation sites, there is uncertainty in applying the model to soils from other geological origins and soils with substantially different properties.

4.7 Conclusion

CPT parameters (q_t, f_s) with a laboratory soil parameter (σ_{vo}) showed the best prediction of unconsolidated undrained could not significantly estimate the s_u. Similarly, q_t with σ_{vo} also showed acceptable s_u prediction. However, no significant correlations were found between cone factor and laboratory soil parameters (e.g., moisture content, liquid limit and plasticity index). Finally, a guideline was proposed to estimate mobilized unconsolidated undrained shear strength from regression models.

CHAPTER 5
SOIL CLASSIFICATION ANALYSIS

This chapter will provide a brief overview of the modification of existing popular CPT/PCPT soil classification methods. All types of soil classification approach, e.g., experimental approach, statistical/probability approach and soil behavioral type approach were investigated. The experimental approaches are, Douglas and Olsen (1981) method and modified Schmertmann method (1978) by Tumay (1985). Moreover, Zhang and Tumay (1999) probability approach was investigated in this study. Lastly, Robertson (1990, 2009 and 2010) charts and Saye et al. (2017) chart are investigated as soil behavioral type approach. Based on the available database, three major soil types (e.g., sand, silt and clay) were modified into the existing charts. In this study corrected cone tip resistance (q_t) is used for plotting the soil classification charts. These soil classification methods are often used in many geotechnical engineering aspects.

5.1 Soil Classification Modification Criteria

A criterion was developed for this study to modify the sandy, silty, and clayey soil zones in the existing CPT/PCPT chats. For a particular soil classification chart, several lines were drawn parallel to present soil zones to select probable silty, clayey or sandy soil zones. Then, the total number of points were calculated. If the selected soil zone was dominant by the respective soil points from USCS soil classification system, the soil zone was selected as the respective soil zone. For example, the clayey zone needs to be selected. Now, the clayey soil points will be calculated in this zone (4 points in Figure 5.1). If clayey soil points are found more than 50% (here 4/7=0.57>0.57) for this zone, then this zone will be called as clayey type soil zone. Otherwise, more lines need to be drawn until more than 50% clayey soil points will be found. The procedure is represented in Figure 5.1.

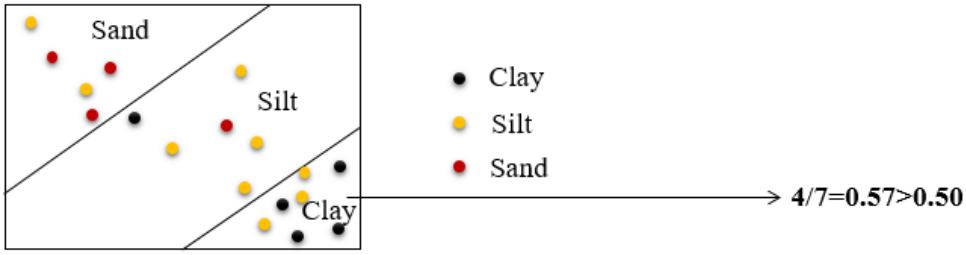

Figure 5.1: Incorporation of soil zones

5.2 Douglas and Olsen (1981) Method

Douglas and Olsen (1981) chart was based on data obtained from electric cone penetrometer. The chart also incorporates the unified soil classification (Figure 2.9). The available cone tip resistance, q_t and friction ratio, F_r data from 70 different sites of Louisiana were plotted in Douglas and Olsen (1981) chart to check the accuracy of the chart (Figure 5.2).

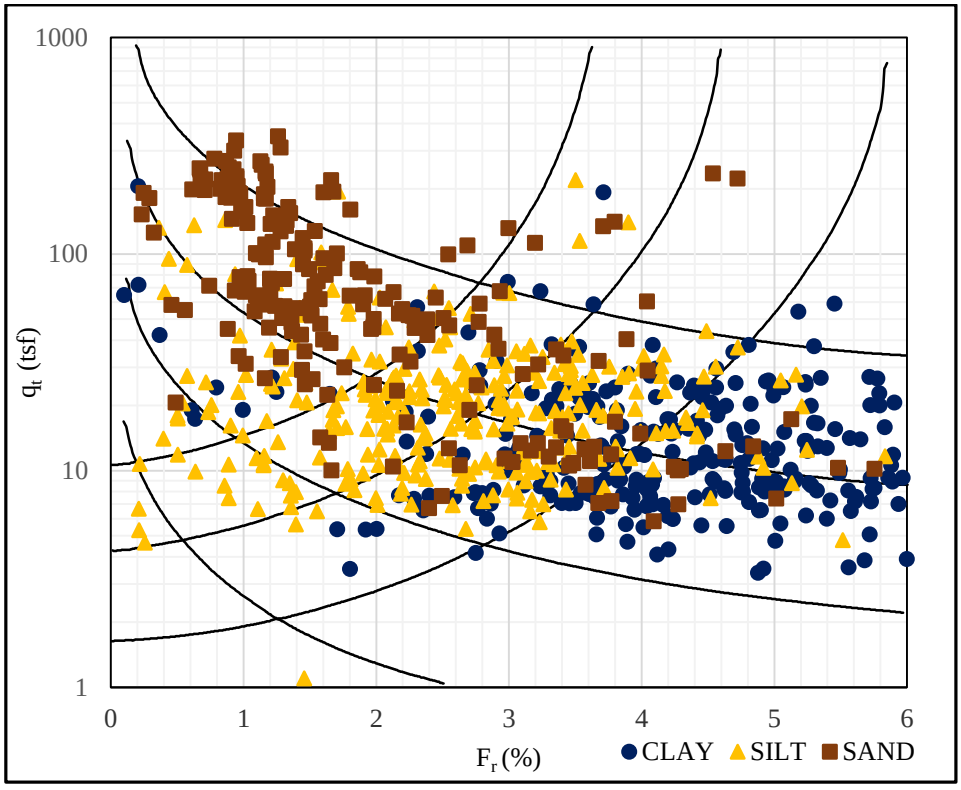

Figure 5.2: Douglas and Olsen (1981) chart with CPT data

The soil was classified based on USCS soil classification. The average q_t and f_s data were calculated from each soil layer. From Figure 5.2, it was clear that the clayey soil spreads more on left. Similarly, the sandy soil was denser on the top left zone. It was observed from Figure 5.2, the clayey zone had 70% clayey points, the silty zone had 59% silt points and the sandy zone had 55% sand points. Thus, more sifting of clayey zone was necessary. The Douglas and Olsen (1981) chart was modified (Figure 5.3) using the criterion proposed in section 5.1. The red boundaries differentiate new soil zones. In between the reds, silty soil zone exits. The new zones have now just more than 50% respective soil points (Figure 5.4). Finally, the proposed modified Douglas and Olsen (1981) chart with three basic soil types (sand, silt, clay) was represented in Figure 5.4.

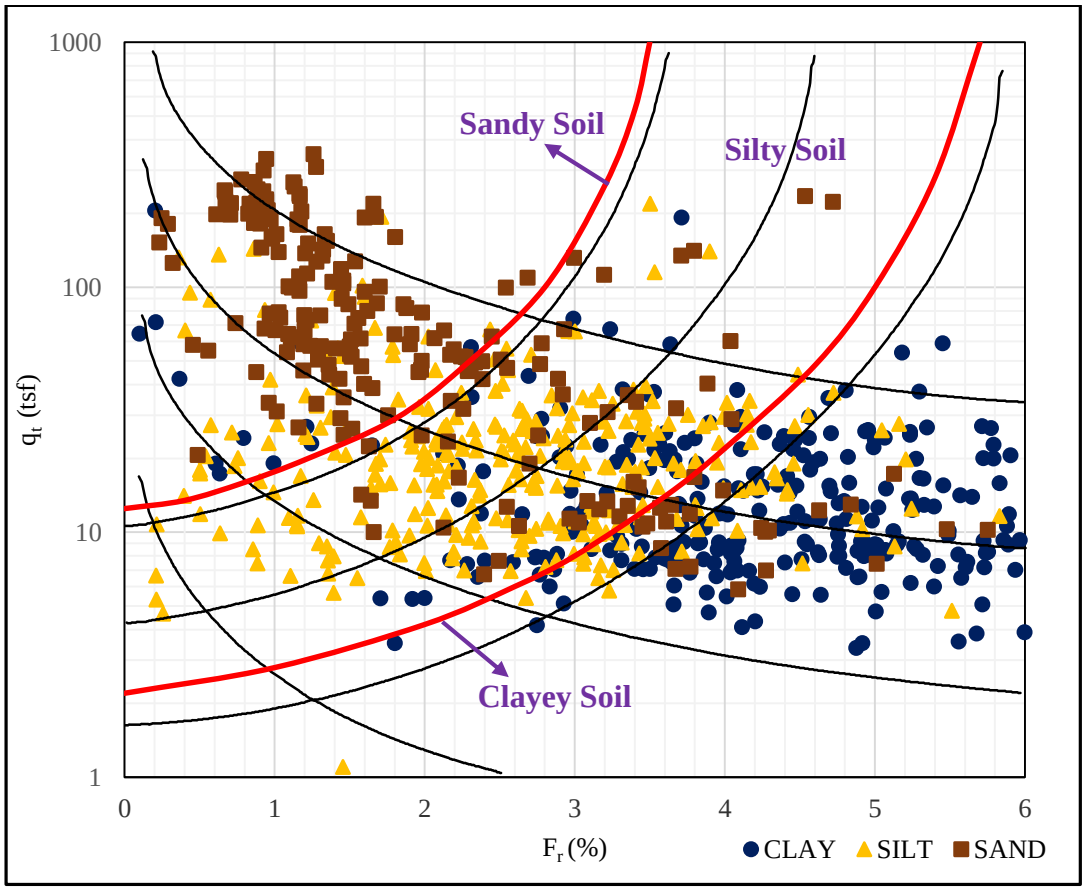

Figure 5.3: Douglas and Olsen (1981) chart with modified zone

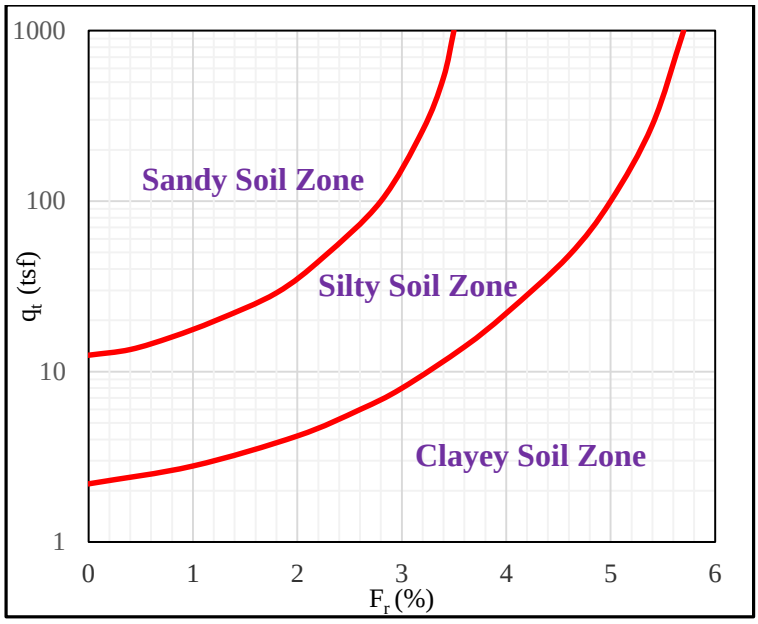

Figure 5.4: Proposed Douglas and Olsen (1981) chart

5.3 Modified Schmertmann (1985) method

Tumay (1985) modified the Schmertmann (1978) soil classification chart. He modified this chart by incorporating Douglas and Olsen (1981) soil classification chart with Schmertmann (1978) chart. The original Schmertmann (1978) was demonstrated in Figure 2.8 and the modified Schmertmann (1978) chart by Tumay (1985) was presented in Figure 2.13. Original and modified both Schmertmann chart presented the q_c as a plot against the F_r. Thus, the available q_t and F_r data from 70 different sites of Louisiana were plotted in modified Schmertmann (1978) soil classification chart by Tumay (1985) (Figure 5.5). After applying soil chart modification criterion, a new boundary was suggested to adjust the data points (Figure 5.6). Silty soil zone exists between the two red boundaries. The percentage of soil points were similar to previous Douglas and Olsen chart (Figure 5.2) as Tumay (1985) adopted Douglas and Olsen chart to modify Schmertmann (1978) chart. Finally, the proposed modified Schmertmann chart was presented in Figure 5.7 that modifies three basic soil zones.

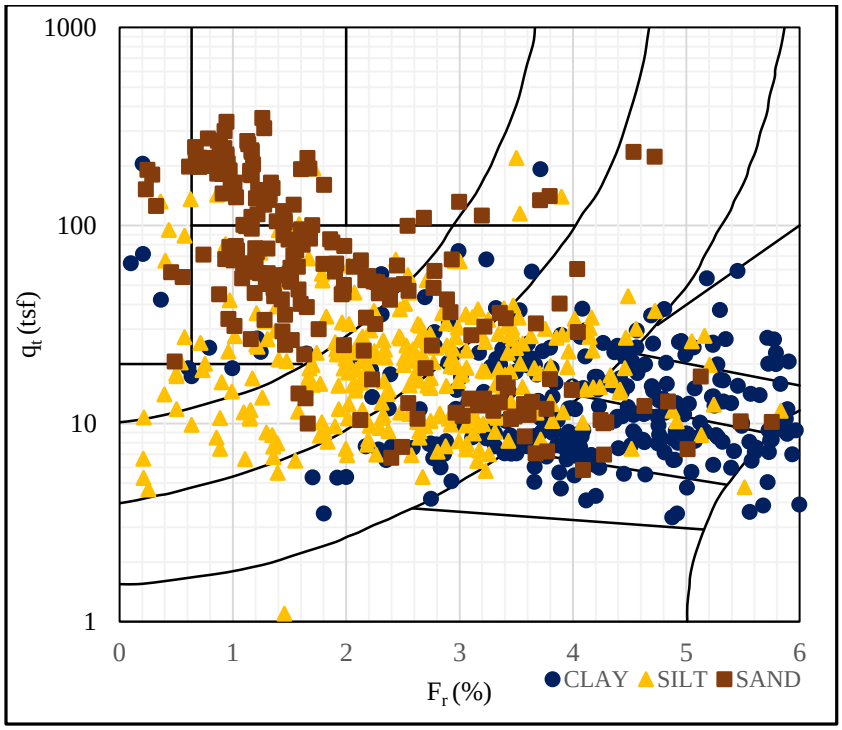

Figure 5.5: Modified Schmertmann chart with CPT data

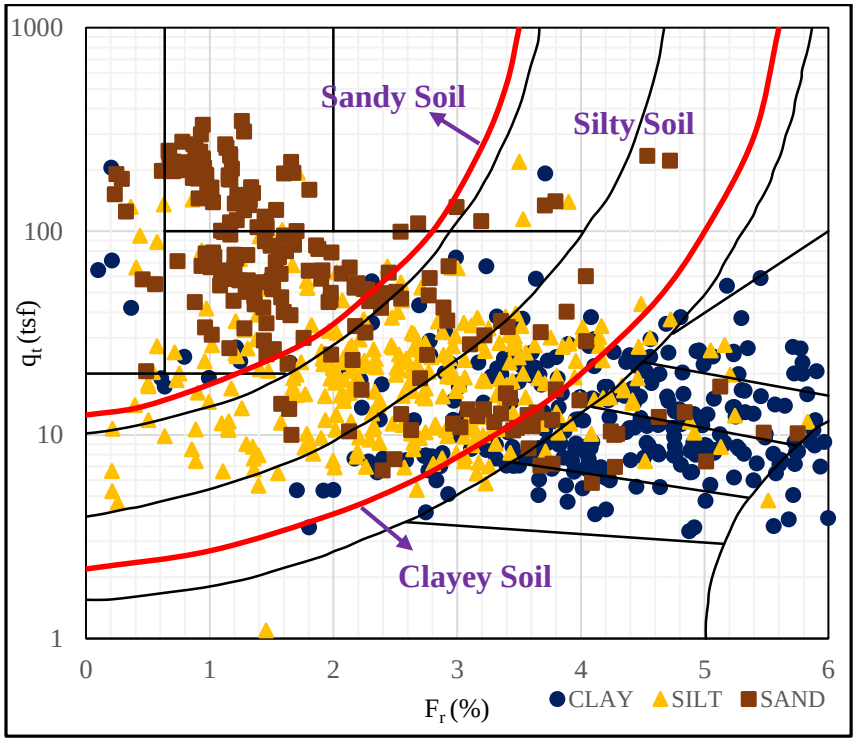

Figure 5.6: Modified Schmertmann chart with modified zone

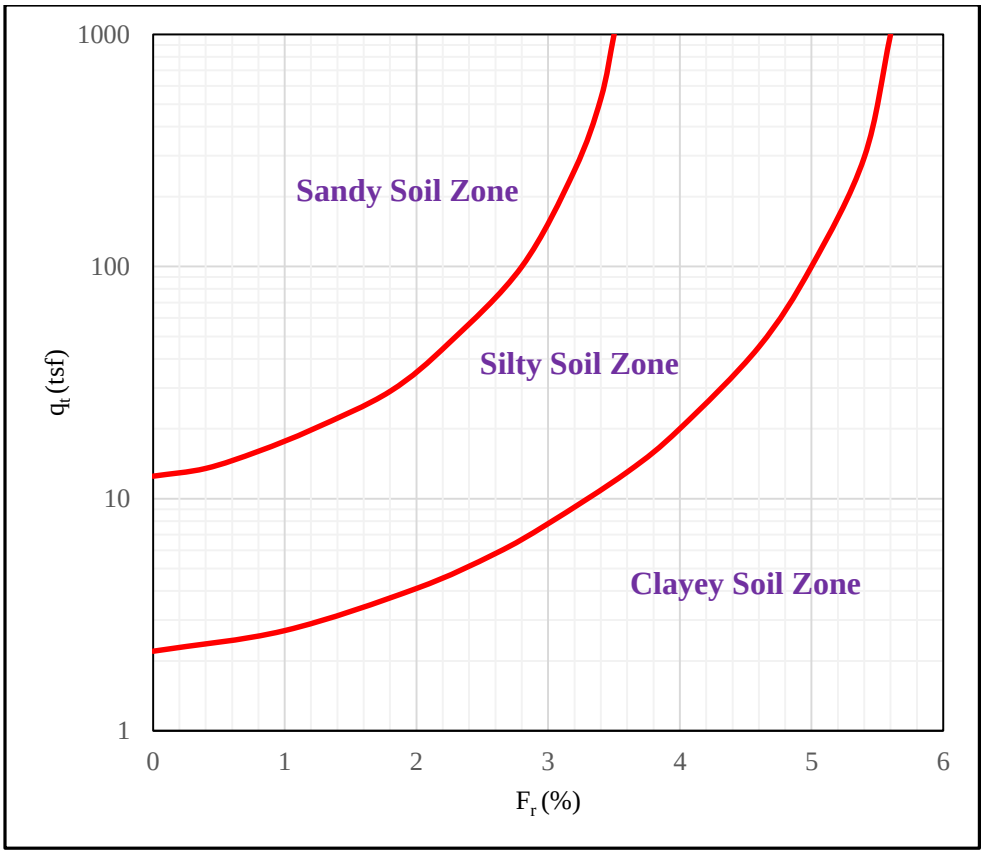

Figure 5.7: Proposed modified Schmertmann chart

5.4 Robertson (1990) Soil Classification Chart

Robertson (1990) modified his previous chart (Robertson, 1986) and defined 9 soil zones instead of 12 zones (Figure 2.18). In this chart, he first used three normalized parameters (Q, F_{rn} and B_q). However excess porewater pressure measurements were not available for most of the test locations. Therefore, only the Q - F_{rn} chart was investigated for this study. The available q_t and F_r data were normalized with respect to σ_{vo} and σ'_{vo} respectively to use in the Robertson (1990) chart. CPT/PCPT, borehole, and laboratory soil data from 70 different sites were plotted in the existing Robertson (1990) soil classification chart (Figure 5.8).

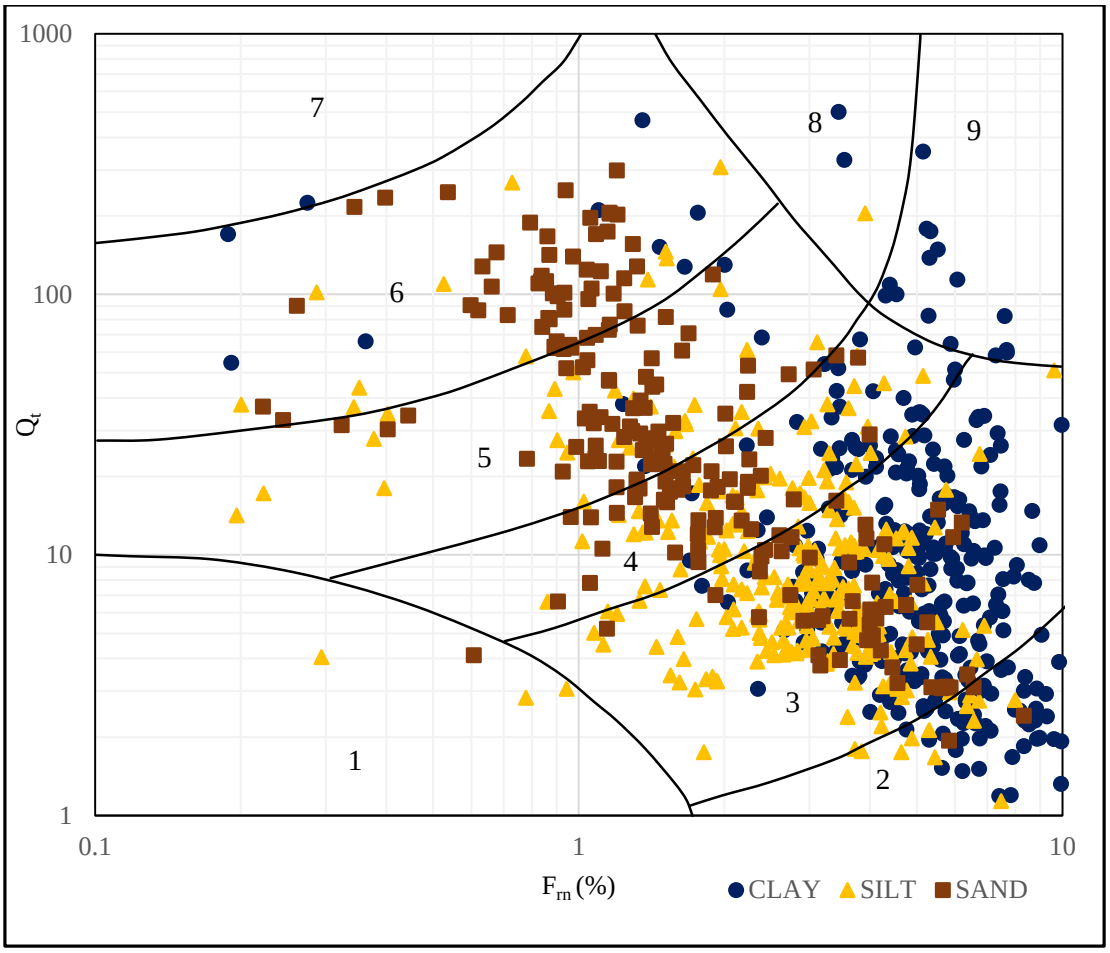

Figure 5.8: Robertson (1990) chart with CPT data

From Figure 5.8, it was clear that clayey and sandy type soil didn't fit it the zone mentioned by Robertson (1990). The clayey zone had 56% clayey points, the silty zone had 41% silt points and the sandy zone had 68% sand points. Therefore, it was necessary to adjust the soil zones according to the soil zone modification criteria. Based on USCS soil classification, the sandy, silty, and clayey type soil zone were adjusted in Robertson (1990) chart (Figure 5.9). Later, the proposed Robertson (1990) chart based on three major soil types was presented in Figure 5.10. Newly proposed zone 2 and 5 are clayey soil zones. Zone 1 and 3 are silty soil zones and zone 4 is sandy soil zone (Figure 5.10). The new proposed zones have now just more than 50% respective soil points.

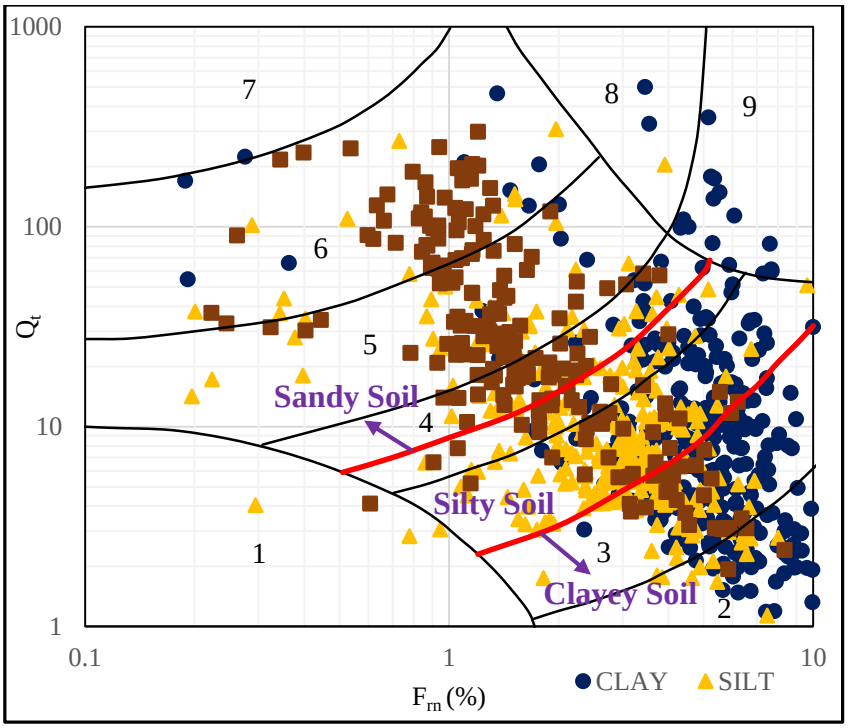

Figure 5.9: Robertson (1990) chart with modified zone

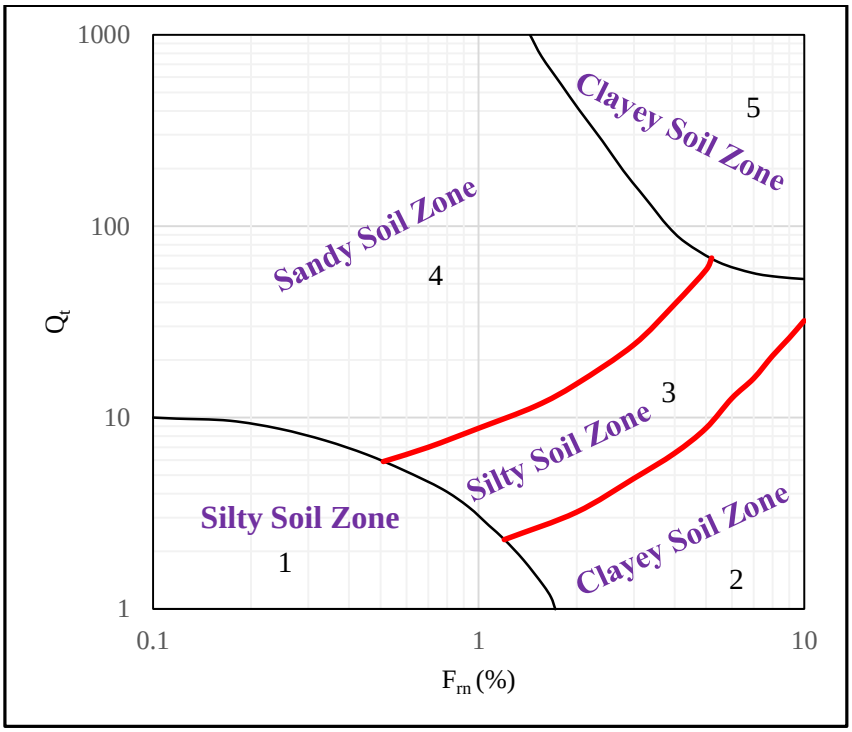

Figure 5.10: Proposed Robertson (1990) chart

5.5 Robertson (2009) Soil Classification Chart

Robertson (2009) incorporated soil behavioral type index, I_c, proposed by Jefferies & Davies (1993). This chart is similar to the Robertson (1990) chart with 9 soil boundaries. However, the new chart follows an iterative approach. It suggests soil classification based on soil behavioral. The original chart was shown in Figure 2.19 b. The exponent component, n, was calculated. Then The q_t and F_r were calculated with iterations. Then, the available data points were plotted in Robertson (2009) chart (Figure 5.11).

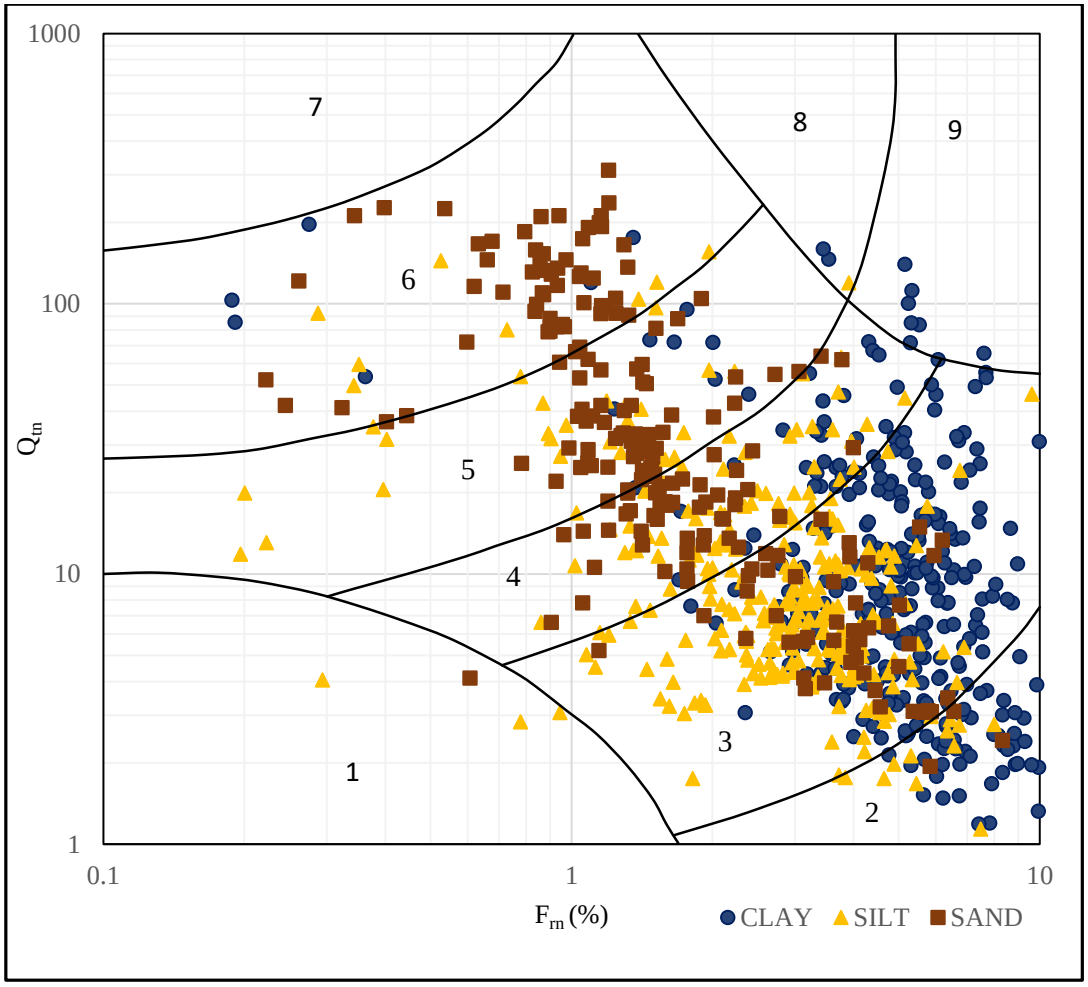

Figure 5.11: Robertson (2009) chart with CPT data

It was observed from Figure 5.11 that the silty type soil is denser in-between zone 3 and 4, however, scattered other zones. Similarly, sandy type soil was denser in zone 5 and 6 and somewhat in zone 4. On the other hand, clayey type of soil was denser on zone 2 and some portions of zone 3. In Figure 5.11, the clayey zone had 56% clayey points, the silty zone had 43% silt points and the sandy zone had 66% sand points. Therefore, a new soil boundary was suggested that modified the previous sandy, silty and clayey soil zones (Figure 5.12). Finally, the modified Robertson (2009) soil classification chart was represented in Figure 5.13. In modified Robertson (2009) soil classification chart, newly proposed zone 2 and 5 are clayey soil zones, zone 1 and 3 are silty soil zones and zone 4 is sandy soil zone. The new proposed zones have now just more than 50% respective soil points.

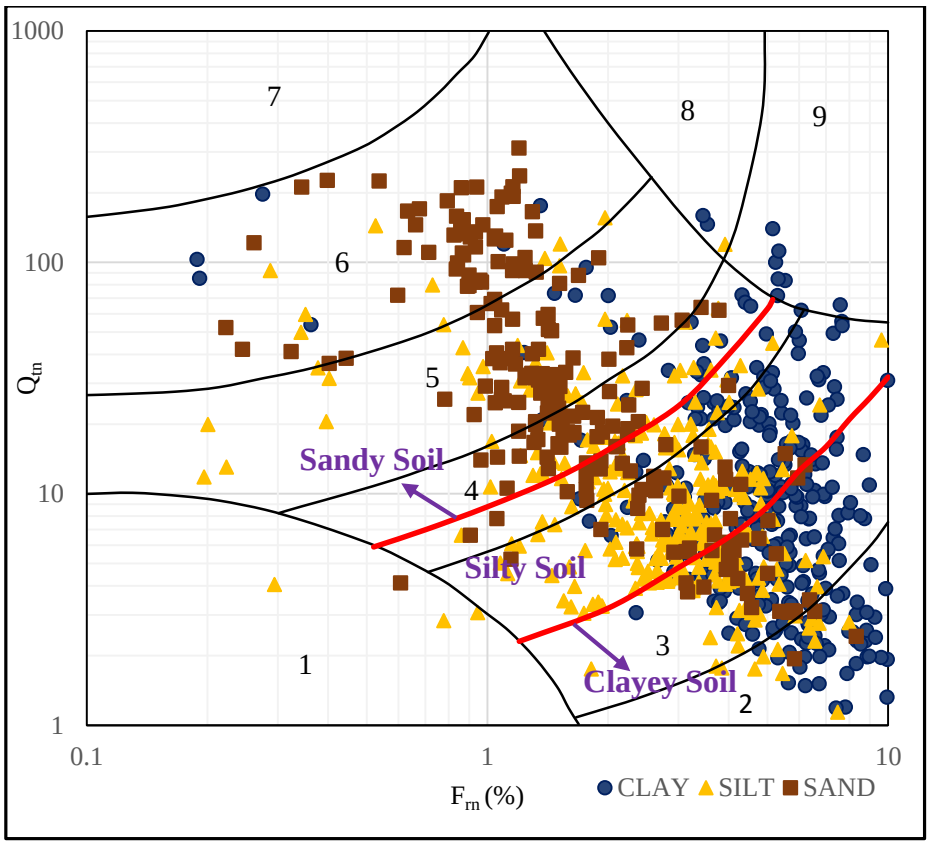

Figure 5.12: Robertson (2009) chart with modified zones

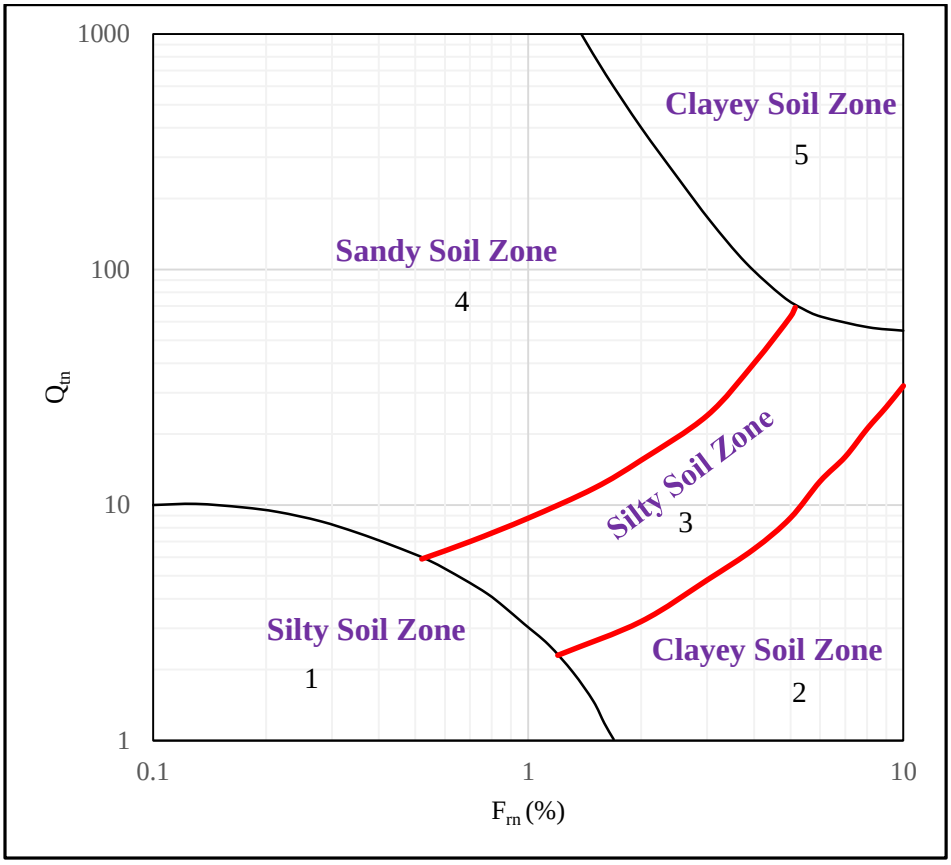

Figure 5.13: Proposed Robertson (2009) chart with CPT data

5.6 Robertson (2010) Soil Classification Chart

Robertson (2010) simplified his previous Robertson (2009) chart. The vertical axis of Robertson (2010) chart is normalized with respect to atmospheric pressure and the horizontal axis uses the F_r. The chart is global in nature and can provide reasonable predictions of soil behavior type for CPT soundings up to a reasonable depth. The original Robertson (2010) chart was shown in Figure 2.19 a. It has still 9 zones, however, it is more simple in nature. The q_t values used in tsf unit throughout the study. Thus, an atmospheric pressure of approximately 1.06 tsf was used. Then, the data points from 70 different sites were plotted in the Robertson (2010) chart with our available data points and then represented in Figure 5.14.

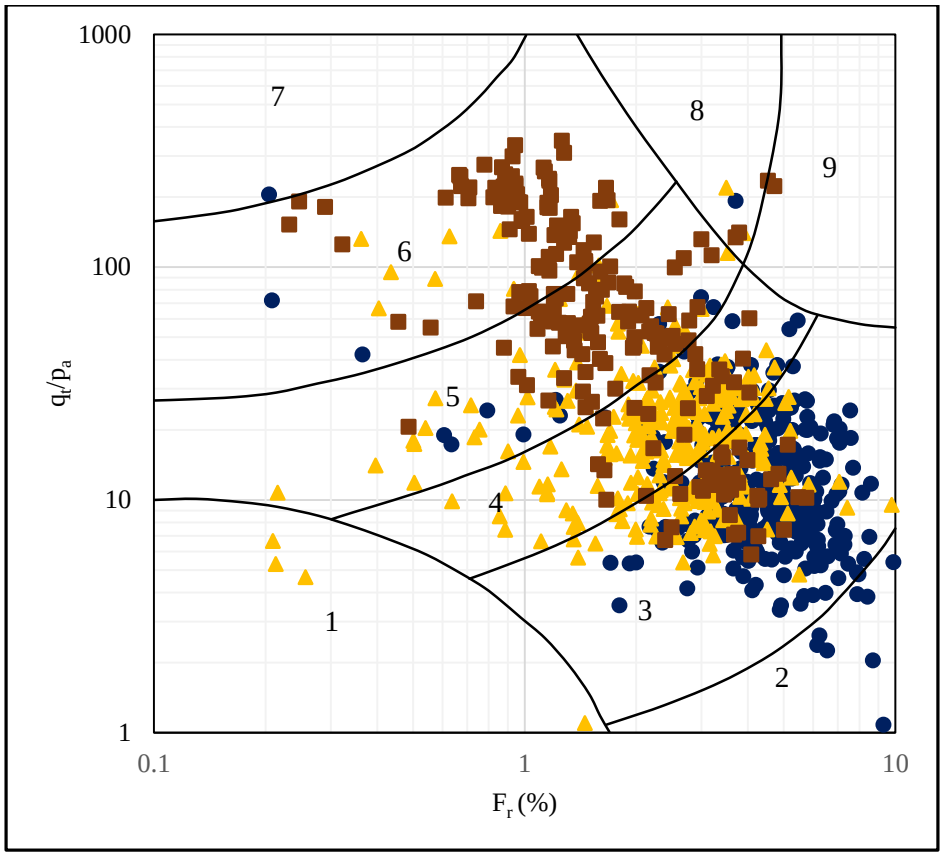

Figure 5.14: Robertson (2010) chart with CPT data

Roberson (2010) matched the data points quite well. However, still, some minor adjustments were necessary. In Figure 5.14, the silts were mainly on zone 4, however, some silty soils were also present in zone 3. Though zone 1 had only silty soils, zone 8 and 9 had mixed soils, however, sandy soils were dominant in that region. In Figure 5.14, the clayey zone had 53% clayey points, the silty zone had 54% silt points and the sandy zone had 57% sand points. Thus, new sandy, silty and clayey soil boundaries were proposed following the soil classification chart modification criterion (Figure 5.15). In modified Robertson (2010) chart, newly proposed zone 2 is clayey type soil zone, however, zone 1 and zone 3 are silty soil zones, and zone 4 and 5 are sandy soil zones (Figure 5.16). The new proposed zones have now just more than 50% respective soil points.

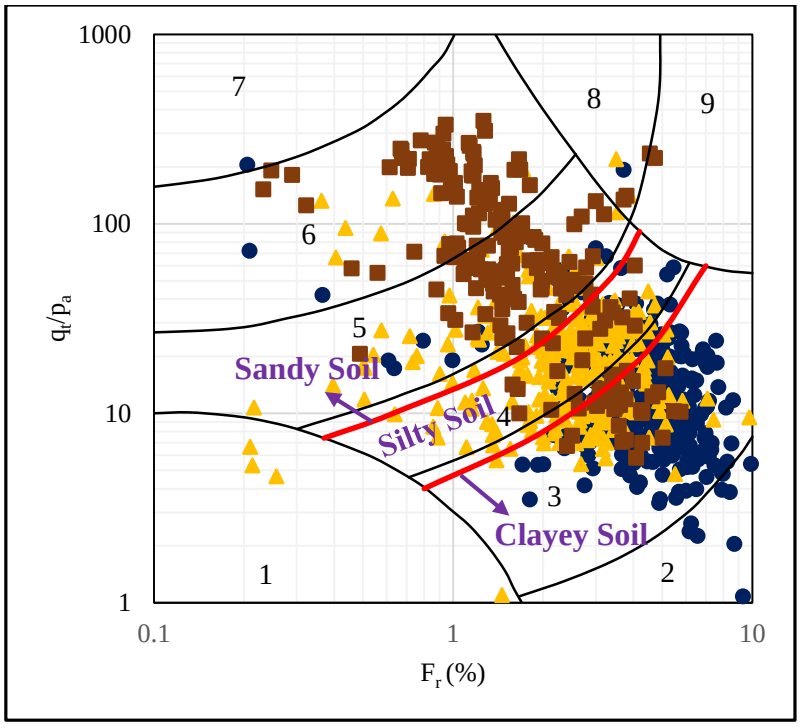

Figure 5.15: Robertson (2010) chart with modified zones

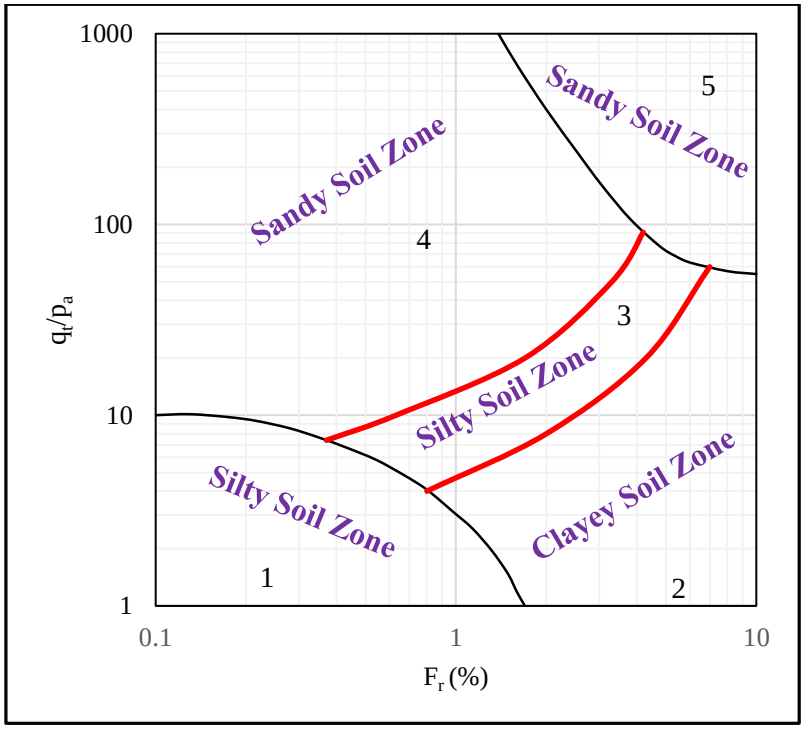

Figure 5.16: Proposed Robertson (2009) chart with CPT data

5.7 Saye et al. (2017) Soil Classification Chart

The soil classification chart of Saye et al. (2017) was based on Q_t–f_s/σ'_{vo} space and it was shown in Figure 2.25. They observed a linear relationship with a slope of Δ_Q. According to this chart, the sand percentage of the soil increases with increasing Δ_Q. If the slope is low, then the soil is clayey type soil. However, the data from 70 different sites were plotted in the Saye et al. (2017) chart (Figure 5.17).

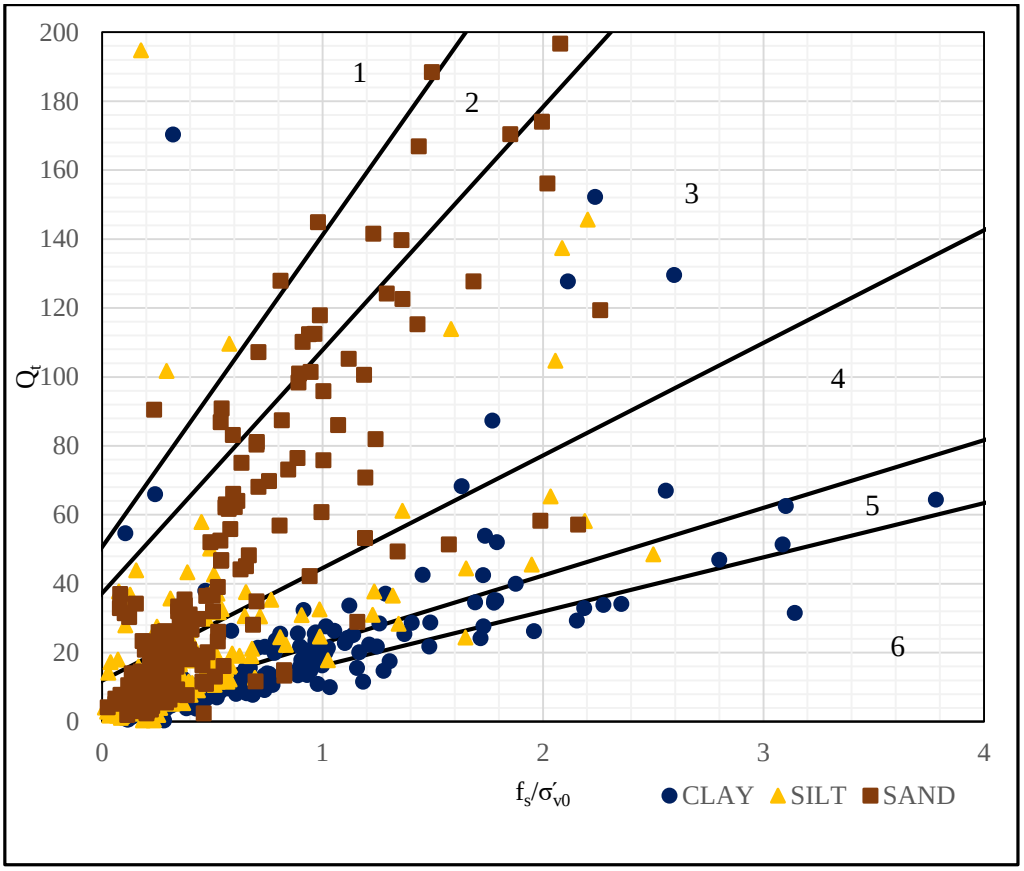

Figure 5.17: Saye et al. (2017) chart with CPT data

The plotted data points were very scattered in Figure 5.17 to modify new soil zones. Incorporating three soil type zones in Saye et al. (2017) chart was found ineffective. Too many sand data points were presented in the clayey zone and vice versa. Therefore, no attempt had been made to modify/adjust this chart.

5.8 Zhang and Tumay (1999) Probabilistic Approach

An approach was made to analyze Zhang and Tumay (1999) soil probability chart based on the available database from 70 test sites. Sandy soil layers were identified with respect to USCS soil classification and later it matched with Zhang and Tumay (1999) chart. Practically, the Zhang and Tumay (1999) chart should match well with USCS soil classification. However, it was observed in Figure 5.18 that if the soil was sandy according to USCS, the probability of soil was being sandy was quite higher. An upward trend of data frequency was observed. Similarly, in sandy soil region, a downward trend was observed for clayey and silty type soil behavior (Figure 5.19). In addition, if silty and clayey type soil behavior together was assumed as a particular type of soil behavior (i.e., silty + clayey), a linear upward frequency was observed for sandy type soil probability and linear downward frequency was observed for silty + clayey type of soil probability (Figure 5.20). Thus, the Zhang and Tumay (1999) chart provides a good estimation of sandy type soil behavior.

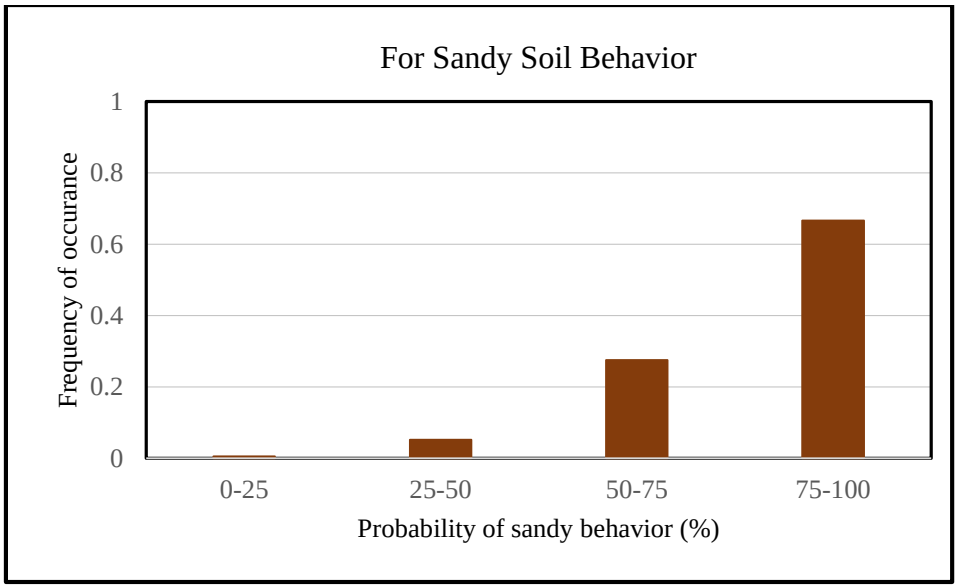

Figure 5.18: Increasing trend of probability for sandy soil behavior

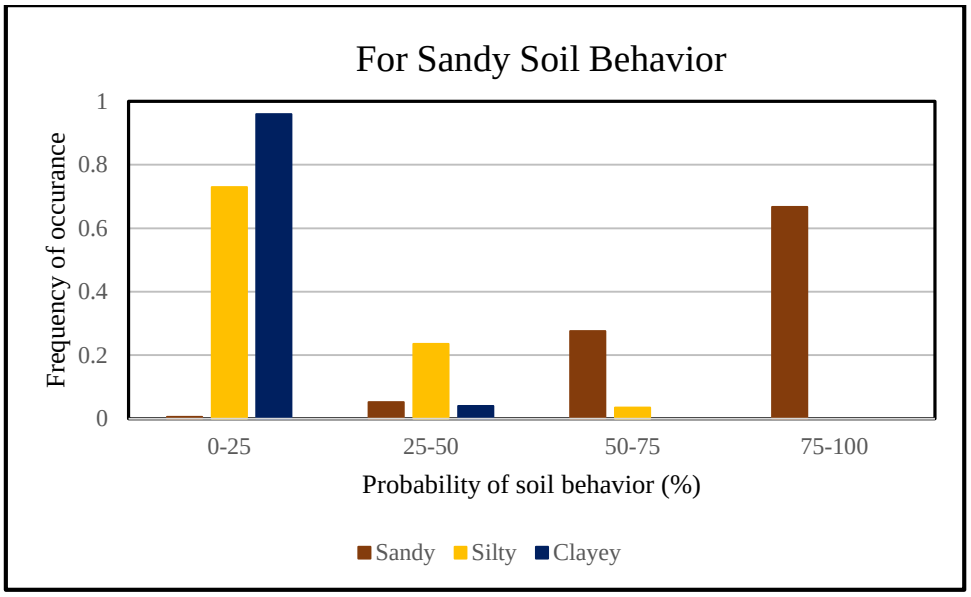

Figure 5.19: Increasing trend of probability for sandy soil behavior and decreasing trend of probability for silty, clayey soil behavior

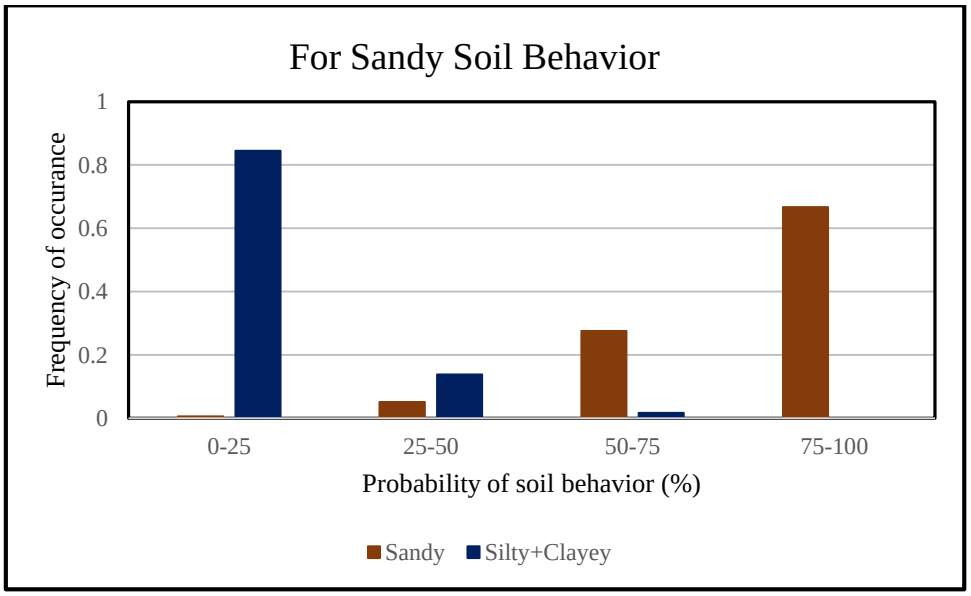

Figure 5.20: Increasing trend of probability for sandy soil behavior and decreasing trend of probability for silty + clayey soil behavior

A similar approach had been applied for the silty type of soil behavior. For silty soil behavior, an increasing trend of data frequency had been observed to a certain soil probability (75% probability of being silty soil behavior) (Figure 5.21). This is because silt is basically a mixture of sand and clay and there is nothing called 100% silt. On the other hand, a decreasing trend had been noticed for the sandy type of soil behavior. However, for the clayey type of soil, an increasing trend had been observed to a certain probability (for 50% of the soil being clayey) and then the trend decreased (Figure 5.22). This was because, when the silt percentage was low, the probability clay percentage was higher. Therefore, for silty soil behavior type, the Zhang and Tumay (1999), soil probability chart did not follow the data trends like the sandy soil behavior type. In addition, when silt and clay were considered as a same soil type entity, a decreasing trend was observed for sandy type soil, however, a steady state trend was observed for the silty + clayey soil up to 75% (Figure 5.23). That means Zhang and Tumay (1999) chart could not represent soil behavior satisfactorily when silt + clay was considered as the same soil type.

Like previous approaches, a similar trend was observed for clayey type of soil behavior. An increasing soil data trend was observed for clayey type of soil (Figure 5.24) and a decreasing trend was observed for sandy and silty soil behavioral type (Figure 5.25).

On the other hand, if silt and sand were considered as same soil type, a steady trend was observed, however, for sandy soil a decreasing trend was observed (Figure 5.26). Thus, if silt and clay were considered as a similar type of soil, Zhang and Tumay (1999) chart could not represent soil behavior perfectly. However, for sandy soil behavioral type, this method showed good prediction.

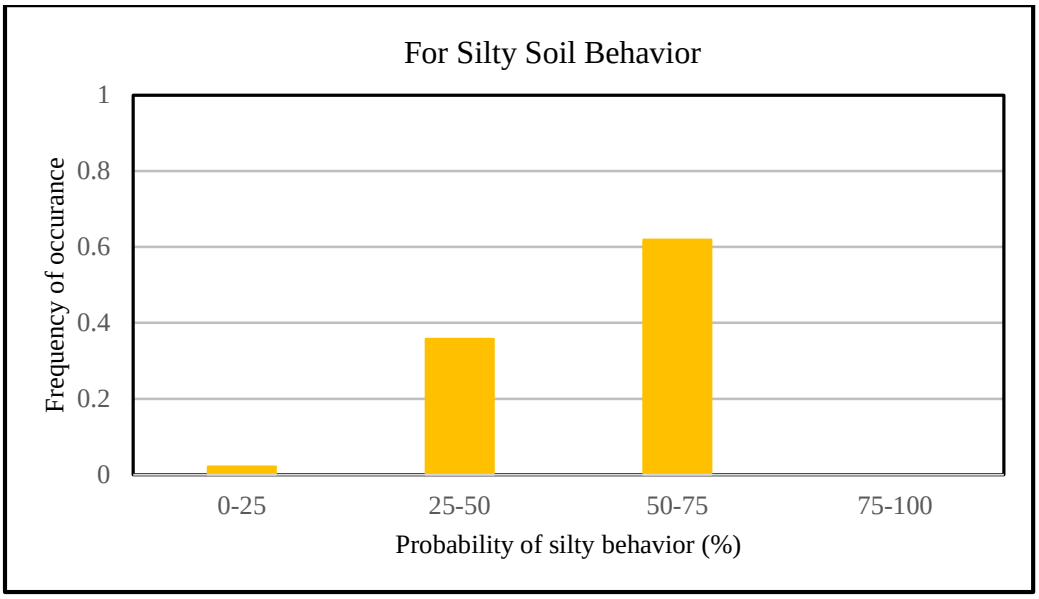

Figure 5.21: Increasing trend of probability for silty soil behavior

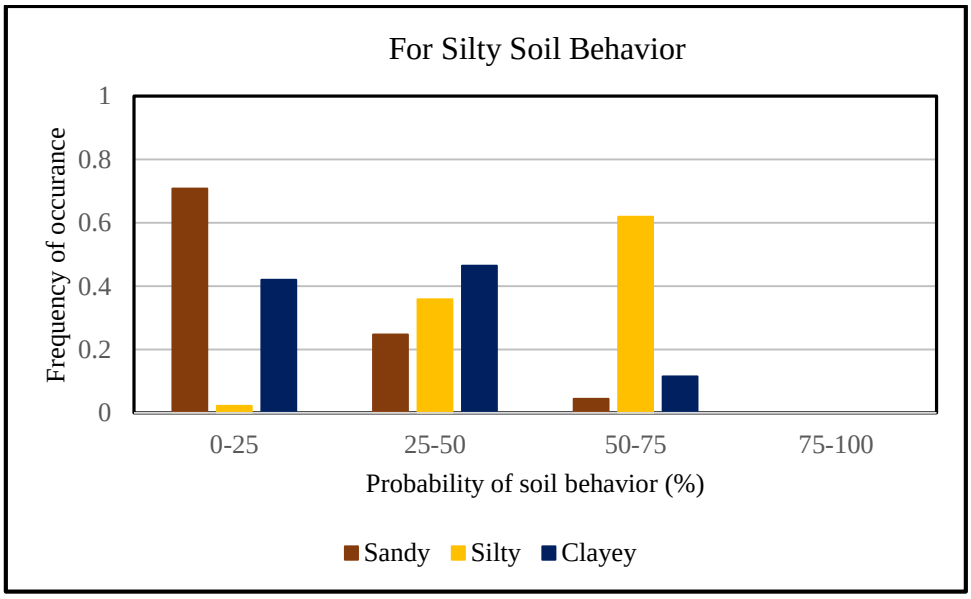

Figure 5.22: Increasing trend of probability for silty soil behavior and decreasing trend of probability for sandy, clayey soil behavior

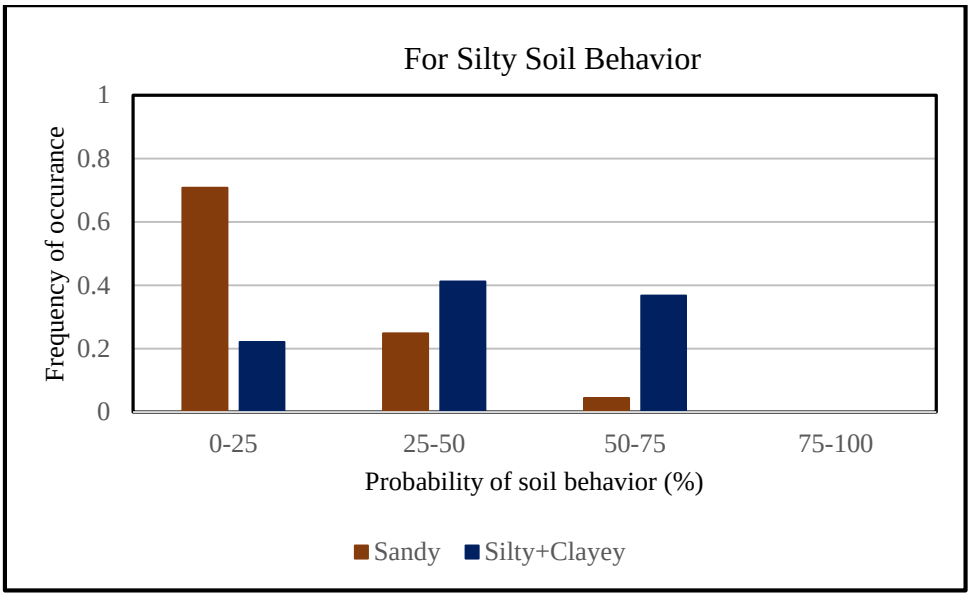

Figure 5.23 : Steady trend of probability for silty + clayey soil behavior up to 75% and decreasing trend of probability for sandy soil behavior

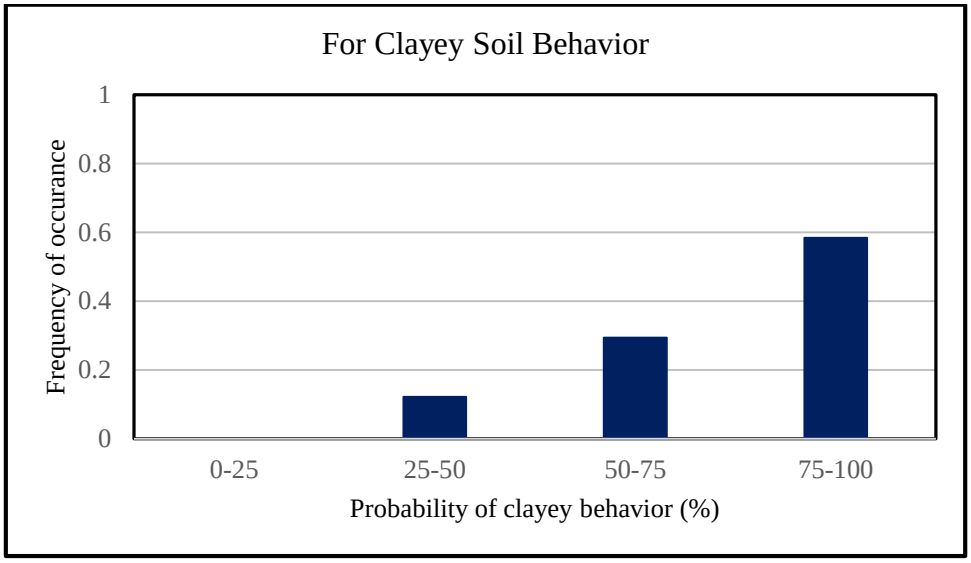

Figure 5.24 : Increasing trend of probability for clayey soil behavior

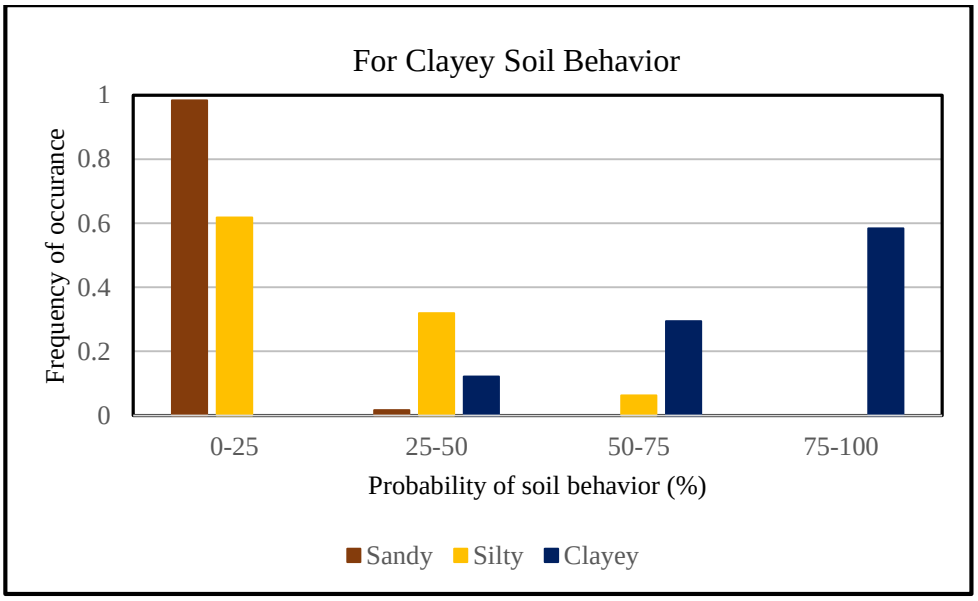

Figure 5.25 : Increasing trend of probability for clayey soil behavior and decreasing trend of probability for sandy, silty soil behavior

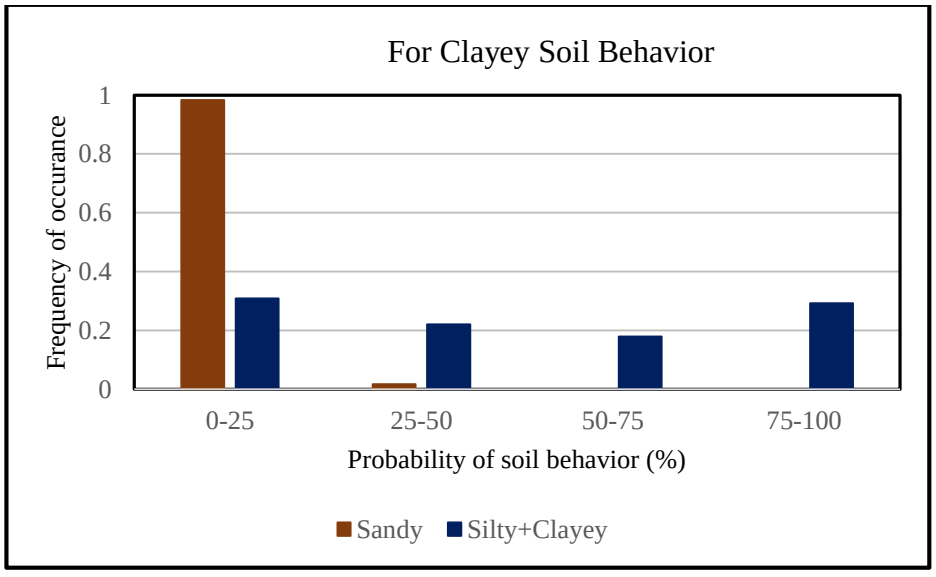

Figure 5.26 : Steady trend of probability for silty + clayey soil behavior and decreasing trend of probability for sandy soil behavior

5.9 Conclusion

To modify the three major soil type zones, e.g., sand, silt and clay, into the selected CPT/PCPT soil classification charts, some adjustments were necessary. However, Saye et al. (2017) chart exhibited many sandy and silty points in clayey zone. Similarly, sandy zone had lots of clayey and silty points. Therefore, no attempts had been made to modify the Saye et al. (2017) chart. Among the selected six soil classification charts, the Robertson (2010) chart showed the best prediction with the USCS soil classification. In addition, the Zhang and Tumay (1999) soil probability method exhibited best soil probability predictions for the clayey and the sandy soil types. However, the chart found ineffective for the identification of silty type of soils.

CHAPTER 6
CONCLUSIONS AND RECOMMENDATIONS

This thesis work investigated the possibility of utilizing the CPT/PCPT data to evaluate the undrained shear strength (s_u) of clayey soils and to adjust/modify existing CPT/PCPT based soil classification charts/methods. The s_u of clayey soil was estimated by CPT/PCPT statistical developed regression models, and comparisons were made with laboratory soil parameters. Additionally, three main soil behavior type (i.e., clayey, silty and sandy) zones had been modified in five CPT/PCPT soil classification charts according to CPT/PCPT and laboratory soil test results in Louisiana. Using CPT data for estimating the undrained shear strength and/or classifying subsurface soil will result in a cost reduction and limitation of laboratory tests.

6.1 Conclusions

The s_u of soil was evaluated using CPT data alone and in combination with other soil properties, such as overburden pressure (σ_{vo}). Moreover, an indirect approach was attempted to evaluate s_u from the cone tip factor, N_{kt}, with different soil parameters (i.e., *LL*, I_p, *MC*). In addition, an attempt was made to modify three soil type behavioral zones in some existing CPT/PCPT soil classification charts. Moreover, the Zhang and Tumay (1999) soil probability method was also investigated in the current study. Based on the findings of this study, the following conclusions can be drawn:

a) A guideline for correcting the cone tip resistance has been developed and proposed to be used whenever the measurement of excess pore water pressure is not available (i.e., no u_1, u_2 measurements with cone penetrometer).

b) An attempt was made to incorporate some soil properties (e.g., σ_{vo}, *MC*, *LL* and I_p) in the development of s_u models. The results of ANOVA analyses showed that the three parameters, *MC*, *LL* and I_p, were not statistically significant at a 5% significance level,

and therefore, they were removed from consideration in developing s_u models.

c) New correlations were developed to estimate the undrained shear strength (s_u) of clayey soil by either using the corrected cone tip resistance (q_t) alone or using the combination of CPT data (q_t, f_s) and the total overburden pressure (σ_{vo}). This study showed that using CPT parameters (q_t, f_s) with total overburden pressure (σ_{vo}) gives the best prediction of s_u measurement of the clayey soil. Using q_t alone gives quite acceptable s_u prediction. However, using f_s alone cannot predict s_u properly.

d) No significant trends were found between the cone tip factor, N_{kt}, and selected soil parameters such as liquid limit, *LL*, plasticity index, I_p, and moisture content, *MC*. Therefore, it was not possible to develop a model for N_{kt} from soil properties for use to improve the estimation of s_u using equation (4.15).

e) Three basic soil zones (e.g., clay, silt and sand) were modified in five existing CPT/PCPT soil classification charts. These charts include Douglas and Olsen (1981) chart, Modified Schmertmann chart by Tumay (1985), and Robertson (1990, 2009, 2010) charts.

f) Among the selected CPT soil classification charts, the Robertson (2010) chart showed better prediction to categorize soils for Louisiana soil data.

g) The clayey zone had many sandy and silty points in Saye et. al (2017) chart. Similarly, the sandy zone had lots of clayey and silty points. Therefore, no attempts had been made to modify this method.

h) Zhang and Tumay (1999) probability soil classification method showed better predictions for the clayey and sandy type behavior of soils. However, for the silty type behavior, the method sometimes was found to be ineffective.

6.2 Recommendations

a) The CPT correlations of s_u developed in this thesis are based on data acquired from all over Louisiana. Therefore, it is suggested that the proposed s_u correlation models are valid for Louisiana soils with certain data ranges, and for soils with similar engineering characteristics. The range of $q_t \leq 50$ tsf (4788 kPa), the range of $f_s \leq 2$ tsf (191.5 kPa) and the range of $\sigma_{vo} \leq 9$ tsf (861.8 kPa), and the range of soil collection depth should be between 4 feet (1.2 meters) to 110 feet (33.5 meters).

b) It is recommended to use advanced statistical regression analysis tools for future research accuracy and to increase the reliability of CPT/PCPT predictions. For example, use the Artificial Neural Network analysis (ANN) to improve the existing s_u correlations.

c) The database used in this study did not include pore pressure measurement in the cone. Additionally, the laboratory tests were also limited for this study. Therefore, more laboratory tests, such as consolidated undrained (c_u) triaxial tests, consolidation tests, hydraulic conductivity tests, and detailed gradation tests are recommended for future to improve calibration of the s_u correlations.

d) The literature showed that the undrained shear strength could be evaluated indirectly from cone tip factor, N_{kt} from the plasticity index and over consolidation ratio. However, for this study, the stress history was unknown. Therefore, it is recommended to measure stress history in future studies to develop indirect correlations for the estimation of undrained shear strength using N_{kt} factor and equation (4.15).

e) In future, the statistical regression models could be verified using finite element analysis.

f) More attention should be given to frequently calibrate the components that measure the tip resistance or the sleeve friction of cone in order to increase the accuracy and performance of CPT/PCPT data.

REFERENCES

Aas, G., Lacasse, S., Lunne, T., & Hoeg, K. (1986). Use of in situ tests for foundation design on clay. In *Use of In Situ Tests in Geotechnical Engineering* (pp. 1-30). ASCE.

Abu-Farsakh, M., Zhang, Z., Tumay, M., & Morvant, M. (2008). Computerized cone penetration test for soil classification: development of MS-Windows software. *Transportation Research Record: Journal of the Transportation Research Board*, (2053), 47-64.

Abu-Farsakh, M. Y. (2007). Possible evaluation of overconsolidation ratio of clayey soils from piezocone penetration tests. In *Problematic Soils and Rocks and In Situ Characterization* (pp. 1-9).

Abu-Farsakh, M., & Nazzal, M. (2005). Reliability of piezocone penetration test methods for estimating the coefficient of consolidation of cohesive soils. *Transportation Research Record: Journal of the Transportation Research Board*, (1913), 62-76.

Abu-Farsakh, M., Tumay, M., & Voyiadjis, G. (2003). Numerical parametric study of piezocone penetration test in clays. *International Journal of Geomechanics*, *3*(2), 170-181.

Abu-Farsakh, M. Y., Voyiadjis, G. Z., & Tumay, M. T. (1998). Numerical analysis of the miniature piezocone penetration tests (PCPT) in cohesive soils. *International Journal for Numerical and Analytical Methods in Geomechanics*, *22*(10), 791-818.

Alonso, E. E., Pinyol, N. P., & Fernández, P. (2016). Caisson Failure Induced by Wave Action. In *Forensic Geotechnical Engineering* (pp. 45-93). Springer, New Delhi.

Amundsen, T., Lunne, T., Christophersen, H. P., Bayne, J. M., & Barnwell, C. L. (1985). Advanced deep-water soil investigation at the Troll East Field. In *Offshore Site Investigation* (pp. 165-186). Springer, Dordrecht.

ASTM. (1992). Standard test method for classification of soils for engineering purposes. *D2487-90*.

Baligh, M.M. (1985). Strain path method. *Journal of Geotechnical Engineering*, 111(9), (pp.1108-1136).

Baligh, M. M., Vivatrat, V., & Ladd, C. C. (1980). Cone penetration in soil profiling. *Journal of Geotechnical and Geoenvironmental Engineering*, *106*(ASCE 15377).

Been, K., Crooks, J. H. A., Becker, D. E., & Jefferies, M. G. (1986). The cone penetration test in sands: part I, state parameter interpretation. *Geotechnique*, *36*(2), 239-249.

Begemann, H. K. S. (1965). The friction jacket cone as an aid in determining the soil profile. In *Proceedings of the 6th International Conference on Soil Mechanics and Foundation Engineering, ICSMFE, Montreal, September* (pp. 8-15).

Bishop, R. F., Hill, R., & Mott, N. F. (1945). The theory of indentation and hardness tests. *Proceedings of the Physical Society*, *57*(3), 147.

Broms, B. B., & Flodin, N. (1990). History of soil penetration testing: Proc 1st International Symposium on Penetration Testing, ISOPT-1, Orlando, 20–24 March 1988 V1, P157–220. Rotterdam: AA Balkema, 1988. In *International Journal of Rock Mechanics and Mining Sciences & Geomechanics Abstracts* (Vol. 27, No. 2, p. A91). Pergamon.

Brown, D. N., & Mayne, P. W. (1993). Stress history profiling of marine clays by piezocone. In *Proceedings of the 4th Canadian Conference on Marine Geotechnical Engineering, Memorial University, St. John's, Newfoundland* (Vol. 1, pp. 176-191).

Budhu, M., & Wu, C. S. (1992). Numerical analysis of sampling disturbances in clay soils. *International journal for numerical and analytical methods in geomechanics*, *16*(7), 467-492.

Cai, G., Liu, S., & Puppala, A. J. (2012). Predictions of coefficient of consolidation from CPTU dissipation tests in Quaternary clays. *Bulletin of Engineering Geology and the Environment*, *71*(2), 337-350.

Cai, G., Liu, S., & Puppala, A. J. (2011). Comparison of CPT charts for soil classification using PCPT data: Example from clay deposits in Jiangsu Province, China. *Engineering geology*, *121*(1-2), 89-96.

Cetin, K. O., & Ozan, C. (2009). CPT-based probabilistic soil characterization and classification. *Journal of Geotechnical and Geoenvironmental Engineering*, *135*(1), 84-107.

Chandler, R. J. (1988). The in-situ measurement of the undrained shear strength of clays using the field vane. In *Vane shear strength testing in soils: field and laboratory studies*. ASTM International.

Chen, B. S., & Mayne, P. W. (1994). Profiling the overconsolidation ratio of clays by piezocone tests. *Rep. No. GIT-CEEGEO-94*, *1*.

Cividini, A., & Gioda, G. (1988). A simplified analysis of pile penetration. In *Proc., 6th Int. Conf. on Numerical Methods in Geomechanics* (pp. 1043-1049).

Clausen, C. J. F., Aas, P. M., & Karlsrud, K. (2005). Bearing capacity of driven piles in sand, the NGI approach. In *Proceedings of Proceedings of International Symposium. on Frontiers in Offshore Geotechnics, Perth* (pp. 574-580).

Das, S. K., & Basudhar, P. K. (2009). Utilization of self-organizing map and fuzzy clustering for site characterization using piezocone data. *Computers and Geotechnics*, *36*(1-2), 241-248.

De Beer, E. (1977). Static cone penetration testing in clay and loam. In *Sondeer Symposium, Utrecht, 1977*.

DeJong, J. T., & Randolph, M. (2012). Influence of partial consolidation during cone penetration on estimated soil behavior type and pore pressure dissipation measurements. *Journal of Geotechnical and Geoenvironmental Engineering*, *138*(7), 777-788.

Demers, D., & Leroueil, S. (2002). Evaluation of preconsolidation pressure and the overconsolidation ratio from piezocone tests of clay deposits in Quebec. *Canadian Geotechnical Journal*, *39*(1), 174-192.

de Ruiter, J. (1971). Electric penetrometer for site investigations. *Journal of the Soil Mechanics and Foundations Division*, 97(2), 457-472.

Douglas, B. J., and Olsen, R. S. (1981). "Soil classification using electric cone penetrometer. Cone penetration testing and experience." Proc., Cone Penetration Testing and Experience, ASCE, New York, 209–227.

Durgunoglu, H. T., & Mitchell, J. K. (1975). Static penetration resistance of soils, evaluation of theory and implication for practice. *Proceedings of the in-situ measurement of soil properties, Raleigh, NC, ASCE, New York, NY*.

Eslami, A., & Fellenius, B. H. (1997). Pile capacity by direct CPT and CPTu methods applied to 102 case histories. *Canadian Geotechnical Journal*, *34*(6), 886-904.

Gebreselassie, B. (2003). Experimental, Analytical and Numerical Investigations of Excavations in Normally Consolidated Soft Soils.

Gibson, R. E. (1950). Discussion. *J. Inst. Civ. Eng*. 34, p. 382.

Gorman, J.L. and Espy, L.E. (1975). Soil survey of Fayette and Raleigh Counties, West Virginia. US *Govt. Print. Off.*

Griffiths, D. V. (1982). Elasto-plastic analyses of deep foundations in cohesive soil. *International Journal for Numerical and Analytical Methods in Geomechanics*, *6*(2), 211-218.

Hansen, J. B. (1970). A revised and extended formula for bearing capacity.

Hegazy, Y.A. (1998). Delineating geostratigraphy by cluster analysis of piezocone data. *PhD Thesis, School of Civil and Environmental Engineering, Georgia Institute of Technology, Atlanta*, 464 p.

Hong, S. J., Lee, M. J., Kim, J. J., & Lee, W. J. (2010). Evaluation of undrained shear strength of Busan clay using CPT. In *Proceedings of the 2nd International Symposium on Cone Penetration Testing, CPT* (Vol. 10).

Huang, W., Sheng, D., Sloan, S. W., & Yu, H. S. (2004). Finite element analysis of cone penetration in cohesionless soil. *Computers and Geotechnics*, *31*(7), 517-528.

ISSMFE (1989) International reference test procedure for cone penetration test (CPT). Report of the ISSMFE Technical Committee on Penetration Testing of soils- TC 16. Linkoping: Swedish Geotechnical Institute,7,6-16.

Jefferies, M. G., & Davies, M. P. (1993). Use of CPTU to estimate equivalent SPT N 60. *Geotechnical Testing Journal*, *16*(4), 458-468.

Jones, G. A. (1982). Piezometer penetration testing CUPT. In *Proceedings of the 2nd European Symposium on Penetration Testing, 1982* (pp. 607-613).

Karlsrud K, Lunne T, Brattlieu K. (1996). Improved CPTu correlations based on block samples. *Nordisk Geoteknikermote. Reykjavik.*

Keverling Buisman, A. S. (1940). Grondmechanica, new. *Balkema, fig*, *70*, 110.

Kim, H., Prezzi, M., & Salgado, R. (2010). Use of dynamic cone penetration and clegg hammer tests for quality control of roadway compaction and construction.

Kiousis, P. D., Voyiadjis, G. Z., & Tumay, M. T. (1988). A large strain theory and its application in the analysis of the cone penetration mechanism. *International Journal for Numerical and Analytical Methods in Geomechanics*, *12*(1), 45-60

Konrad, J. M., & Law, K. T. (1987). Undrained shear strength from piezocone tests. *Canadian Geotechnical Journal*, *24*(3), 392-405.

Kulhawy, F. H., & Mayne, P. W. (1990). *Manual on estimating soil properties for foundation design* (No. EPRI-EL-6800). Electric Power Research Inst., Palo Alto, CA (USA); Cornell Univ., Ithaca, NY (USA). Geotechnical Engineering Group.

Kurup, P. U., & Griffin, E. P. (2006). Prediction of soil composition from CPT data using general regression neural network. *Journal of Computing in Civil Engineering*, *20*(4), 281-289.

La Rochelle, P., Leroueil, S., Trak, B., Blais-Leroux, L., & Tavenas, F. (1988). Observational approach to membrane and area corrections in triaxial tests. In *Advanced triaxial testing of soil and rock*. ASTM International.

Ladanyi, B. (1967). Expansion of cavities in brittle media. In *International Journal of Rock Mechanics and Mining Sciences & Geomechanics Abstracts* (Vol. 4, No. 3, pp. 301-328). Pergamon.

Larsson, R., & Mulabdic, M. (1991). *Piezocone tests in clay. Swedish Geotechnical Institute, Linköping, Sweden* (No. 42). Report.

Lee, M. J., Choi, S. K., Kim, M. T., & Lee, W. (2011). Effect of stress history on CPT and DMT results in sand. *Engineering geology*, *117*(3-4), 259-265.

Levesques, C. L., Locat, J., & Leroueil, S. (2007). Characterization of postglacial sediments of the Saguenay Fjord, Quebec. *Characterization and engineering properties of natural soils, (IS-Singapore). Taylor & Francis Group, London*, *4*, 2645-2677.

Levadoux, J. N., & Baligh, M. M. (1986). Consolidation after undrained piezocone penetration. I: Prediction. *Journal of Geotechnical Engineering*, *112*(7), 707-726.

Long, M. (2008). Design parameters from in situ tests in soft ground–recent developments. In *Proceedings of the 3rd International Conference on Geotechnical and Geophysical Site Characterisation, ISC* (Vol. 3, pp. 89-116).

Louisiana Geological Survey (2010). Generalized geology of Louisiana. Baton Rouge: *Louisiana State University*.

Lunne, T., Robertson, P. K., & Powell, J. J. M. (1997). Cone penetration testing in geotechnical practice. Blackie Academic. Chapman.

Lunne, T., Powell, J. J., & Robertson, P. K. (2014). *Cone penetration testing in geotechnical practice*. CRC Press.

Lunne, T., & Kleven, A. (1981). Role of CPT in North Sea foundation engineering. In *Cone penetration testing and experience* (pp. 76-107). ASCE.

Lunne, T., Eide, O. and Ruiter, J.D. (1976). Correlations between cone resistance and vane shear strength in some Scandinavian soft to medium stiff clays. *Canadian Geotechnical Journal*, 13(4), 430-441.

Marr, L. S., & Endley, S. N. (1981). Offshore geotechnical investigation using cone penetrometer. In *Offshore technology conference*. Offshore Technology Conference.

Masood, T., & Mitchell, J. K. (1993). Estimation of in situ lateral stresses in soils by cone-penetration test. *Journal of geotechnical engineering*, 119(10), 1624-1639.

Massarsch, K.R. and Broms, B.B. (1981). Pile driving in clay slopes. *International Conference on Soil Mechanics and Foundation Engineering, Stockholm*, Vol. 3, 469-474.

Mayne, P. W. (2014). Interpretation of geotechnical parameters from seismic piezocone tests. In *Proceedings of 3rd International Symposium on Cone Penetration Testing, CPT14, Las Vegas, Nevada, Gregg Drilling & Testing, Inc*. www. cpt14. com.

Mayne, P. W. (2007). *Cone penetration testing* (Vol. 368). Transportation Research Board.

Mayne, P. W., & Campanella, R. G. (2005, September). Versatile site characterization by seismic piezocone. In *Proceedings of the International Conference on Soil Mechanics and Geotechnical Engineering* (Vol. 16, No. 2, P. 721). AA Balkema Publishers.

Mayne, P. W., Christopher, B. R., & DeJong, J. (2001). Manual on subsurface investigations. *Nat. Highway Inst. Sp. Pub. FHWA NHI-01–031. Fed. Highway Administ, Washington, DC*.

Mayne, P. W., Schneider, J. A., Yu, H. S., & Mitchell, J. K. (1999). Analysis of Cone Resistance: Review of Methods. *Journal of Geotechnical and Geoenvironmental Engineering*, *125*(9), 812-814.

Mayne, P. W., & Rix, G. J. (1993). G max-qc relationships for clays. *Geotechnical Testing Journal*, *16*(1), 54-60.

Mayne, P.W., Kulhawy, F.H., and Kay, J.N. (1990). "Observations on the development of pore water pressures during piezocone tests in clays". Canadian Geotechnical Journal, Vol. 27 (4), 418-428.

Mesri, G., & Huvaj, N. (2007). Shear strength mobilized in undrained failure of soft clay and silt deposits. In *Advances in Measurement and Modeling of Soil Behavior* (pp. 1-22).

Mesri, G. (2001). Undrained shear strength of soft clays from push cone penetration test. *Geotechnique*, *51*(2).

Meyerhof, G. G. (1951). The ultimate bearing capacity of foudations. *Geotechnique*, *2*(4), 301-332.

Mitchell, J.K. and Brandon, T.L. (1998). Analysis and use of CPT in earthquake and environmental engineering, Keynote Lecture, *Proceedings of ISC'98*, Vol.1, 69-97.

Molle, J. (2005). The accuracy of the interpretation of CPT-based soil classification methods in soft soils. *Delft University of Technology*.

Moss, R. E., Seed, R. B., & Olsen, R. S. (2006). Normalizing the CPT for overburden stress. *Journal of Geotechnical and Geoenvironmental Engineering*, *132*(3), 378-387.

Newcomb, D. E., & Birgisson, B. (1999). *Measuring in situ mechanical properties of pavement subgrade soils* (Vol. 278). Transportation Research Board.

Oliveira, J. R., Almeida, M. S., Motta, H. P., & Almeida, M. C. (2010). Influence of penetration rate on penetrometer resistance. *Journal of Geotechnical and Geoenvironmental Engineering*, *137*(7), 695-703.

Olsen, R. S., and Malone, P. G. (1988). "Soil classification and site characterization using the cone penetrometer test." Penetration testing 1988, Proc., First Int. Symp. on Penetration Testing ISOPT-1, J. De Ruiter, ed., A. A. Balkema, Rotterdam, The Netherlands, 887–893.

Olsen, R. S., and Koester, J. P. (1995). "Prediction of liquefaction resistance using the CPT." Proc., Int. Symp. on Cone Penetration Testing, CPT 95, 251–256.

Olsen, R. S. and Mitchell, J. K. (1995). "CPT stress normalization and prediction of soil classification." Proc., Int. Symp. on Cone Penetration Testing, CPT 95, Linkoping, Sweden, 257–262.

Pamukcu, S., & Fang, H. Y. (1989). Development of a chart for preliminary assessments in pavement design using some in situ soil parameters. *Transportation Research Record*, *1235*, 38-44.

Pant, R. R. (2007). Evaluation of consolidation parameters of cohesive soils using PCPT method.

Powell, J. J. M., Quarterman, R. S. T., & Lunne, T. (1989). Interpretation and use of the piezocone test in UK clays. In *Penetration testing in the UK: Proceedings of the geotechnology conference organized by the Institution of Civil Engineers and held in Birmingham on 6–8 July 1988* (pp. 151-156). Thomas Telford Publishing.

Pradhan, T. B. (1998). Soil identification using piezocone data by fuzzy method. *Soils and foundations*, *38*(1), 255-262.

Prandlt, L. (1921). Eindringungsfestigkeit und Festigkeit von Schneiden. Z. Angew. *Math. Mech*. 1,15.

Rad, N. S., Sollie, S., Lunne, T., & Torstensson, B. A. (1988). A new offshore soil investigation tool for measuring the in-situ coefficient of permeability and sampling pore water and gas. *Norwegian Geotechnical Institute Publication*, (176).

Randolph, M. F., Carter, J. P., & Wroth, C. P. (1979). Driven piles in clay—the effects of installation and subsequent consolidation. *Geotechnique*, *29*(4), 361-393.

Rémai, Z. (2013). Correlation of undrained shear strength and CPT resistance. *Periodica Polytechnica. Civil Engineering*, *57*(1), 39.

Robertson, P. K. (2016). Cone penetration test (CPT)-based soil behaviour type (SBT) classification system—an update. *Canadian Geotechnical Journal*, *53*(12), 1910-1927.

Robertson, P.K. and Cabal, K.L. (2015). Guide to cone penetration testing for geotechnical engineering. edn. Martinez, *California, Gregg Drilling & Testing Inc*.

Robertson, P.K. & Cabal, K. L. (2012). Guide to Cone Penetration Testing for Geotechnical Engineering.

Robertson, P. K., & Cabal, K. L. (2010). Guide to cone penetration testing for geotechnical engineering. *Gregg Drilling & Testing*.

Robertson, P. K. (2010). Soil behaviour type from the CPT: an update. In *2nd international symposium on cone penetration testing, USA* (pp. 9-11).

Robertson, P. K. (2009). Interpretation of cone penetration tests—a unified approach. *Canadian geotechnical journal*, *46*(11), 1337-1355.

Robertson, P. K., and Wride, C. E. (1997). Cyclic liquefaction and its evaluation based on the SPT and CPT. *Proc., NCEER Workshop on Evaluation of Liquefaction Resistance of Soil*, 41–87.

Robertson, R. (1992a). *Globalization: Social theory and global culture* (Vol. 16). Sage.

Robertson, P. K. (1990). Soil classification using the CPT. *Can. Geotech. J.*, 27(1), 151–158.

Robertson, P. K., & Campanella, R. G. (1988). Guidelines for geotechnical design using CPT and CPTU data. *Civil Engineering Department, University of British Columbia*.

Robertson, P. K., and Wride, C. E. (1998). Evaluating cyclic liquefaction potential using the cone penetration test. *Can. Geotech. J.*, 35(3), 442–459.

Robertson, P. K., Campanella, R. G., Gillespie, D., and Greig, J. (1986). Use of piezometer cone data. *Proc., In Situ '86: Use of In Situ Tests in Geotechnical Engineering, ASCE, New York*, 1263–1280.

Robertson, P.K., R.G. Campanella, and A. Wightman. (1983). SPT–CPT Correlations. *Journal of the Geotechnical Engineering Division*, Vol. 108, No. GT 11, pp. 1449–1459.

Salgado, R., Lyamin, A. V., Sloan, S. W. and Yu, H. S. (2004). Two- and three dimensional bearing capacity of foundations in clay, *Géotechnique* 54 (5), 297-306.

Salgado, R. and Randolph, M.F. (2001). Analysis of cavity expansion in sand. International Journal of *Geomechanics*, 1(2), 175-192.

Salgado, R., Boulanger, R. W., & Mitchell, J. K. (1997). Lateral stress effects on CPT liquefaction resistance correlations. *Journal of geotechnical and geoenvironmental engineering*, *123*(8), 726-735.

Salgado, R. (1993). Analysis of penetration resistance in sands. *University of California, Berkeley*.

Sandven, R. (1990). Strength and deformation parameters of fine-grained soils determined from piezocone tests. *Department of Geotechnical Engineering, NTNU (former NTH), Trondheim, Norway. PhD thesis 1990, 3*.

Sanglerat, G., Nhim, T. V., Sejourne, M., and Andina, R. (1974). Direct soil classification by static penetrometer with special friction sleeve. *Proceedings of the First European Symposium on Penetration Testing, ESOPT-1*, June 5 - 7, Stockholm, Vol. 2.2, pp. 337 - 344.

Sanglerat, G. (1972). The Penetrometer and Soil Exploration; Interpretation of Penetration Diagrams—*Theory and Practice. Elsevier, Amsterdam*, pp. 464.

Schmertmann, J. H. (1978). Guidelines for cone test, performance, and design. *Federal Highway Administration, Report FHWA-TS-78209, Washington*, 145 p.

Saye, S. R., Santos, J., Olson, S. M., & Leigh, R. D. (2017). Linear Trendlines to Assess Soil Classification from Cone Penetration Test Data. *Journal of Geotechnical and Geoenvironmental Engineering*, *143*(9), 04017060.

Schneider, J. A., Hotstream, J. N., Mayne, P. W., & Randolph, M. F. (2012). Comparing CPTU Q–F and Q–Δ u 2/σv0′ soil classification charts. *Géotechnique Letters*, *2*(4), 209-215.

Schneider, J. A., & Moss, R. E. S. (2011). Linking cyclic stress and cyclic strain based methods for assessment of cyclic liquefaction triggering in sands. *Géotechnique Letters*, *1*(April-June), 31.

Senneset, K., Sandven, R., & Janbu, N. (1989). Evaluation of soil parameters from piezocone tests. *Transportation Research Record*, (1235).

Senneset, K., and Janbu, N. (1985). Shear strength parameters obtained from static cone penetration tests. *Proc., Strength Testing of Marine Sediments; Laboratory and in situ Measurement, ASTM Special Technical Publication, STP* 883, 41–54.

Senneset, K. (1982). Strength and Defomation parameters form cone penetortion. *ESOPT II*, 863-870.

Song, C. R., & Voyiadjis, G. Z. (2005). Pore pressure response of saturated soils around a penetrating object. *Computers and Geotechnics*, *32*(1), 37-46.

Teh, C.I. and Houlsby, G.T. (1991). An analytical study of the cone penetration test in clay. *Geotechnique*, 41(1), 17-34.

Terzaghi, K., Peck, R. B., & Mesri, G. (1996). *Soil mechanics in engineering practice*. John Wiley & Sons.

Terzaghi, K. (1943). Theory of consolidation. *John Wiley & Sons, Inc*. 265-296.

Tumay, M. T., Abu-Farsakh, M. Y., & Zhang, Z. (2008). From theory to implementation of a CPT-based probabilistic and fuzzy soil classification. In *From Research to Practice in Geotechnical Engineering* (pp. 259-276).

Tumay, M. T. (1985). Field calibration of electric cone penetrometers in soft soil. *Executive summary* (No. FHWA/LA/LSU-GE-85/02).

van den Berg, P. (1994). Analysis of soil penetration. *PhD thesis*, Delft University of Technology, Delft, The Netherlands.

Vesic, A.S. (1977). Design of pile foundations. *NCHRP synthesis of highway practice*, (42).

Vesic, A.S. (1972). Expansion of cavities in infinite soil mass. *Journal of Soil Mechanics & Foundations Div*, 98 (sm3).

Vesić, A. (1969). Experiments with instrumented pile groups in sand. *In Performance of deep foundations. ASTM International*.

Vos, J. D. (1982, May). The practical use of CPT in soil profiling. In *Proceedings of the Second European Symposium on Penetration Testing, ESOPT-2, Amsterdam, May* (pp. 24-27).

Voyiadjis, G. Z., & Kim, D. (2003). Finite element analysis of the piezocone test in cohesive soils using an elastoplastic–viscoplastic model and updated Lagrangian formulation. *International Journal of Plasticity*, *19*(2), 253-280.

Voyiadjis, G. Z., & Song, C. R. (2003). Determination of hydraulic conductivity using piezocone penetration test. *International Journal of Geomechanics*, *3*(2), 217-224.

Voyiadjis, G. Z., Kurup, P. U., & Tumay, M. T. (1993). Preparation of large-size cohesive specimens for calibration chamber testing. *Geotechnical Testing Journal*, *16*(3), 339-349.

Walker, J., & Yu, H. S. (2006). Adaptive finite element analysis of cone penetration in clay. *Acta Geotechnica*, *1*(1), 43-57.

Wroth, C. P. (1984). Interpretation of in situ soil tests. *Geotechnique*, *34*(4), 449-489.

Yu, H. S., Herrmann, L. R., & Boulanger, R. W. (2000). Analysis of steady cone penetration in clay. *Journal of Geotechnical and Geoenvironmental Engineering*, *126*(7), 594-605.

Yu, H. S., & Whittle, A. J. (1999). Combining strain path analysis and cavity expansion theory to estimate cone resistance in clay. *Unpublished notes*.

Yu, H.S. and Houlsby, G.T. (1991). Finite cavity expansion in dilatant soils: loading analysis.

Zhang, Z., & Tumay, M. T. (1999). Statistical to fuzzy approach toward CPT soil classification. *Journal of Geotechnical and Geoenvironmental Engineering*, *125*(3), 179-186.

Zhang, Z. (1994). Use of Uncertainty Methodology in Identification and Classification of Soils Based Upon CPT.

APPENDIX A
CPT AND LABORATORY SOIL DATA

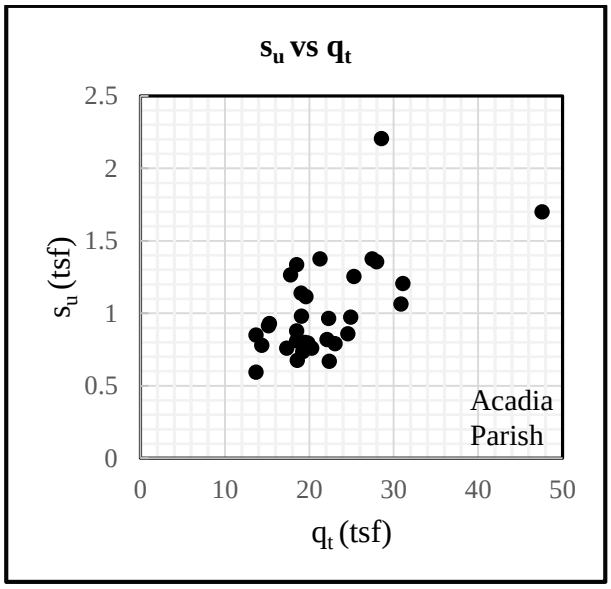

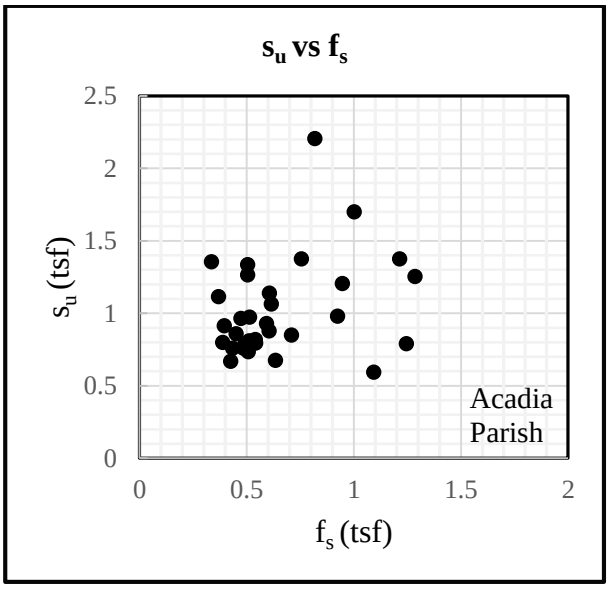

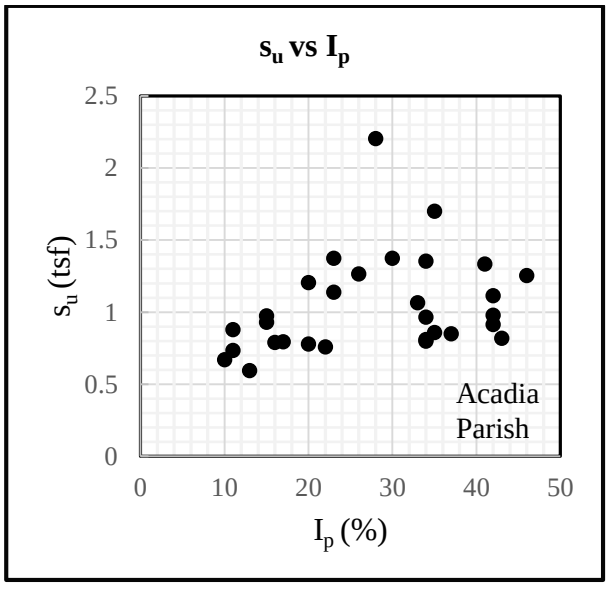

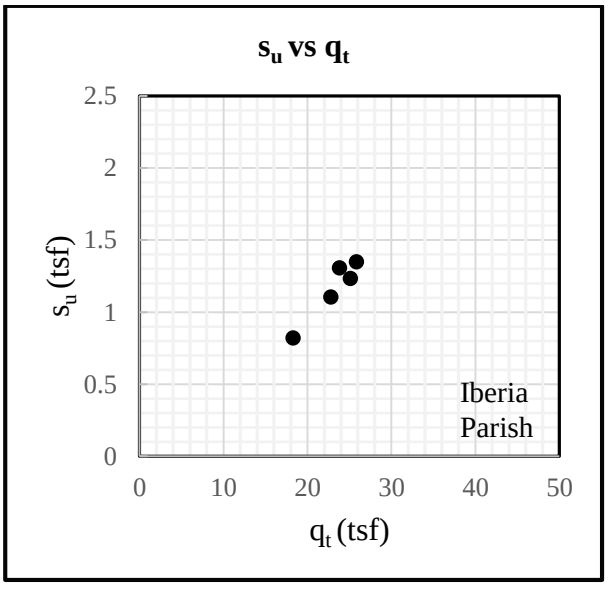

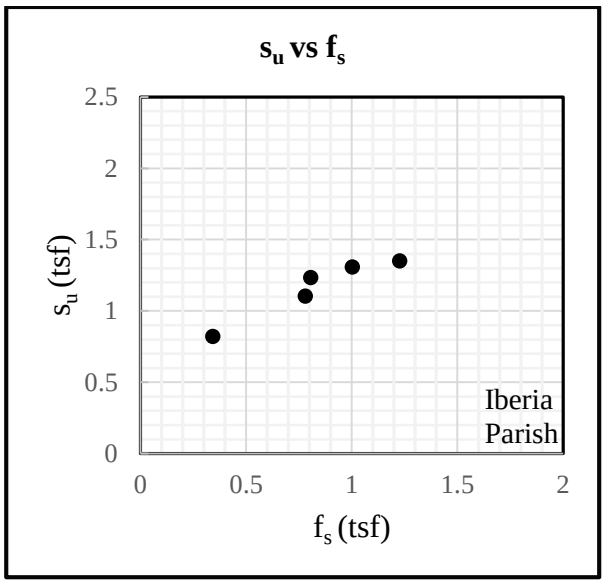
s_u vs f_s
2.5
2
1.5
1
0.5
0
0
0.5
1
1.5
2
s_u (tsf)
f_s (tsf)
Iberia
Parish

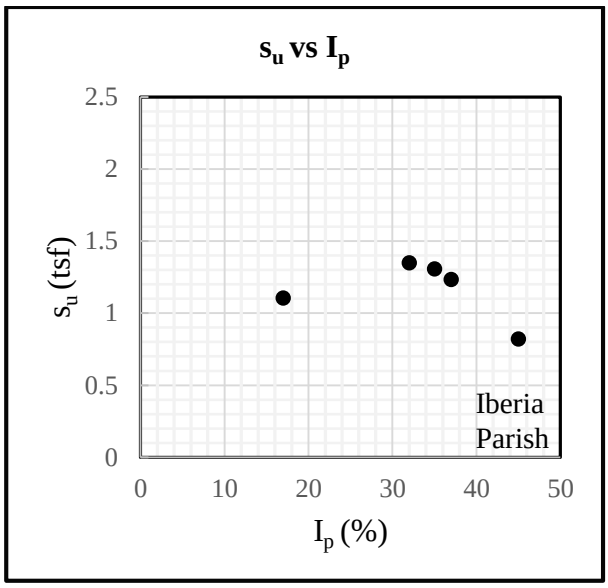
s_u vs I_p
2.5
2
1.5
1
0.5
0
0
10
20
30
40
50
s_u (tsf)
I_p (%)
Iberia
Parish

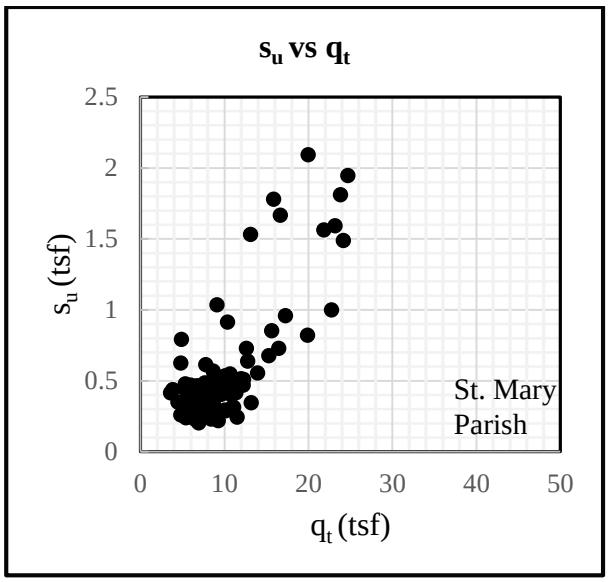
s_u vs q_t
2.5
2
1.5
1
0.5
0
0
10
20
30
40
50
s_u (tsf)
q_t (tsf)
St. Mary
Parish

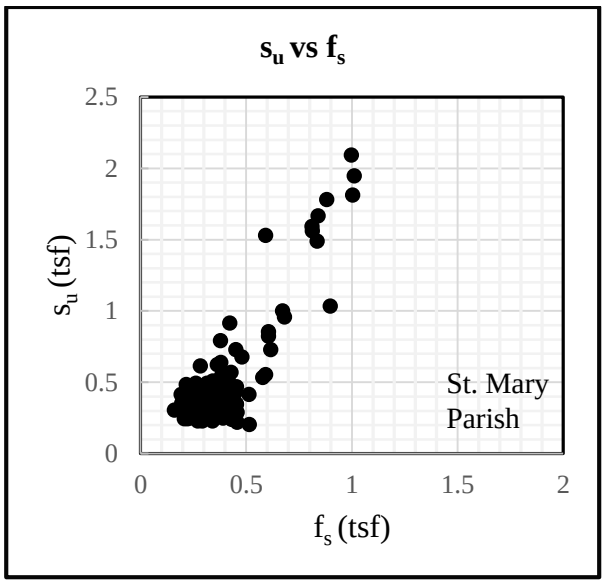
s_u vs f_s
2.5
2
1.5
1
0.5
0
0
0.5
1
1.5
2
s_u (tsf)
f_s (tsf)
St. Mary
Parish

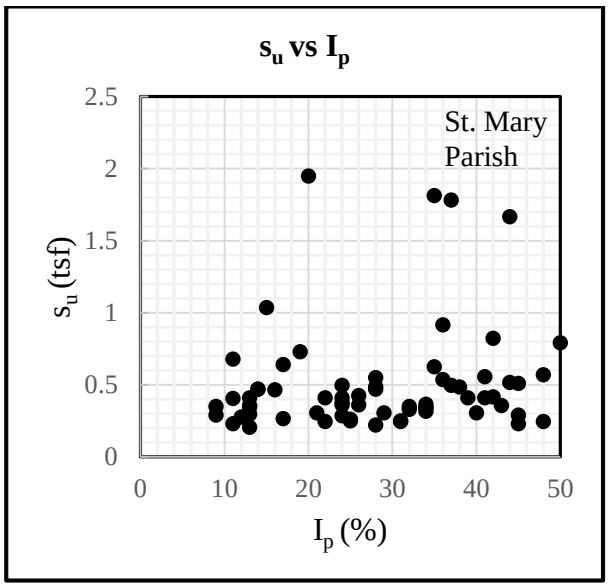
s_u vs I_p
St. Mary Parish
s_u (tsf)
I_p (%)
0
0.5
1
1.5
2
2.5
0
10
20
30
40
50

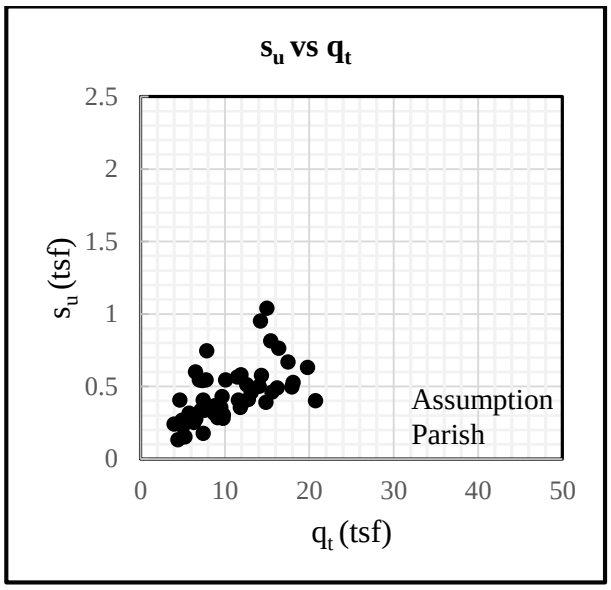
s_u vs q_t
Assumption Parish
s_u (tsf)
q_t (tsf)
0
0.5
1
1.5
2
2.5
0
10
20
30
40
50

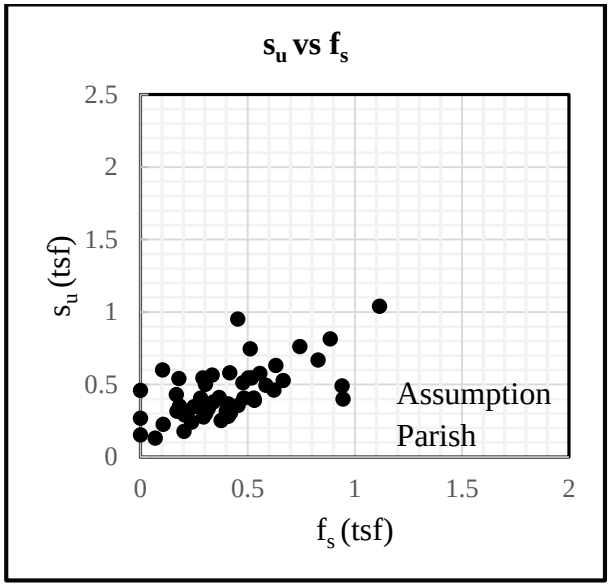
s_u vs f_s
Assumption Parish
s_u (tsf)
f_s (tsf)
0
0.5
1
1.5
2
2.5
0
0.5
1
1.5
2

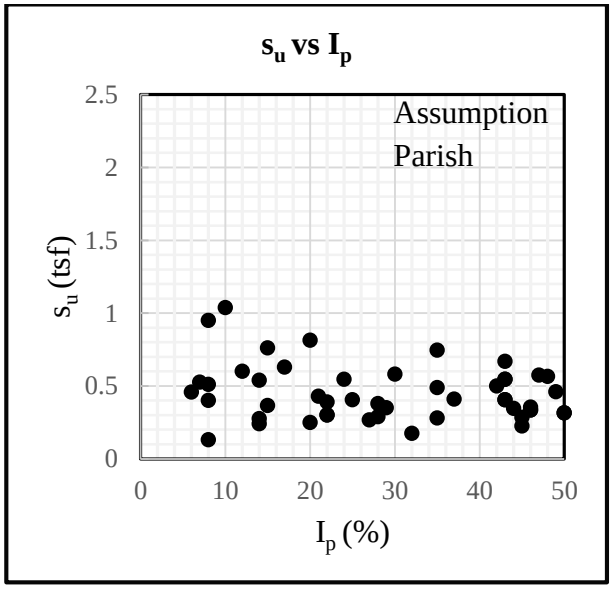
s_u vs I_p
Assumption Parish
s_u (tsf)
I_p (%)
0
0.5
1
1.5
2
2.5
0
10
20
30
40
50

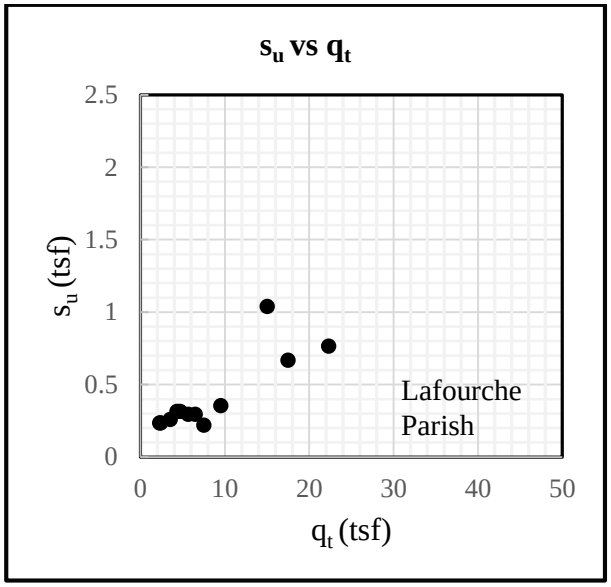
s_u vs q_t
2.5
2
1.5
1
0.5
0
s_u (tsf)
0
10
20
30
40
50
q_t (tsf)
Lafourche Parish

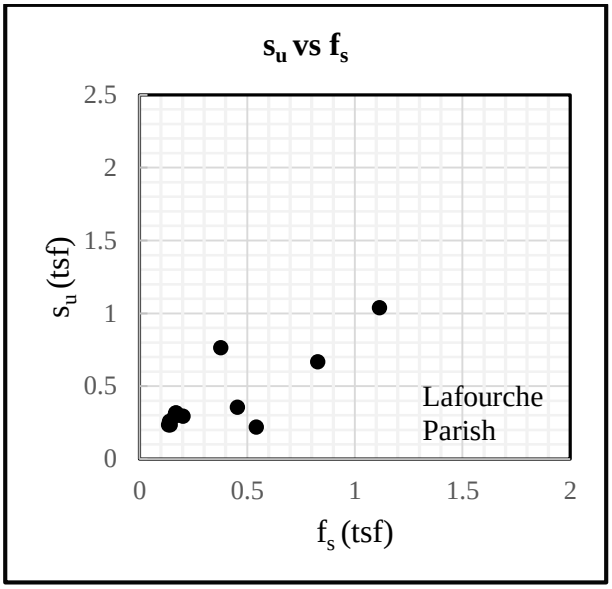
s_u vs f_s
2.5
2
1.5
1
0.5
0
s_u (tsf)
0
0.5
1
1.5
2
f_s (tsf)
Lafourche Parish

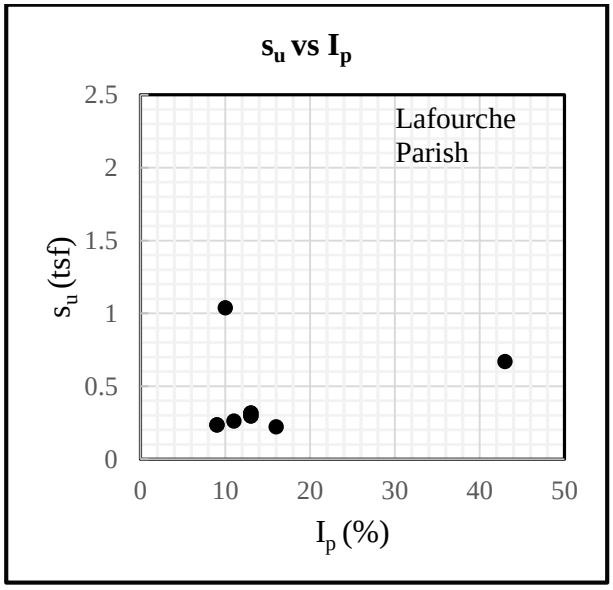
s_u vs I_p
2.5
2
1.5
1
0.5
0
s_u (tsf)
0
10
20
30
40
50
I_p (%)
Lafourche Parish

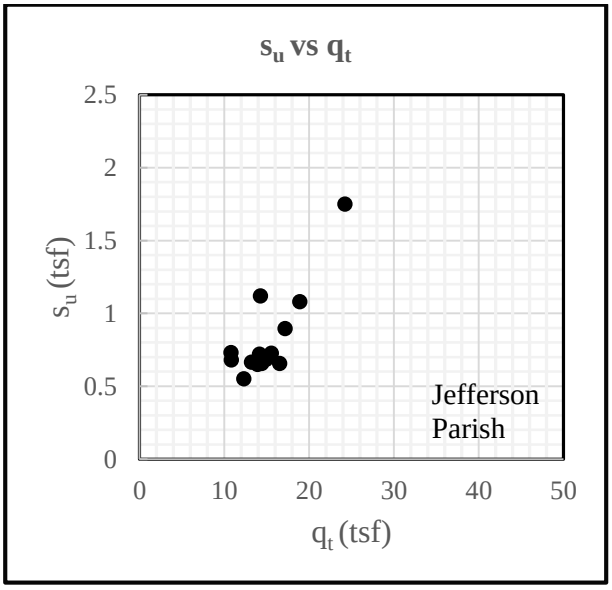
s_u vs q_t
2.5
2
1.5
1
0.5
0
s_u (tsf)
0
10
20
30
40
50
q_t (tsf)
Jefferson Parish

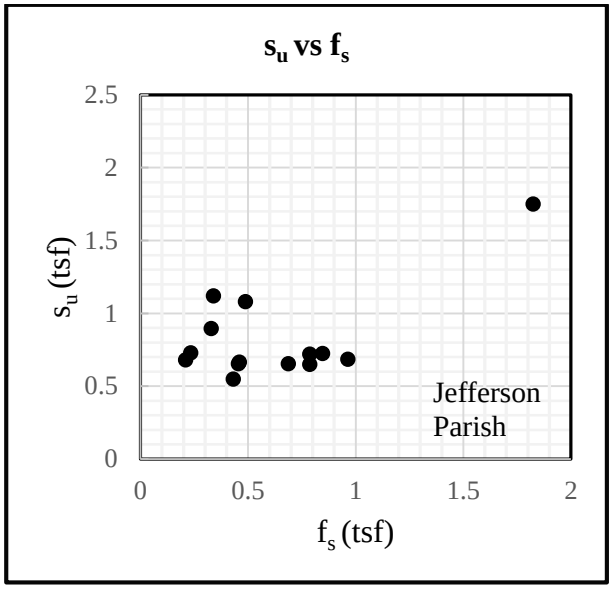
s_u vs f_s
2.5
2
1.5
1
0.5
0
0
0.5
1
1.5
2
s_u (tsf)
f_s (tsf)
Jefferson Parish

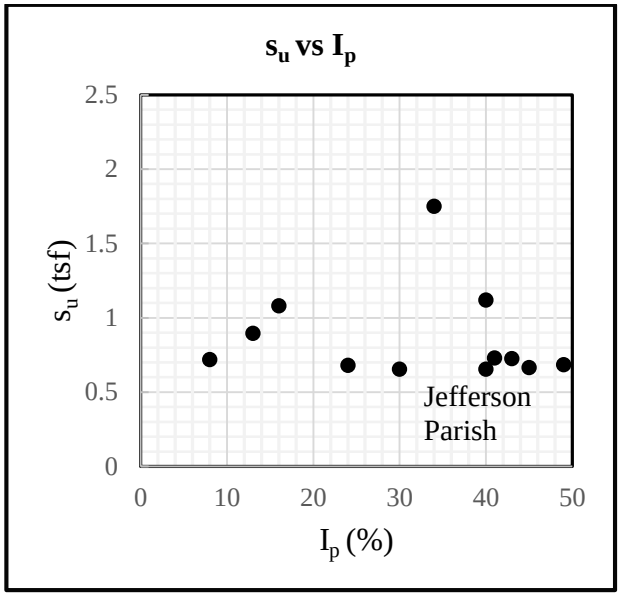
s_u vs I_p
2.5
2
1.5
1
0.5
0
0
10
20
30
40
50
s_u (tsf)
I_p (%)
Jefferson Parish

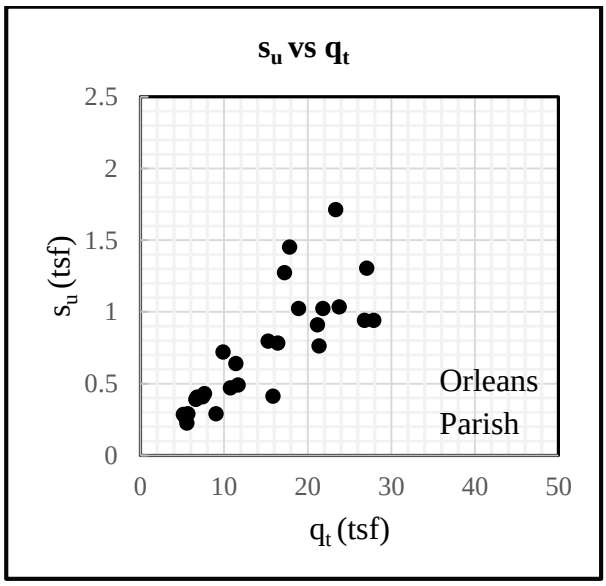
s_u vs q_t
2.5
2
1.5
1
0.5
0
0
10
20
30
40
50
s_u (tsf)
q_t (tsf)
Orleans Parish

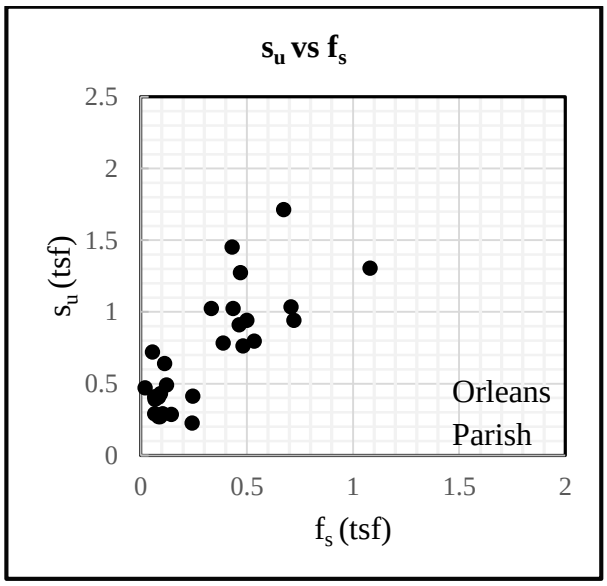
s_u vs f_s
2.5
2
1.5
1
0.5
0
0
0.5
1
1.5
2
s_u (tsf)
f_s (tsf)
Orleans Parish

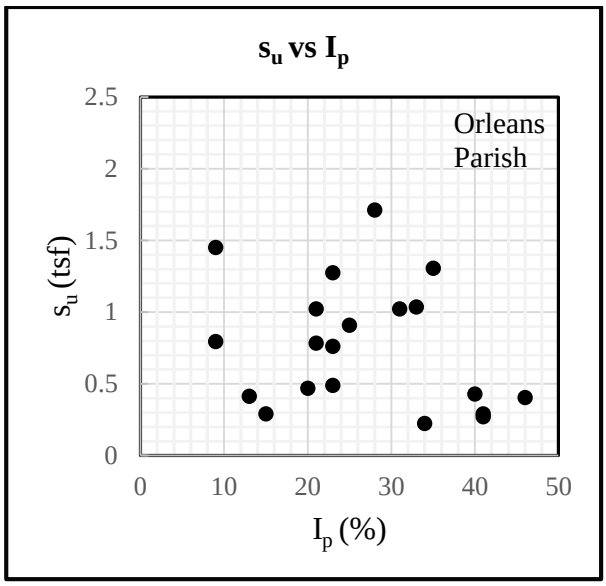
s_u vs I_p
Orleans Parish
s_u (tsf)
I_p (%)
0
0.5
1
1.5
2
2.5
0
10
20
30
40
50

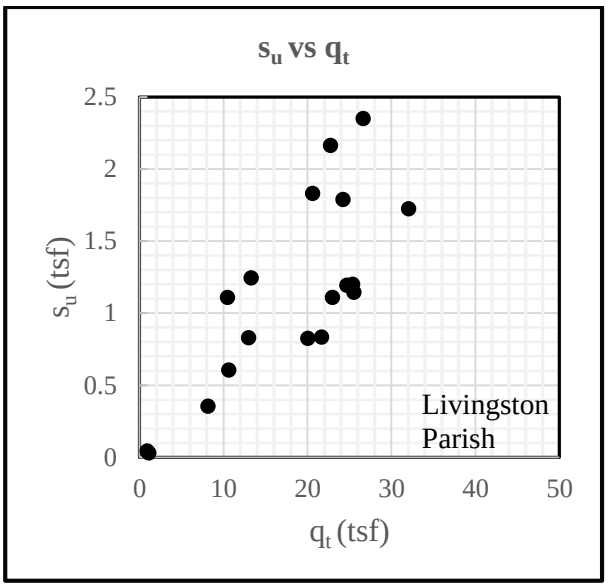
s_u vs q_t
Livingston Parish
s_u (tsf)
q_t (tsf)
0
0.5
1
1.5
2
2.5
0
10
20
30
40
50

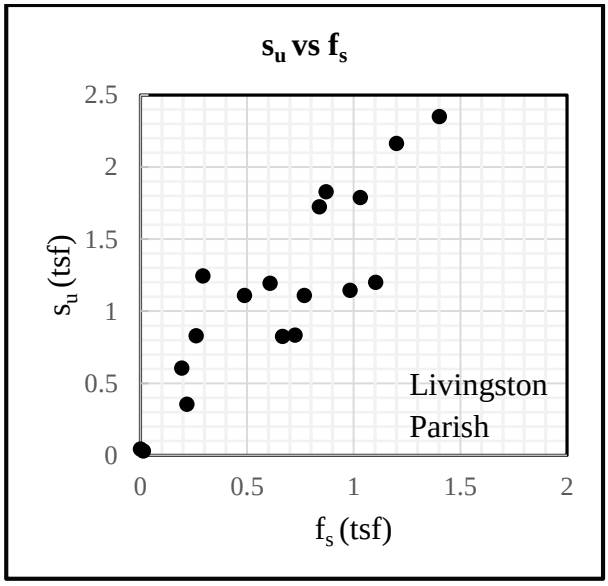
s_u vs f_s
Livingston Parish
s_u (tsf)
f_s (tsf)
0
0.5
1
1.5
2
2.5
0
0.5
1
1.5
2

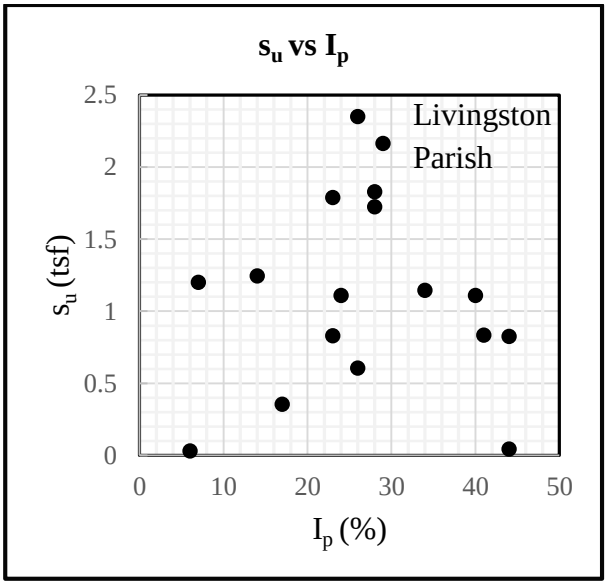
s_u vs I_p
Livingston Parish
s_u (tsf)
I_p (%)
0
0.5
1
1.5
2
2.5
0
10
20
30
40
50

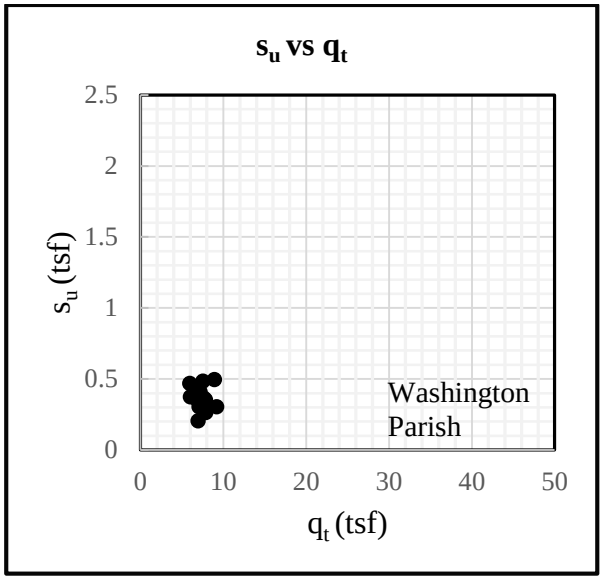
s_u vs q_t
2.5
2
1.5
1
0.5
0
s_u (tsf)
0
10
20
30
40
50
q_t (tsf)
Washington Parish

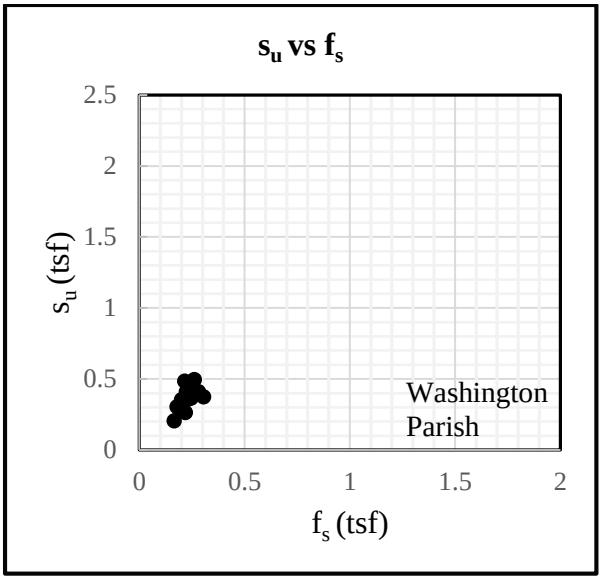
s_u vs f_s
2.5
2
1.5
1
0.5
0
s_u (tsf)
0
0.5
1
1.5
2
f_s (tsf)
Washington Parish

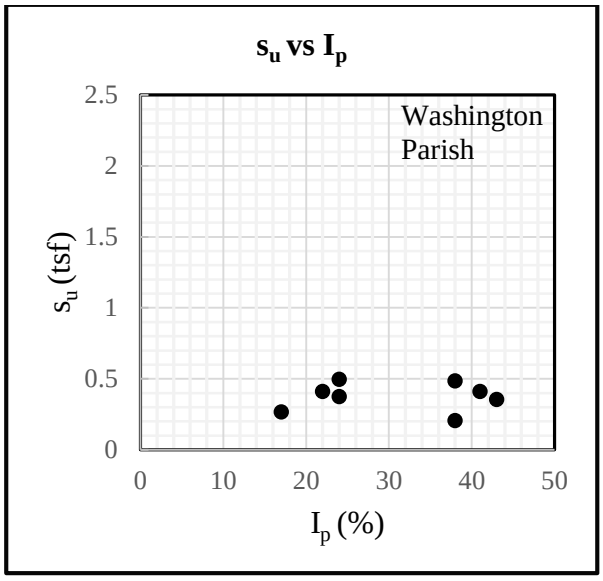
s_u vs I_p
2.5
2
1.5
1
0.5
0
s_u (tsf)
0
10
20
30
40
50
I_p (%)
Washington Parish

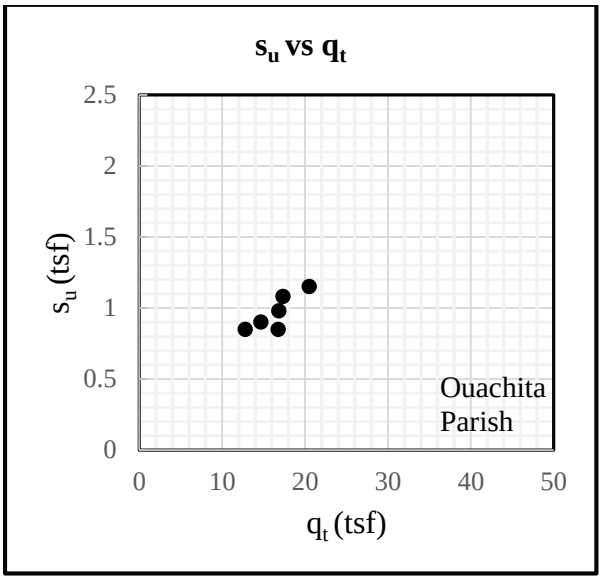
s_u vs q_t
2.5
2
1.5
1
0.5
0
s_u (tsf)
0
10
20
30
40
50
q_t (tsf)
Ouachita Parish

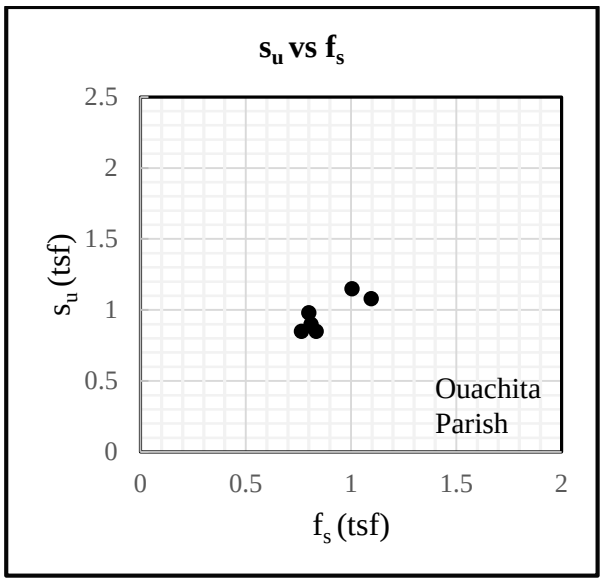
s_u vs f_s
2.5
2
1.5
1
0.5
0
0
0.5
1
1.5
2
s_u (tsf)
f_s (tsf)
Ouachita Parish

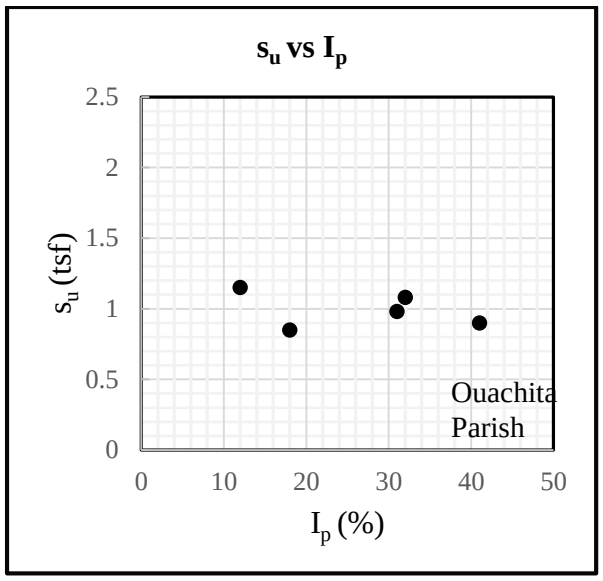
s_u vs I_p
2.5
2
1.5
1
0.5
0
0
10
20
30
40
50
s_u (tsf)
I_p (%)
Ouachita Parish

APPENDIX B
SAS® PROGRAM AND SAMPLE OUTPUTS

A brief description of SAS® program to analyze the data and perform regression analyses is given in following sections.

Statistical Analyses for Selecting Significant Model Parameters

```
ods rtf file="C:\Users\rdas5\Desktop\PREG_F.rtf";
ods graphics on;
data  PER;
input su qt fs σvo LL Ip MC @@;
datalines;
0.6850    14.9332    0.9633    0.7585    38.0000    49.0000    38.0000
0.7250    15.5388    0.8451    0.9280    76.0000    43.0000    42.0000
0.6500    13.9247    0.7861    1.0690    75.0000    53.0000    41.0000
0.7200    14.1425    0.7865    1.1860    92.0000    8.0000     43.0000
……
……
1.0388    14.9996    1.1151    0.7213    72.0000    10.0000    31.0000
0.5116    12.6065    0.4772    3.2184    82.0000    8.0000     8.0000
0.8143    15.4352    0.8860    3.4957    45.0000    20.0000    42.0000
0.7621    16.3690    0.7438    4.1202    42.0000    15.0000    36.0000
;
PROC glm data = PER;
Model su = qt fs σvo LL Ip MC ;
```

run;

ods rtf close;

quit; quit;

Sample Output

The SAS System

The GLM Procedure

Dependent Variable; s_u

Source	DF	Sum of Squares	Mean Square	F Value	Pr > F
Model	6	3597.397705	599.566284	115.98	<0.0001
Error	198	1023.591980	5.169656		
Corrected Total	204	4620.989684			

R-Square	Coeff Var	Root MSE	s_u Mean
0.778491	75.65191	2.273688	3.005460

Source	DF	Type III SS	Mean Square	F Value	Pr > F
q_t	1	14.7450767	14.7450767	3.85	0.0428
f_s	1	197.5341418	197.5341418	38.21	<.0001
σ_{vo}	1	272.9295441	272.9295441	52.79	<.0001
LL	1	15.2878106	15.2878106	2.96	0.0871
PI	1	0.1654521	0.1654521	0.03	0.8582
MC	1	20.5445887	20.5445887	3.17	0.0676

Source	Estimate	Standard Error	t Value	Pr > |t|
Intercept	2.313600262	0.65564957	3.53	0.0005
q_t	-0.037372722	0.02212901	-3.69	0.0428
f_s	1.207793222	0.19539001	6.18	<.0001
σ_{vo}	0.095054377	0.01308211	7.27	<.0001
LL	-0.014888379	0.00865776	-1.72	0.0871
PI	0.001903961	0.01064272	0.18	0.8582
MC	-0.023902493	0.01199017	-1.89	0.0676

Collinearity Test

Pearson Coefficient Test

```
ods rtf file="temp.rtf";
ods graphics on;
data  PER;
input su qt fs σvo @@;
datalines;
1.7500    24.2087      1.8250    0.3895
0.6850    14.9332      0.9633    0.7585
0.7250    15.5388      0.8451    0.9280
0.6500    13.9247      0.7861    1.0690
……
……
0.8143    15.4352      0.8860    3.4957
0.5272    18.0883      0.6655    3.8022
0.9500    14.2282      0.4535    4.1202
0.7621    16.3690      0.7438    4.1202
;
PROC Corr data = PER;
Var su qt fs σvo ;
run;
ods rtf close;
quit;
```

VIF Test

```
ods rtf file="temp.rtf";
ods graphics on;
data  PER;
input su qt fs σvo @@;
datalines;
1.7500    24.2087       1.8250    0.3895
0.6850    14.9332       0.9633    0.7585
0.7250    15.5388       0.8451    0.9280
0.6500    13.9247       0.7861   1.0690
……
……
0.8143     15.4352      0.8860     3.4957
0.5272     18.0883      0.6655     3.8022
0.9500     14.2282      0.4535     4.1202
0.7621     16.3690      0.7438     4.1202
;
PROC reg data = PER;
Model su = qt fs σvo / tol vif collin;
run;
ods rtf close;
quit;
```

Sample Output

The SAS System

The CORR Procedure

4 Variables:	s_u	q_t	f_s	σ_{vo}

Simple Statistics						
Variable	**N**	**Mean**	**Std Dev**	**Sum**	**Minimum**	**Maximum**
s_u	322	0.64992	0.41073	209.27380	0.03000	2.35000
q_t	322	12.72700	6.95472	4098	0.91750	47.56810
f_s	322	0.44390	0.29243	142.93600	0.0001000	1.82500
σ_{vo}	322	2.82320	1.77452	909.07090	0.02070	7.54880

Pearson Correlation Coefficients, N = 322 Prob > |r| under H0: Rho=0				
	s_u	**q_t**	**f_s**	**σ_{vo}**
s_u	1.00000	0.78045 <.0001	0.75287 <.0001	0.22104 <.0001
q_t	0.78045 <.0001	1.00000	0.71724 <.0001	0.49999 <.0001
f_s	0.75287 <.0001	0.71724 <.0001	1.00000	0.10333 0.0640
σ_{vo}	0.22104 <.0001	0.49999 <.0001	0.10333 0.0640	1.00000

The SAS System

The REG Procedure

Model: MODEL1

Dependent Variable: s_u

Number of Observations Read	322
Number of Observations Used	322

Analysis of Variance					
Source	**DF**	**Sum of Squares**	**Mean Square**	**F Value**	**Pr > F**
Model	3	39.19450	13.06483	277.74	<.0001
Error	318	14.95862	0.04704		
Corrected Total	321	54.15312			

Root MSE	0.21689	**R-Square**	0.7238
Dependent Mean	0.64992	**Adj R-Sq**	0.7212
Coeff Var	33.37130		

Parameter Estimates							
Variable	**DF**	**Parameter Estimate**	**Standard Error**	**t Value**	**Pr > |t|**	**Tolerance**	**Variance Inflation**
Intercept	1	0.06348	0.03177	2.00	0.0466	.	0
q_t	1	0.04099	0.00372	11.00	<.0001	0.28714	3.48257
f_s	1	0.35867	0.07601	4.72	<.0001	0.39245	2.54810
σ_{vo}	1	-0.03231	0.01000	-3.23	0.0014	0.56504	1.76979

Collinearity Diagnostics						
Number	**Eigenvalue**	**Condition Index**	**Proportion of Variation**			
			Intercept	**q_t**	**f_s**	**σ_{vo}**
1	3.54750	1.00000	0.01304	0.00524	0.00825	0.01162
2	0.26889	3.63222	0.01186	0.00596	0.20411	0.32592
3	0.13968	5.03965	0.95347	0.05957	0.01720	0.16759
4	0.04393	8.98632	0.02163	0.92923	0.77044	0.49487

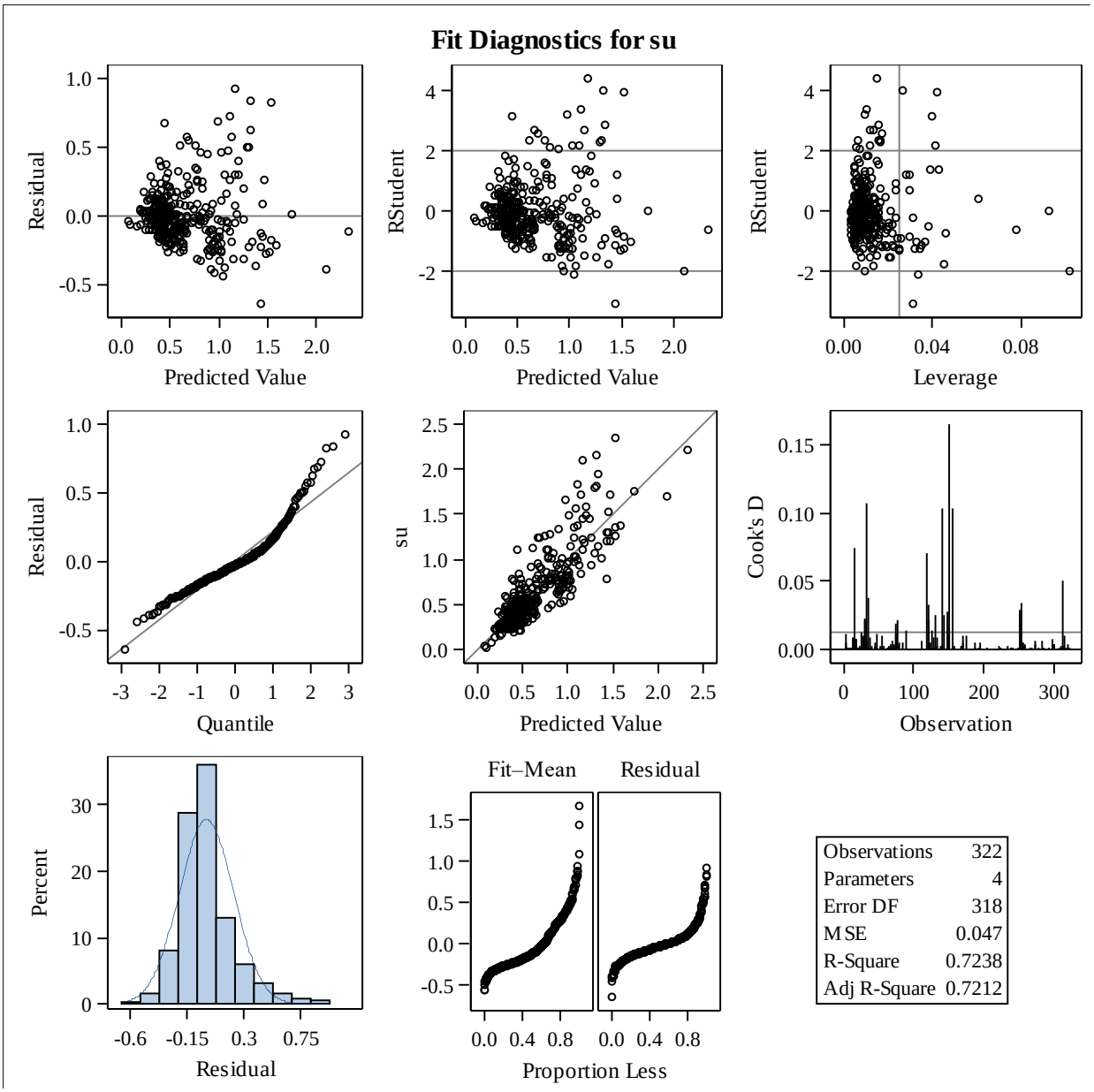
Fit Diagnostics for su
Residual
Predicted Value
RStudent
Predicted Value
RStudent
Leverage
Residual
Quantile
su
Predicted Value
Cook's D
Observation
Percent
Residual
Fit–Mean
Residual
Proportion Less
Observations 322
Parameters 4
Error DF 318
MSE 0.047
R-Square 0.7238
Adj R-Square 0.7212

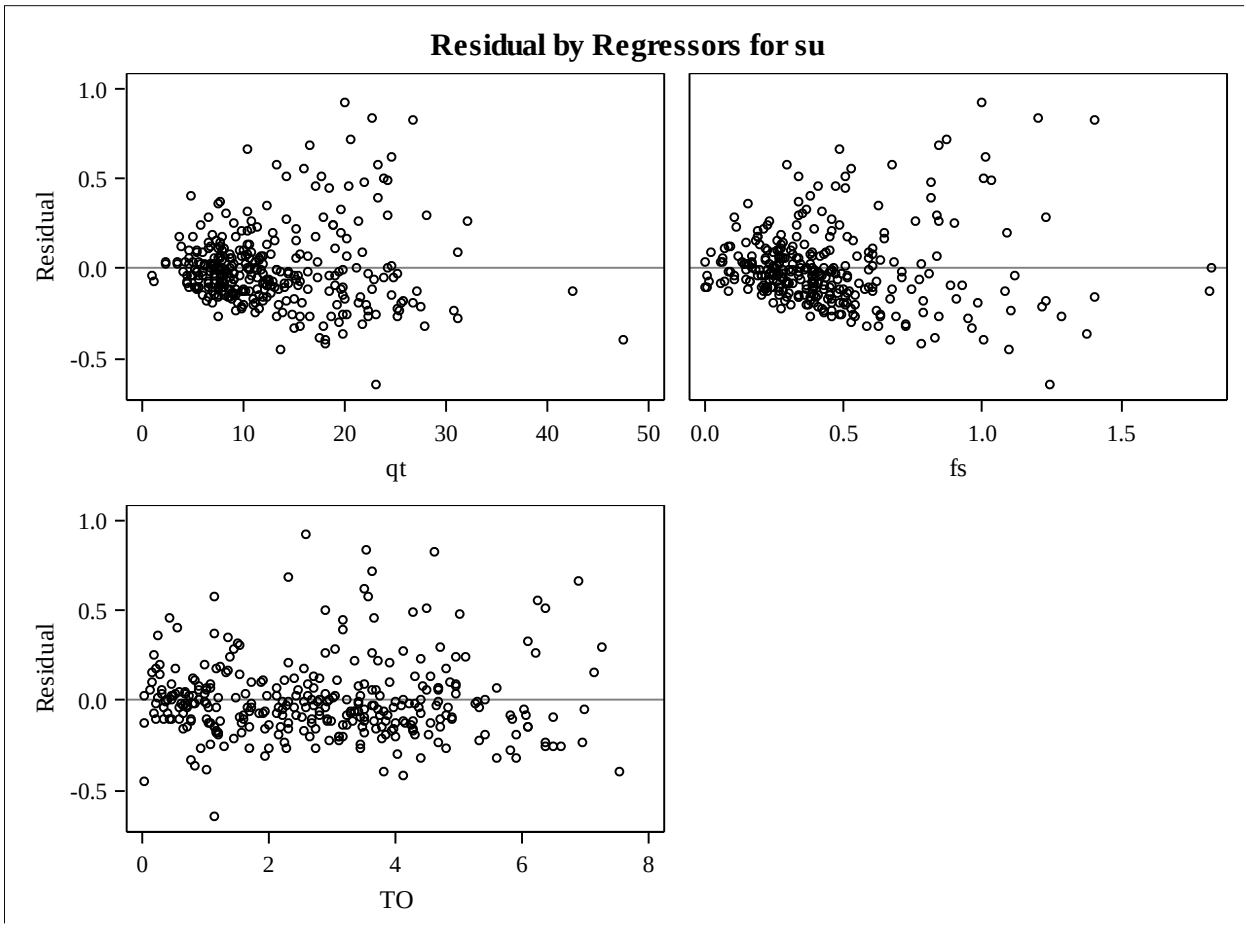

Linear Regression Model Using Cone Tip Resistance (f_s) and Sleeve Friction (f_s)

dm 'log; clear; output; clear';

title1 's_u q_t f_s MODEL';

options nodate nocenter pageno=1 ls=78 PS=55;

ods rtf file="C:\Users\rdas5\Desktop\PREG_F.rtf";

DATA PER; TITLE 's_u q_t f_s Linear Model';

input s_u q_t f_s @@;

CARDS;

1.7500 24.2087 1.8250

0.6850 14.9332 0.9633

0.7250 15.5388 0.8451

0.6500 13.9247 0.7861

……...

……

0.8143 15.4352 0.8860

0.5272 18.0883 0.6655

0.9500 14.2282 0.4535

0.7621 16.3690 0.7438

;

* CALCULATE SUMMARY STATISTICS;

proc means n mean std min max clm css cv ALPHA=0.05;

run;

* Fit the linear model;

proc lin data=PER method=marquardt hougaard ;

parms A=.05 ;

Model $s_u = A*(q_t+f_s)$;

output out=nlinout predicted=pred l95m=l95mean u95m=u95mean

l95=l95ind u95=u95ind;

run;

proc print data=nlinout; run;

ods rtf close;

quit;

Sample Output

s_u, q_t, f_s linear model

The MEANS Procedure

Variable	N	Mean	Std Dev	Minimum	Maximum	Lower 95% CL for Mean	Upperr 95% CL for Mean	Corrected SS	Coeff of Variation
s_u	322	0.6499186	0.4107327	0.0300000	2.3500000	0.6048868	0.6949505	54.1531211	63.1975498
q_t	322	12.7270037	6.9547238	0.9175000	47.5681000	11.9645024	13.4895050	15526.19	54.6454138
f_s	322	0.4439006	0.2924336	0.0001000 00	1.8250000	0.4118388	0.4759624	27.4510947	65.8781758

The LIN Procedure

Dependent Variable s_u

Method: Marquardt

Iterative Phase		
Iter	**A**	**Sum of Squares**
0	0.0500	18.7263
1	0.0487	18.6033

NOTE: Convergence criterion met.

Estimation Summary	
Method	**Marquardt**
Iteration	1
R	0
PPC	0
RPC(A)	0.026076

Object	0.006568
Objective	18.60334
Observations Read	322
Observations Used	322
Observations Missing	0

Note: An intercept was not specified for this model.

Source	DF	Sum of Squares	Mean Square	F Value	Approx Pr > F
Model	1	171.6	171.6	2960.27	<0.0001
Error	321	18.6033	0.0580		
Uncorrected Total	321	190.2			

Parameter	Estimate	Approx Std Error	Approximate 95% confidence Limits		Skewness
			Limits		
Error	321	18.6033	0.0469	0.0505	0

Obs	s_u	q_t	f_s	pred	I95mean	U95mean	I95ind	U95ind
1	1.7500	24.2087	1.8250	1.26774	1.22190	1.31358	0.79191	1.74358
2	0.6850	14.9332	0.9633	0.77410	0.74611	0.80209	0.29965	1.24855
3	0.7250	15.5388	0.8451	0.79783	0.76898	0.82668	0.32333	1.27233
4	0.6500	13.9247	0.7861	0.71636	0.69046	0.74226	0.24203	1.19069
-	-	-	-	-	-	-	-	-
319	0.8143	15.4352	0.8860	0.79478	0.76604	0.82352	0.32029	1.26927
320	0.5272	18.0883	0.6655	0.91324	0.88022	0.94626	0.43847	1.38801
321	0.9500	14.2282	0.4535	0.71494	0.68909	0.74079	0.24062	1.18927
322	0.7621	16.3690	0.7438	0.83333	0.80319	0.86346	0.35875	1.30791

Nonlinear Regression Model Using Cone Tip Resistance (f_s) and Sleeve Friction (f_s)

```
dm 'log; clear; output; clear';
title1 's_u q_t f_s MODEL';
options nodate nocenter pageno=1 ls=78 PS=55;
ods rtf file="C:\Users\rdas5\Desktop\PREG_F.rtf";
DATA PER; TITLE 's_u q_t f_s Nonlinear Model';
input s_u q_t f_s @@;
CARDS;
1.7500    24.2087    1.8250
0.6850    14.9332    0.9633
0.7250    15.5388    0.8451
0.6500    13.9247    0.7861
……...
……
0.8143 15.4352       0.8860
0.5272 18.0883       0.6655
0.9500 14.2282       0.4535
0.7621 16.3690       0.7438
;
* CALCULATE SUMMARY STATISTICS;
proc means n mean std min max clm css cv ALPHA=0.05;
run;
* Fit the nonlinear model;
proc nlin data=PER method=marquardt hougaard ;
```

parms A=.06, B=0.85 C=.1 ;

Model s_u = A*(q_t+f_s)**B+C ;

output out=nlinout predicted=pred l95m=l95mean u95m=u95mean

l95=l95ind u95=u95ind;

run; proc print data=nlinout; run; ods rtf close; quit;

s_u, q_t, f_s linear model

The MEANS Procedure

Variable	N	Mean	Std Dev	Minimum	Maximum	Lower 95% CL for Mean	Upperr 95% CL for Mean	Corrected SS	Coeff of Variation
s_u	322	0.6499255	0.4107509	0.0300000	2.3500000	0.6048916	0.6949593	54.1579382	63.1996962
q_t	322	12.6556025	6.7296814	0.9170000	47.5681000	11.9177744	13.3934306	14537.64	53.1755119
f_s	322	0.4422609	0.2821007	0	1.8250000	0.4113319	0.4731898	25.5454381	63.7860407

The NLIN Procedure

Dependent Variable s_u

Method: Marquardt

Iterative Phase				
Iter	**A**	**B**	**C**	**Sum of Squares**
0	0.0400	0.1000	1.4000	20.5205
1	0.0357	0.1012	1.3664	19.2023
2	0.0358	0.1002	1.3730	19.2023
3	0.0358	0.1004	1.3716	19.2022
4	0.0358	0.1004	1.3719	19.2022
5	0.0358	0.1004	1.3718	19.2022

NOTE: Convergence criterion met.

Estimation Summary	
Method	**Marquardt**
Iteration	5
R	4.918E-6
PPC	0.000018
RPC(A)	0.000087
Object	4.21E-10
Objective	19.20225
Observations Read	322
Observations Used	322
Observations Missing	0

Note: An intercept was not specified for this model.

Source	DF	Sum of Squares	Mean Square	F Value	Approx Pr > F
Model	3	171.0	56.9898	946.75	<0.0001
Error	319	19.2022	0.0602		
Uncorrected Total	322	190.2			

Parameter	Estimate	Approx Std Error	Approximate 95% confidence Limits		Skewness
			Limits		
A	0.0358	0.00275	0.0304	0.0412	0.0235
B	0.1004	0.0255	0.0502	0.1505	0.0763
C	1.3718	0.1494	1.0779	1.6657	0.4364

Approximate Correlation Matrix			
	A	**B**	**C**
A	1.0000000	-0.8802421	0.5442836
B	-0.8802421	1.0000000	-0.8254971
C	0.5442836	-0.8254971	1.0000000

Obs	s_u	q_t	f_s	pred	I95mean	U95mean	I95ind	U95ind
1	1.750	24.209	1.825	2.09383	1.75829	2.42937	1.50596	2.68170
2	0.685	14.933	0.963	0.91063	0.85784	0.96343	0.42505	1.39622
3	0.725	15.539	0.845	0.87609	0.83634	0.91584	0.39176	1.36043
4	0.650	13.925	0.786	0.79345	0.75465	0.83226	0.30919	1.27771
-	-	-	-	-	-	-	-	-
-	-	-	-	-	-	-	-	-
319	0.814	15.435	0.886	0.89089	0.84745	0.93432	0.40623	1.37554
320	0.527	18.088	0.666	0.89730	0.86308	0.93152	0.41339	1.38121
321	0.950	14.228	0.454	0.69608	0.66681	0.72534	0.21249	1.17967
322	0.7621	16.3690	0.7438	0.86440	0.83123	0.89756	0.38055	1.34824

VITA

Md Imran Hossain was born on February 15, 1993, in Sirajganj, Bangladesh. His father, Md Amzad Hossain, is a teacher and his mother, Ismot Ara, is a housewife. He finished his secondary school level education from Bogra Zilla School and higher secondary in Science from Notre Dame College, Dhaka, Bangladesh. He attended Bangladesh University of Engineering and Technology, Dhaka, Bangladesh from 2010 to 2015, for Bachelor of Science degree in civil engineering. After finishing Bachelor of Science degree, he was employed at Uttara University as an instructor. Later he joined Bangladesh Water Development Board under the Peoples Republic of Bangladesh as an assistant engineer. He joined Louisiana State University, Baton Rouge in the Spring semester, 2017. Upon completion of his master's degree, he will begin work in the industry.